

The MAD Program
(Methodical Accelerator Design)
Version 8.13
Physical Methods Manual

F. Christoph Iselin

Abstract

MAD is a tool for charged-particle optics in alternating-gradient accelerators and beam lines. It can handle from very large to very small accelerators, and solve various problems on such machines.

This document outlines the physical models used in MAD. It should help the physicist in understanding the precise function of the program, and to appreciate possible limits of its validity.

Geneva, Switzerland
September 15, 1994

Contents

1	Basic Conventions and Notations	1
1.1	Canonical Variables	1
1.2	Phase Space Vector	1
1.3	Auxiliary Functions and Their Integrals	2
2	Hamiltonian Representations	3
2.1	Magnetic Field and Vector Potential (Transverse Field, Curved Reference)	3
2.2	Magnetic Field and Vector Potential (Multipole)	3
2.3	Magnetic Field and Vector Potential (Solenoid Fields)	4
2.4	Electric Field for an RF Cavity	4
2.5	Electric Field for an Electrostatic Separator	4
2.6	General Form for the Hamiltonian	4
3	Lie Algebraic Maps	6
3.1	Definitions	6
3.2	Tilted Elements	6
3.3	Map Composition	6
3.4	Reverse Factorisation	8
3.5	Map Inversion	9
3.6	Reflection of a Lie Algebraic Map	9
3.7	Fixed Points	9
3.8	Tracking	9
4	TRANSPORT Maps	11
4.1	Definition	11
4.2	Tilted Elements	11
4.3	Map Composition	11
4.4	Map Inversion	11
4.5	Map Reflection	12
4.6	Closed Orbit	12
4.7	Making First-Order Matrix Symplectic	13
4.8	Tracking	13
5	Maps for Physical Elements	14
5.1	Marker	14
5.2	Drift Space and Similar Objects	14
5.2.1	Hamiltonian for a Drift Space	14
5.2.2	Exact Solution for Equations of Motion	14
5.2.3	Lie-Algebraic Map for a Drift Space	15
5.2.4	TRANSPORT Map	15
5.3	Dipoles	15
5.3.1	Dipole Fringing Fields	15
5.3.2	Body of a Sector Dipole	17
5.3.3	Body of a Rectangular Dipole	21
5.4	Quadrupole	22
5.4.1	Hamiltonian for a Quadrupole	22
5.4.2	Lie-Algebraic map for a Quadrupole	22
5.4.3	TRANSPORT Map for a Quadrupole	24

5.5	Sextupole	24
5.5.1	Hamiltonian for a Sextupole	24
5.5.2	Lie-Algebraic Map for a Sextupole	25
5.5.3	TRANSPORT Map for a Sextupole	25
5.6	Octupole	26
5.6.1	Lie-Algebraic Map for an Octupole	26
5.6.2	TRANSPORT Map for a Thin Octupole	26
5.7	Thin Multipole	26
5.7.1	Lie-Algebraic Map for a Thin Multipole	27
5.7.2	TRANSPORT Map for a Thin Multipole	27
5.8	Solenoid	28
5.8.1	Hamiltonian for a Solenoid	28
5.8.2	Lie-Algebraic Map for a Solenoid	28
5.8.3	TRANSPORT Map for a Solenoid	29
5.9	Orbit Correctors	29
5.10	RF Cavity	29
5.10.1	Exact Solution for a Thin RF Cavity	30
5.10.2	Lie-Algebraic Map for a Thin RF Cavity	30
5.10.3	TRANSPORT Map for a Thin RF Cavity	30
5.10.4	Electrostatic Separator	31
5.10.5	Hamiltonian for an Electrostatic Separator	31
5.10.6	Exact Solution for an Electrostatic Separator	31
5.10.7	Lie-Algebraic Map for an Electrostatic Separator	31
5.10.8	TRANSPORT Map for an Electrostatic Separator	32
5.11	Misalignments	32
5.11.1	Exact Map for Misalignments	33
5.11.2	Linear Approximation for Misalignments	33
5.11.3	Misalignment at Exit	34
5.12	Rotation of Reference about the s -Axis	35
5.13	Rotation of Reference About y -Axis	35
5.14	Beam-Beam Interactions	35
5.14.1	Lie-Algebraic Map for Beam-Beam Interaction	35
5.14.2	TRANSPORT Map for Beam-Beam Interactions	35
6	Uncoupled Linear Optics	38
6.1	Courant-Snyder Lattice Functions	38
6.1.1	Initial Conditions for the Periodic Case	38
6.1.2	Tracking the Lattice Functions	39
6.2	Dispersion	39
6.2.1	Initial Values for Dispersion	39
6.2.2	Tracking the Dispersion	40
6.3	Chromatic Effects	41
6.3.1	Initial Values for Chromatic Functions	41
6.3.2	Tracking the Chromatic Functions	41
7	Transverse Coupling (Method by Edwards and Teng)	43
7.1	Initial Values	43
7.2	Tracking the Edwards-Teng Functions	44

8 Fully Coupled Motion	45
8.1 Eigenvectors of a $2N \times 2N$ Symplectic Matrix	45
8.2 Everything is Real	46
8.3 Linear Invariants	48
8.4 Phase Factors	49
8.5 TRANSPORT Sigma Matrix	49
8.6 Coupling Angles	50
8.7 Implementation	50
8.7.1 EMIT Command	50
8.7.2 Eigenvectors	51
8.7.3 Linear Invariants	51
8.7.4 Phase advances	51
8.7.5 Envelopes	51
8.7.6 Mais-Ripken Lattice Functions	52
8.8 Transformations between Representations of Beam	52
8.8.1 Eigenvectors to Internal Sigma Matrix	52
8.8.2 Internal Sigma Matrix to TRANSPORT Notation	52
8.8.3 TRANSPORT Notation to Internal Sigma Matrix	53
9 Survey	54
9.1 Global Reference System	54
9.2 Single Elements	55
9.2.1 Markers	55
9.2.2 Straight Elements	55
9.2.3 Dipoles	56
9.2.4 Rotation of Reference System about s -Axis	57
9.2.5 Rotation of Reference System about y -Axis	57
9.3 Sequences of Elements	58
10 Closed Orbit and Dispersion Correction	59
10.1 Influence of a Kick in a Plane on the Orbit	59
10.2 Orbit Correction by MICADO Algorithm	59
10.3 Influence Matrix for Orbit and Dispersion for a Plane	59
10.4 Orbit and Dispersion Correction by MICADO Algorithm	60
11 Synchrotron Radiation and Equilibrium Emittances	61
11.1 Local Curvature for Different Elements	61
11.1.1 Dipole	61
11.1.2 Quadrupole, Sextupole, Octupole	62
11.1.3 Thin Multipole	62
11.2 Systematic Energy Loss by Synchrotron Radiation	62
11.3 Quantum Excitation by Synchrotron Radiation in Tracking	62
11.4 Equilibrium Emittances	63
12 HARMON Module	64
12.1 General Organisation of HARMON	64
12.2 First-Order Chromaticity	64
12.3 Higher-order Chromaticities	65
12.4 Variation of the Dispersion with Energy	66
12.5 Variation of β with Energy	67
12.6 Variation of Tunes with Amplitude	67

12.7 Resonances	67
12.7.1 HRESONANCE Command	67
12.7.2 Sum Resonances	68
12.8 Third-Integer Resonances in HFUNCTION Command	68
12.9 Fourth-Order Resonances	68

List of Figures

8.1 Projection of the phase space ellipsoid onto one plane	51
9.1 Global Reference System	54
9.2 Reference System for Straight Beam Elements	56
9.3 Reference System for a Rectangular Bending Magnet	56
9.4 Reference System for a Sector Bending Magnet	57
9.5 Reference System for a Rotation Around the s-Axis	58
9.6 Reference System for a Rotation Around the y-Axis	58

List of Tables

Chapter 1. Basic Conventions and Notations

1.1 Canonical Variables

Many beam optics programs work on the set of variables

$$x, \quad x', \quad y, \quad y', \quad \Delta s, \quad \frac{\Delta p}{p_0}. \quad (1.1)$$

These variables do not form a set of canonical pairs in six-dimensional phase space. For this reason MAD uses the set of canonical variables

$$(x, p_x/p_s), \quad (y, p_y/p_s), \quad (-c\Delta t, p_t = \Delta E/p_s c). \quad (1.2)$$

In earlier versions MAD used $p_s = p_0$, the *design momentum*, to normalise the momentum components. As from Version 8.13, MAD normalises with the *average momentum* $p_s = p_0(1 + \delta_s) = m\beta_s\gamma_s$ of the particle. The quantity $\delta_s = (p_s - p_0)/p_0$ can be arbitrarily large and is imposed by the user. This makes the momentum dependence of the expanded Hamiltonian exact for particles with constant momentum p_s . For particles with variable momentum, there is an additional differential momentum error p_t , whose average over the machine will be close to zero. This should keep the errors due to the truncation of maps down to an acceptable level.

From the equation of motion in reference [16] one easily derives the relations between the slopes x', y' and the normalised canonical momenta p_x, p_y :

$$x' \approx p_x(1 + hx - p_t\beta_s), \quad y' \approx p_y(1 + hx - p_t\beta_s), \quad (1.3)$$

where h is the curvature of the reference orbit in the mid-plane. The relative energy error p_t is related to the relative momentum error $\Delta p/p_s$ by

$$p_t = (E/p_s c) - (1/\beta_s) = \Delta E/p_s c \approx \beta_s(\Delta p/p_s). \quad (1.4)$$

The special choice of variables affects those second-order terms in the transfer maps which contain p_t . For constant momentum calculations we have $p_t = 0$, and the momentum dependence is correct.

1.2 Phase Space Vector

MAD normally works on the phase space vector

$$Z = \begin{pmatrix} z_1 \\ z_2 \\ z_3 \\ z_4 \\ z_5 \\ z_6 \end{pmatrix} = \begin{pmatrix} x \\ p_x \\ y \\ p_y \\ t \\ p_t \end{pmatrix}. \quad (1.5)$$

and handles coupling effects by means of full 6×6 matrices.

1.3 Auxiliary Functions and Their Integrals

To simplify notations we introduce the abbreviations

$$\begin{aligned}
c(k, l) &= \cos(kl) = \cosh(ikl) \\
s(k, l) &= \int_0^l c(k, t) dt = \sin(kl)/k = \sinh(ikl)/ik \\
d(k, l) &= \int_0^l s(k, t) dt = (1 - c(k, l))/k^2 \\
f(k, l) &= \int_0^l d(k, t) dt = (l - s(k, l))/k^2
\end{aligned} \tag{1.6}$$

The quantities in reference [2] are related to the above quantities as follows:

$$\begin{aligned}
c_x &= c(k_x, l), & s_x &= s(k_x, l), & d_x &= hd(k_x, l), \\
c_y &= c(k_y, l), & s_y &= s(k_y, l)
\end{aligned} \tag{1.7}$$

For evaluating transfer maps we shall need the integrals:

$$\begin{aligned}
J_1 &= \int_0^s d_x(t) dt = (L - s_x)/k_x^2, \\
J_2 &= \int_0^s d_x^2(t) dt = (3L - 4s_x + s_x c_x)/(2k_x^4), \\
J_3 &= \int_0^s d_x^3(t) dt = (15L - 22s_x + 9s_x c_x - 2s_x c_x^2)/(6k_x^6), \\
J_c &= (c(2k_y, s) - c(k_x, s))(k_x^2 - 4k_y^2), \\
J_s &= \int_0^s J_c(t) dt = (s(2k_y, s) - s(k_x, s))(k_x^2 - 4k_y^2), \\
J_d &= \int_0^s J_s(t) dt = (d(2k_y, s) - d(k_x, s))(k_x^2 - 4k_y^2), \\
J_f &= \int_0^s J_d(t) dt = (f(2k_y, s) - f(k_x, s))(k_x^2 - 4k_y^2).
\end{aligned} \tag{1.8}$$

Chapter 2. Hamiltonian Representations

MAD derives most equations of motion from a Hamiltonian. The Hamiltonian governing particle motion in magnetic elements has been given in reference [11]. Below the reader can find the forms used in MAD for different elements.

2.1 Magnetic Field and Vector Potential (Transverse Field, Curved Reference)

For all mid-plane symmetric elements MAD defines the magnetic field on the mid-plane of a sector dipole by its Taylor expansion:

$$B_x(x, 0, s) = 0, \quad B_y(x, 0, s) = B_0 + B_1 \frac{x}{1!} + B_2 \frac{x^2}{2!} + B_3 \frac{x^3}{3!} + \dots \quad B_s(x, 0, s) = 0. \quad (2.1)$$

For positive x a positive field coefficient gives a contribution to the field in positive y -direction. The vector potential has a longitudinal component A_s depending on x, y only. Expanded to order four it takes the form

$$\begin{aligned} A_x(x, y, s) &= 0, \\ A_y(x, y, s) &= 0, \\ A_s(x, y, s) &= -B_0 \left(x - \frac{hx^2}{2(1+hx)} \right) - B_1 \left(\frac{1}{2}(x^2 - y^2) - \frac{h}{6}x^3 + \frac{h^2}{24}(4x^4 - y^4) + \dots \right) \\ &\quad - B_2 \left(\frac{1}{6}(x^3 - 3xy^2) - \frac{h}{24}(x^4 - y^4) + \dots \right) - B_3 \left(\frac{1}{24}(x^4 - 6x^2y^2 + y^4) + \dots \right) + \dots \end{aligned} \quad (2.2)$$

where h is the curvature of the reference orbit. Taking the curl of A_s in curvilinear coordinates the field components are to order three

$$\begin{aligned} B_x(x, y, s) &= +B_1 \left(y + \frac{h^2}{6}y^3 + \dots \right) + B_2 \left(xy - \frac{h^3}{6}y^3 + \dots \right) \\ &\quad + B_3 \left(\frac{1}{6}(3x^2y - y^3) + \dots \right) + \dots \\ B_y(x, y, s) &= +B_0 + B_1 \left(x - \frac{h}{2}y^2 + \frac{h^2}{2}xy^2 + \dots \right) + B_2 \left(\frac{1}{2}(x^2 - y^2) - \frac{h}{2}xy^2 + \dots \right) \\ &\quad + B_3 \left(\frac{1}{6}(x^3 - 3xy^2) + \dots \right) + \dots \\ B_s(x, y, s) &= 0. \end{aligned} \quad (2.3)$$

2.2 Magnetic Field and Vector Potential (Multipole)

For zero curvature ($h = 0$) the field coefficients may be complex. The field expansion then takes the form of a complex Taylor series:

$$B_y(x, y, s) + iB_x(x, y, s) = \sum_{k=0}^{\infty} C_k \frac{(x + iy)^k}{k!}, \quad B_s(x, y, s) = 0. \quad (2.4)$$

The vector potential can still be written with a longitudinal component A_s only:

$$A_x(x, y, s) = 0, \quad A_y(x, y, s) = 0, \quad A_s(x, y, s) = \Re \left(\sum_{k=0}^{\infty} C_k \frac{(x + iy)^{k+1}}{(k+1)!} \right). \quad (2.5)$$

2.3 Magnetic Field and Vector Potential (Solenoid Fields)

The magnetic field in a solenoid has the constant value

$$B_x(x, y, s) = 0, \quad B_y(x, y, s) = 0, \quad B_s(x, y, s) = B_0. \quad (2.6)$$

The vector potential requires two transverse components:

$$A_x(x, y, s) = -\frac{1}{2}B_0y, \quad A_y(x, y, s) = +\frac{1}{2}B_0x, \quad A_s(x, y, s) = 0. \quad (2.7)$$

2.4 Electric Field for an RF Cavity

The voltage in a thin cavity is

$$V = \hat{V} \sin(\phi_s - 2\pi f_{RF}t), \quad (2.8)$$

where \hat{V} is the peak RF voltage, ϕ_s is the RF phase relative to a time reference to be defined below, and f_{RF} is the RF frequency. The field can be derived from a vector potential

$$A_x(x, y, s) = 0, \quad A_y(x, y, s) = 0, \quad A_s(x, y, s) = c\hat{V} \sin(\phi_s - 2\pi f_{RF}t)/(2\pi f_{RF}). \quad (2.9)$$

2.5 Electric Field for an Electrostatic Separator

The vertical electrostatic field in a separator has the constant value

$$E_x(x, y, s) = 0, \quad E_y(x, y, s) = E_0, \quad E_s(x, y, s) = 0. \quad (2.10)$$

The scalar potential depends on y only:

$$\phi(x, y) = -E_0y. \quad (2.11)$$

2.6 General Form for the Hamiltonian

The general Hamiltonian in a curved reference system with the curvature h

$$H = -(1 + hx) \left(qA_s + \sqrt{\frac{1}{c^2}(E - q\phi)^2 - (mc)^2 - (p_x - qA_x)^2 - (p_y - qA_y)^2} \right), \quad (2.12)$$

is expressed using the arc length s as the independent variable. The particle charge is q and the canonical pairs of variables are

$$(x, p_x), \quad (y, p_y), \quad (E, -t). \quad (2.13)$$

The Hamiltonian is normalised in MAD by the following transformations:

$$H_1 = \frac{H}{p_s}, \quad (x_1 = x, p_{x1} = \frac{p_x}{p_s}), \quad (y_1 = y, p_{y1} = \frac{p_y}{p_s}), \quad (E_1 = \frac{E}{p_s c}, t_1 = ct), \quad (2.14)$$

giving

$$H_1 = -(1 + hx_1) \left(\frac{qA_s}{p_s} + \sqrt{\left(E_1 - \frac{q\phi}{p_s}\right)^2 - \frac{1}{\beta_s^2 \gamma_s^2} - \left(p_{x1} - \frac{qA_x}{p_s}\right)^2 - \left(p_{y1} - \frac{qA_y}{p_s}\right)^2} \right). \quad (2.15)$$

In the unperturbed machine, and ignoring any momentum change, a reference particle with constant momentum p_s would travel with a constant velocity $v_s = \beta_s c = p_s/m$ on an orbit of the length

$C_s = C(1 + \eta\delta_s)$, where C is the machine circumference and $\eta = \alpha - 1/\gamma_s^2$ is the momentum compaction factor. Hence it would take the time $T_s = C_s/v_s$ to complete one revolution.

The two variables t_1 and E_s can take on large values. To make a perturbation approach feasible, the two variables must be replaced by their deviations from a fixed reference. To this effect MAD introduces a time reference frame such that $\partial t_{\text{ref}}/\partial s = -T_s/C$. The generating function

$$F = x_1 p_{x2} + y_1 p_{y2} - \left(t_1 + \frac{1 + \eta\delta_s}{\beta_s} s \right) \left(p_t + \frac{1}{\beta_s} \right). \quad (2.16)$$

generates a canonical transformation with the following properties:

- The transverse variables are unchanged.
- For a general particle the time difference relative to the reference frame is

$$t_2 = t_1 + \frac{1 + \eta\delta_s}{\beta_s} s. \quad (2.17)$$

- The relative energy deviation is defined as

$$p_t = E_1 - E_{s1} = \frac{E}{p_s c} - \frac{1}{\beta_s}. \quad (2.18)$$

- The closed orbit has $t = 0$ before and after one turn, i. e. it also closes in the longitudinal plane. The average momentum on the closed orbit is approximately p_s .

This canonical transformation generates the new Hamiltonian

$$\begin{aligned} H_2 &= -\frac{\partial F}{\partial s} - (1 + hx_2) \frac{qA_s}{p_s} \\ &\quad - (1 + hx_2) \sqrt{\left(p_t - \frac{q\phi}{p_s} + \frac{1}{\beta_s} \right)^2 - \frac{1}{\beta_s^2 \gamma_s^2} - \left(p_{x2} - \frac{qA_x}{p_s} \right)^2 - \left(p_{y2} - \frac{qA_y}{p_s} \right)^2} \\ &= + \frac{1 + \eta\delta_s}{\beta_s} \left(p_t + \frac{1}{\beta_s} \right) - (1 + hx_2) \frac{qA_s}{p_s} \\ &\quad - (1 + hx_2) \sqrt{\left(1 + p_t - \frac{q\phi}{p_s} \right)^2 - \left(p_x - \frac{qA_x}{p_s} \right)^2 - \left(p_y - \frac{qA_y}{p_s} \right)^2 - \frac{1}{\beta_s^2 \gamma_s^2} \left(p_t - \frac{q\phi}{p_s} \right)^2}. \end{aligned} \quad (2.19)$$

In the latter form the Hamiltonian can easily be expanded as a Taylor series.

Chapter 3. Lie Algebraic Maps

3.1 Definitions

Let the functions $f(p, q)$ and $g(p, q)$ be differentiable functions of the canonical variables p and q . The Poisson bracket of f and g is defined as

$$[f, g] = \sum_{k=1}^3 \left(\frac{\partial f}{\partial q_k} \frac{\partial g}{\partial p_k} - \frac{\partial f}{\partial p_k} \frac{\partial g}{\partial q_k} \right). \quad (3.1)$$

The Lie operator associated with f is defined as the Poisson bracket

$$:f:g = [f, g], \quad (3.2)$$

Iterated Lie operators are defined recursively:

$$:f:^n g = [f, :f:^{n-1} g] \quad (3.3)$$

and we also use the abbreviations for iterated Lie operators

$$[f, g, h] = [f, [g, h]], \quad [f, g, h, i] = [f, [g, [h, i]]], \quad \text{etc.} \quad (3.4)$$

The Lie transformation associated with f is defined as the exponential

$$e^{:f:} g = \sum_{k=0}^{\infty} \frac{:f:^k}{k!} g. \quad (3.5)$$

An arbitrary Lie transformation acting on the components of the phase space vector Z always represents a canonical transformation, or in other terms, a symplectic map. In MAD, like in the program MARYLIE, a Lie algebraic map is represented as the composition of Lie transformations

$$z_j^{(2)} = e^{:f_1:} e^{:f_2:} e^{:f_3:} e^{:f_4:} \dots Z_j^{(1)}, \quad \text{for } j = 1 \dots 6. \quad (3.6)$$

where each f_k is a homogeneous polynomials of order k . The polynomial f_2 generates the ordinary transfer matrix. It is normally not stored, but replaced by that matrix. For details refer to [10, 11, 14].

Maps for various elements have been derived in [10, 16]. Note that the signs of energy and time are inverted in MAD with respect to [10] and to MARYLIE. For most elements MAD carries terms up to order four in the Hamiltonian.

3.2 Tilted Elements

The effect of the TILT parameter on an element is that the reference system is rotated by the angle $\psi = TILT$ at element entrance, and by $-\psi$ at element exit. Such a rotation \mathcal{R} has been described in Section 5.12. The transfer map \mathcal{F} for the element must be transformed to

$$\overline{\mathcal{F}} = \mathcal{R} \mathcal{F} \mathcal{R}^{-1}. \quad (3.7)$$

3.3 Map Composition

Let us assume that the two maps $\mathcal{F} = \{F, f_i\}$ and $\mathcal{G} = \{G, g_i\}$ occur in this order in a beam line. The problem is to build their composition as follows:

$$e^{:f_1:} e^{:f_2:} e^{:f_3:} e^{:f_4:} e^{:f_5:} e^{:f_6:} \dots e^{:g_1:} e^{:g_2:} e^{:g_3:} e^{:g_4:} e^{:g_5:} e^{:g_6:} \dots \approx e^{:h_1:} e^{:h_2:} e^{:h_3:} e^{:h_4:} e^{:h_5:} e^{:h_6:} \dots = \mathcal{H} = \{H, h_i\} \quad (3.8)$$

with truncation at a predefined order. Formulas valid up to order 6 have been given in Appendix B of [13]. These formulas have first been implemented in MARYLIE 5.1 and have been copied and modified for use in MAD. The formulas are listed here for reference; for the theory refer to [13].

Using the exchange formula

$$e^{f \cdot} e^{g \cdot} = e^{g \cdot} e^{\exp \cdot - g \cdot f \cdot} \quad (3.9)$$

composition is done in three steps. First consider the problem of moving the first-order term g_1 to the left:

$$e^{f_1 \cdot} e^{f_2 \cdot} e^{f_3 \cdot} e^{f_4 \cdot} e^{f_5 \cdot} e^{f_6 \cdot} e^{g_1 \cdot} e^{g_2 \cdot} e^{g_3 \cdot} e^{g_4 \cdot} e^{g_5 \cdot} e^{g_6 \cdot} = e^{h_1 \cdot} e^{f_2 \cdot} e^{t_2 \cdot} e^{t_3 \cdot} e^{t_4 \cdot} e^{t_5 \cdot} e^{t_6 \cdot} e^{g_2 \cdot} e^{g_3 \cdot} e^{g_4 \cdot} e^{g_5 \cdot} e^{g_6 \cdot} \quad (3.10)$$

To move g_1 successively over the polynomials f_i we define:

$$j_m^{(n)} = \frac{1}{(n-m)!} : -g_1 :^{(n-m)} f_n, \quad m = 0, 1, \dots, n, \quad n = 6, 5, 4, 3. \quad (3.11)$$

and then we regroup the various Lie transformations arising:

$$\begin{aligned} k_1^{(3)} &= j_1^{(3)} + \frac{1}{2} [j_2^{(3)}, j_1^{(3)}] - \frac{1}{6} [j_1^{(3)}, j_3^{(3)}, j_1^{(3)}] + \frac{1}{6} [j_2^{(3)}, j_2^{(3)}, j_1^{(3)}] \\ &\quad - \frac{1}{8} [j_1^{(3)}, j_3^{(3)}, j_2^{(3)}, j_1^{(3)}] - \frac{1}{24} [j_2^{(3)}, j_1^{(3)}, j_3^{(3)}, j_1^{(3)}] + \frac{1}{24} [j_2^{(3)}, j_2^{(3)}, j_2^{(3)}, j_1^{(3)}] \\ k_2^{(3)} &= j_2^{(3)} + \frac{1}{2} [j_3^{(3)}, j_1^{(3)}] - \frac{1}{12} [j_2^{(3)}, j_3^{(3)}, j_1^{(3)}] + \frac{1}{6} [j_3^{(3)}, j_2^{(3)}, j_1^{(3)}] \\ &\quad - \frac{1}{24} [j_2^{(3)}, j_3^{(3)}, j_2^{(3)}, j_1^{(3)}] - \frac{1}{24} [j_3^{(3)}, j_1^{(3)}, j_3^{(3)}, j_1^{(3)}] + \frac{1}{24} [j_3^{(3)}, j_2^{(3)}, j_2^{(3)}, j_1^{(3)}] \\ k_3^{(3)} &= j_3^{(3)} + \frac{1}{2} [j_3^{(3)}, j_2^{(3)}] - \frac{1}{6} [j_2^{(3)}, j_3^{(3)}, j_2^{(3)}] + \frac{1}{6} [j_3^{(3)}, j_3^{(3)}, j_1^{(3)}] + \frac{1}{24} [j_2^{(3)}, j_2^{(3)}, j_3^{(3)}, j_2^{(3)}] \\ &\quad - \frac{1}{8} [j_2^{(3)}, j_3^{(3)}, j_3^{(3)}, j_1^{(3)}] + \frac{1}{24} [j_3^{(3)}, j_2^{(3)}, j_3^{(3)}, j_1^{(3)}] + \frac{1}{24} [j_3^{(3)}, j_3^{(3)}, j_2^{(3)}, j_1^{(3)}] \\ k_4^{(3)} &= -\frac{1}{12} [j_3^{(3)}, j_3^{(3)}, j_2^{(3)}] + \frac{1}{24} [j_3^{(3)}, j_2^{(3)}, j_3^{(3)}, j_2^{(3)}] - \frac{1}{24} [j_3^{(3)}, j_3^{(3)}, j_3^{(3)}, j_1^{(3)}] \\ k_5^{(3)} &= \frac{1}{24} [j_3^{(3)}, j_3^{(3)}, j_3^{(3)}, j_2^{(3)}] \end{aligned} \quad (3.12)$$

$$\begin{aligned} k_1^{(4)} &= j_1^{(4)} + \frac{1}{2} [j_2^{(4)}, j_1^{(4)}] \\ k_2^{(4)} &= j_2^{(4)} + \frac{1}{2} [j_3^{(4)}, j_1^{(4)}] \\ k_3^{(4)} &= j_3^{(4)} + \frac{1}{2} [j_3^{(4)}, j_2^{(4)}] + \frac{1}{2} [j_4^{(4)}, j_1^{(4)}] \\ k_4^{(4)} &= j_4^{(4)} + \frac{1}{2} [j_4^{(4)}, j_2^{(4)}] \\ k_5^{(4)} &= \frac{1}{2} [j_4^{(4)}, j_3^{(4)}] \end{aligned} \quad (3.13)$$

$$\begin{aligned} k_m^{(5)} &= j_m^{(5)} \\ k_m^{(6)} &= j_m^{(6)} \end{aligned} \quad (3.14)$$

and get the final result:

$$\begin{aligned}
h_1 &= f_1 + e^{:f_2:} (g_1 + k_1^{(3)} + k_1^{(4)} + k_1^{(5)} + k_1^{(6)}) \\
t_2 &= k_2^{(3)} + k_2^{(4)} + k_2^{(5)} + k_2^{(6)} + \frac{1}{2}[k_2^{(3)}, k_2^{(4)} + k_2^{(5)}] + \frac{1}{12}[k_2^{(3)}, k_2^{(3)}, k_2^{(4)}] \\
t_3 &= k_3^{(3)} + k_3^{(4)} + k_3^{(5)} + k_3^{(6)} + [k_3^{(3)}, k_2^{(4)} + k_2^{(5)}] \\
t_4 &= k_4^{(3)} + k_4^{(4)} + k_4^{(5)} + k_4^{(6)} + \frac{1}{2}[k_3^{(3)}, k_3^{(4)} + k_3^{(5)}] \\
t_5 &= k_5^{(3)} + k_5^{(4)} + k_5^{(5)} + k_5^{(6)} - \frac{1}{6}[k_3^{(3)}, k_3^{(3)}, k_3^{(4)}], \\
t_6 &= k_6^{(6)}
\end{aligned} \tag{3.15}$$

The second step converts t_2 to a matrix and combines it with the matrices F and G . We note that

$$t_2 = \frac{1}{2}Z^t W Z, \quad W \text{ symmetric}, \tag{3.16}$$

is of small order 3, and that

$$:t_2:Z = JWZ. \tag{3.17}$$

Hence, using the approximation $\tanh(x) \approx x - x^3/6$, we define a symplectic matrix T by

$$\begin{aligned}
\exp(:t_2:) &= \exp(JW)Z = (I + \tanh(JW/2))(I - \tanh(JW/2))^{-1} \\
&\approx TZ = (I + (W/2 - W^3/24))(I - (W/2 - W^3/24))^{-1}Z.
\end{aligned} \tag{3.18}$$

In the third step the remaining problem is to convert

$$e^{:h_1:} e^{:h_2:} e^{:u_3:} e^{:u_4:} e^{:u_5:} e^{:u_6:} e^{:g_3:} e^{:g_4:} e^{:g_5:} e^{:g_6:} = e^{:h_1:} e^{:h_2:} e^{:h_3:} e^{:h_4:} e^{:h_5:} e^{:h_6:}. \tag{3.19}$$

Due to the exchange formula the t polynomials are converted to

$$u_k = t_k(-g_2:Z), \quad k = 3, 4, 5, 6. \tag{3.20}$$

The solution is

$$\begin{aligned}
h_3 &= f_3 + u_3 \\
h_4 &= f_4 + u_4 + \frac{1}{2}[f_3, u_3] \\
h_5 &= f_5 + u_5 - [u_3, f_4] - \frac{1}{6}:f_3:^2 u_3 + \frac{1}{3}:u_3:^2 f_3 \\
h_6 &= f_6 + u_6 - [u_3, f_5] + \frac{1}{2}:u_3:^2 f_4 + \frac{1}{2}[f_4, u_4] - \frac{1}{4}[f_4, f_3, u_3] \\
&\quad - \frac{1}{4}[u_4, f_3, u_3] + \frac{1}{12}:f_3:^3 u_3 - \frac{1}{8}:u_3:^3 f_3 + \frac{1}{8}[f_3, u_3, f_3, u_3].
\end{aligned} \tag{3.21}$$

3.4 Reverse Factorisation

MAD requires only the case where f_1 vanishes and the order is four:

$$\mathcal{F} = e^{:f_2:} e^{:f_3:} e^{:f_4:} = e^{:g_4:} e^{:g_3:} e^{:g_2:}, \tag{3.22}$$

where the second-order polynomials are represented by the corresponding matrices. The result is:

$$G = F, \quad g_3(Z) = f_3(FZ), \quad g_4(Z) = g_4(FZ). \tag{3.23}$$

3.5 Map Inversion

MAD requires only the case where f_1 vanishes and the order is four. The inverse of a Lie algebraic map \mathcal{F} is found in two steps. First the factorisation is reversed as shown in the previous subsection. The second step uses the formula $(e^{:\mathcal{F}:})^{-1} = e^{:-\mathcal{F}:}$ to find the inverse map:

$$\mathcal{F}^{-1} = e^{:-g_2:} e^{:-g_3:} e^{:-g_4:} \quad (3.24)$$

The matrix of the inverse map is thus F^{-1} , and the polynomials are the negative of the ones found for the reverse factorisation.

3.6 Reflection of a Lie Algebraic Map

Reflection of a transfer map is the transformation needed to simulate traversal through a beam line in reverse direction. Note that this also reverses asymmetric elements. This transformation is equivalent to inversion of the transfer map, followed by a change of sign for the variables p_x, p_y and t .

3.7 Fixed Points

Starting with an arbitrary initial approximation Z_0 , an iterative procedure can be defined as follows:

1. Define a first-order polynomial g_1 such that

$$Z_0 = [g_1, Z]. \quad (3.25)$$

This polynomial represents a map which sends the origin to the initial approximation.

2. Compose the map \mathcal{F} with the “map” g_1 to get h_1 according to the composition algorithm. h_1 then maps the origin onto the orbit at the end of the system. The matrix H is the Jacobian of this map and can be used to find a new approximation:

$$Z_1 = Z_0 - H^{-1}(:h_1:Z - Z_0). \quad (3.26)$$

3. Repeat, until convergence is achieved.

Note that MAD now finds the fixed point by tracking through each element individually, since the above procedure may not give good results when high-order terms resulting from concatenation become important.

3.8 Tracking

When one of the options

METHOD=LIE3|LIE4

occurs on a RUN command, MAD uses the Lie-algebraic tracking method up to f_3 or f_4 terms, respectively. For LUMPs it always uses the order specified on their definition. Note that truncating the exponential series

$$e^{:\mathcal{F}:} Z = \sum_{k=0}^{\infty} \frac{:\mathcal{F}:^k}{k!} \quad (3.27)$$

at a finite k does not produce a symplectic map. MAD therefore tracks the linear terms using the transfer matrix. For the non-linear terms f_n it uses a generating function of the form

$$G(q_1, p_2) = q_1 p_2 + \sum_{k=3}^6 g_k(q_1, p_2). \quad (3.28)$$

This function is set up such that the resulting canonical transformation agrees to the desired order with the mapping. With the temporary values

$$\begin{aligned} t_4 &= \sum_{m=1}^3 \frac{\partial f_3}{\partial q_m} \frac{\partial f_3}{\partial p_m}, \\ t_5 &= \sum_{m=1}^3 \frac{\partial f_3}{\partial q_m} \frac{\partial t_4}{\partial p_m} + \sum_{l=1}^3 \sum_{m=1}^3 \frac{\partial^2 f_3}{\partial q_l \partial q_m} \frac{\partial f_3}{\partial p_l} \frac{\partial f_3}{\partial p_m}, \\ t_6 &= \sum_{m=1}^3 \frac{\partial f_4}{\partial q_m} \frac{\partial t_4}{\partial p_m} + \sum_{l=1}^3 \sum_{m=1}^3 \frac{\partial^2 f_4}{\partial q_l \partial q_m} \frac{\partial f_3}{\partial p_l} \frac{\partial f_3}{\partial p_m}, \\ u_6 &= \sum_{m=1}^3 \frac{\partial f_3}{\partial q_m} \frac{\partial t_5}{\partial p_m} + 3 \sum_{l=1}^3 \sum_{m=1}^3 \frac{\partial^2 f_3}{\partial q_l \partial q_m} \frac{\partial f_3}{\partial p_l} \frac{\partial t_4}{\partial p_m} + \sum_{k=1}^3 \sum_{l=1}^3 \sum_{m=1}^3 \frac{\partial^3 f_3}{\partial q_k \partial q_l \partial q_m} \frac{\partial f_3}{\partial p_k} \frac{\partial f_3}{\partial p_l} \frac{\partial f_3}{\partial p_m}, \end{aligned} \quad (3.29)$$

it can be written as

$$\begin{aligned} g_3 &= f_3, \\ g_4 &= f_4 + \frac{1}{2} t_4, \\ g_5 &= f_5 - \frac{1}{6} t_5 + \frac{1}{2} \sum_{m=1}^3 \frac{\partial f_4}{\partial q_k} \frac{\partial f_3}{\partial p_k}, \\ g_6 &= f_6 + \frac{1}{24} t_6 - \frac{1}{2} u_6 + \sum_{m=1}^3 \frac{\partial f_5}{\partial q_k} \frac{\partial f_3}{\partial p_k} + \frac{1}{2} \sum_{m=1}^3 \frac{\partial f_4}{\partial q_k} \frac{\partial f_4}{\partial p_k}. \end{aligned} \quad (3.30)$$

The generating function is truncated at the order of the Lie transformation given.

Chapter 4. TRANSPORT Maps

4.1 Definition

A TRANSPORT map (see [2, 3]) is the Taylor series for the exact transfer map, truncated at order two:

$$z_j^{(2)} = \Delta z_j + \sum_{k=1}^6 R_{jk} z_k^{(1)} + \sum_{k=1}^6 \sum_{l=1}^6 T_{jkl} z_k^{(1)} z_l^{(1)}, \quad \text{for } j = 1 \dots 6. \quad (4.1)$$

The T_{jkl} array is symmetric with respect to its second and third index. Both indices run from 1 to 6, and by convention the off-diagonal terms in MAD are half those used in TRANSPORT. Below we list only non-zero elements for $k \leq l$ to save space.

Due to truncation a TRANSPORT map is symplectic only in exceptional cases. TRANSPORT maps have been derived for many elements in [2]. However, due to different variables, the second-order terms are changed as explained in [16]. Reference [16] also gives the formula to derive a TRANSPORT map from a Lie-algebraic map (see Chapter 3):

$$\begin{aligned} T_{1kl} &= -\frac{1}{2} \sum_{m=1}^6 \sum_{n=1}^6 F_{2mn} R_{mk} R_{nl}, & T_{2kl} &= +\frac{1}{2} \sum_{m=1}^6 \sum_{n=1}^6 F_{1mn} R_{mk} R_{nl}, \\ T_{3kl} &= -\frac{1}{2} \sum_{m=1}^6 \sum_{n=1}^6 F_{4mn} R_{mk} R_{nl}, & T_{4kl} &= +\frac{1}{2} \sum_{m=1}^6 \sum_{n=1}^6 F_{3mn} R_{mk} R_{nl}, \\ T_{5kl} &= -\frac{1}{2} \sum_{m=1}^6 \sum_{n=1}^6 F_{6mn} R_{mk} R_{nl}, & T_{6kl} &= +\frac{1}{2} \sum_{m=1}^6 \sum_{n=1}^6 F_{5mn} R_{mk} R_{nl}. \end{aligned} \quad (4.2)$$

4.2 Tilted Elements

The effect of the TILT parameter on an element is that the reference system is rotated by the angle $\psi = TILT$ at element entrance, and by $-\psi$ at element exit. Such a rotation \mathcal{R} has been described in Section 5.12. The transfer map \mathcal{F} for the element must be transformed to

$$\overline{\mathcal{F}} = \mathcal{R} \mathcal{F} \mathcal{R}^{-1}. \quad (4.3)$$

4.3 Map Composition

Assume that the two maps $\mathcal{A} = \{R^a, T^a\}$ and $\mathcal{B} = \{R^b, T^b\}$ occur in this order in the beam. The transfer matrix for the composition $\mathcal{C} = \mathcal{B}\mathcal{A} = \{R^c, T^c\}$ is

$$R^c = R^b R^a \quad (4.4)$$

By substitution of \mathcal{A} in \mathcal{B} and truncation at second order one finds the second-order terms of \mathcal{C} :

$$T_{ijk}^c = \sum_{l=1}^6 R_{il}^b T_{ljk}^a + \sum_{l=1}^6 \sum_{m=1}^6 T_{ilm}^b R_{lj}^a R_{mk}^a. \quad (4.5)$$

4.4 Map Inversion

To first order a TRANSPORT map is inverted by inverting its transfer matrix. Since the matrix is symplectic its inverse can be found by the formula

$$R^{-1} = -SR^T S, \quad (4.6)$$

where the superscript T denotes the transpose and the matrix S is the symplectic unit matrix

$$S = \begin{pmatrix} 0 & 1 & 0 & 0 & 0 & 0 \\ -1 & 0 & 0 & 0 & 0 & 0 \\ 0 & 0 & 0 & 1 & 0 & 0 \\ 0 & 0 & -1 & 0 & 0 & 0 \\ 0 & 0 & 0 & 0 & 0 & 1 \\ 0 & 0 & 0 & 0 & -1 & 0 \end{pmatrix} \quad (4.7)$$

The composition of a map and its inverse must reproduce the identity map. The equations for this condition may be solved and give:

$$T_{ijk}^{-1} = - \sum_{l=1}^6 \sum_{m=1}^6 \sum_{n=1}^6 R_{il}^{-1} T_{lmn} R_{mj}^{-1} R_{nk}^{-1}. \quad (4.8)$$

4.5 Map Reflection

The reflection $\overline{\mathcal{T}} = \{\overline{R}, \overline{T}\}$ of a transfer map $\mathcal{T} = \{R, T\}$ represents the traversal of a beam line in inverse order. Note that this also reverses asymmetric elements like RF cavities. Care must be taken if such elements occur, since this may not be the desired effect.

To compute the reflection, first the formulas of the previous section are applied. The signs of all coefficients having an odd number of occurrences of 2, 4, or 5 in their indices must be inverted. The result is:

$$\overline{R}_{ij} = s_i s_j (R^{-1})_{ij}, \quad \overline{T}_{ijk} = s_i s_j s_k (T^{-1})_{ijk}, \quad (4.9)$$

where $s_1 = s_3 = s_6 = 1, s_2 = s_4 = s_5 = -1$.

4.6 Closed Orbit

The closed orbit is the first-order fixed point of the transfer map for one turn around the machine. MAD searches for the closed orbit along the following steps:

1. Set the initial guess to zero for the transverse phase space coordinates and to the specified energy error for $\Delta E/p_0 c$:

$$Z_0 = \begin{pmatrix} x_0 \\ p_x 0 \\ y_0 \\ p_y 0 \\ ct_0 \\ \delta_0 \end{pmatrix} = \begin{pmatrix} 0 \\ 0 \\ 0 \\ 0 \\ 0 \\ \Delta p/p_0 c \end{pmatrix}. \quad (4.10)$$

2. Find the orbit Z_1 after one turn and the Jacobian R of the map for one turn.
3. Use the Jacobian to find a correction to the initial conditions. The transverse coordinates must close.

For dynamic maps (including RF cavities and synchrotron radiation) the flight time is constrained such as to give the specified energy error on average. This leads to the conditions

$$\begin{aligned} x_1 &= x_0 & p_{x1} &= p_{x0} \\ y_1 &= y_0 & p_{y1} &= p_{y0} \\ c \cdot t_1 &= c \cdot t_0 + \frac{C \alpha \Delta p}{\beta_s p_0 c} & \delta_1 &= \delta_0 \end{aligned} \quad (4.11)$$

where C is the machine circumference, α is the momentum compaction, and β_s is the ratio of the particle velocity to the velocity of light. The equation for one iteration affects all three degrees of freedom and reads:

$$Z_1 + R_j \Delta Z = Z_0 + \Delta Z \quad \Rightarrow \quad \Delta Z = -(R_j - I)^{-1}(Z_1 - Z_0). \quad (4.12)$$

Note that when searching for the closed orbit in an OPTICS command the flight time difference is always zero. Thus only $\delta = 0$ is permitted.

For static maps (constant energy around the ring) there is no condition on the flight time difference, and the energy error is constant. Thus the equations affect the transverse degrees of freedom only.

4. Iterate steps 2 and 3 until convergence is achieved.

When the machine is strongly non-linear, the convergence of this algorithm may be bad. In this case MAD first attempts to find the closed orbit with reduced sextupole strengths. This may still fail if the RF phase lags are set such that the zero orbit is close to the unstable fixed point.

4.7 Making First-Order Matrix Symplectic

The Jacobian matrix of a TRANSPORT map is only approximately symplectic, whereas the theory requires an exactly symplectic matrix. An elegant method to make a matrix symplectic has been given in [14]. A symplectic matrix F can be written as $\exp(SM)$ with a symmetric M . We may rewrite this as

$$F = (I + \tanh(SM/2))(I - \tanh(SM/2))^{-1} = (I + W)(I - W)^{-1}, \quad (4.13)$$

where W is symmetric if and only if F is symplectic. Given a matrix F which is approximately symplectic, we define the matrix

$$V = S(I - F)(I + F)^{-1}. \quad (4.14)$$

which is approximately symmetric. Using the exactly symmetric matrix $W = (V + V^T)/2$ we generate an exactly symplectic matrix from the previous equation.

4.8 Tracking

Tracking by the TRANSPORT method is straightforward. It uses the definition of the TRANSPORT map:

$$z_j^{(2)} = \Delta z_j + \sum_{k=1}^6 R_{jk} z_k^{(1)} + \sum_{k=1}^6 \sum_{l=1}^6 T_{jkl} z_k^{(1)} z_l^{(1)}, \quad \text{for } j = 1 \dots 6. \quad (4.15)$$

This method is used by default, or if the option

METHOD=TRANSPORT

is seen on a RUN command. For magnets defined as thin multipoles the thin lens map is used. Note that the TRANSPORT map tracking is not symplectic; for long-term tracking it most certainly causes spurious blow up or shrinking. For long-term tracking it is recommended to use the Lie-algebraic methods, or if CPU time is at premium, thin lens tracking.

Chapter 5. Maps for Physical Elements

5.1 Marker

The MARKER element has no transfer map. It is ignored during optical calculations.

5.2 Drift Space and Similar Objects

There are seven drift-like elements in MAD:

- DRIFT, Ordinary drift space,
- ECOLLIMATOR, Elliptic collimator,
- RCOLLIMATOR, Rectangular collimator,
- INSTRUMENT, Beam instrumentation,
- MONITOR, Monitor for both planes,
- HMONITOR, Monitor for horizontal plane,
- VMONITOR, Monitor for vertical plane.

All these element types act as field-free regions. A beam position monitor also stores the position of the beam in its centre, and a collimator limits the aperture during tracking.

5.2.1 Hamiltonian for a Drift Space

The drift space has no field. Its exact Hamiltonian is

$$H = -\sqrt{\left(1 + \frac{p_t}{\beta_s}\right) - \left(p_x^2 + p_y^2 + \frac{p_t^2}{\beta_s^2 \gamma_s^2}\right)} + \frac{\eta \delta_s}{\beta_s} p_t. \quad (5.1)$$

5.2.2 Exact Solution for Equations of Motion

The exact solution for the equations of motion is

$$\begin{aligned} x_2 &= x_1 + p_{x1} \Big/ \sqrt{\left(1 + \frac{p_t}{\beta_s}\right) - \left(p_x^2 + p_y^2 + \frac{p_t^2}{\beta_s^2 \gamma_s^2}\right)}, & p_{x2} &= p_{x1}, \\ y_2 &= y_1 + p_{y1} \Big/ \sqrt{\left(1 + \frac{p_t}{\beta_s}\right) - \left(p_x^2 + p_y^2 + \frac{p_t^2}{\beta_s^2 \gamma_s^2}\right)}, & p_{y2} &= p_{y1}, \\ t_2 &= t_1 + \frac{L \eta \delta_s}{\beta_s} - \left(1 + \frac{p_{t1}}{\beta_s}\right) \Big/ \sqrt{\left(1 + \frac{p_t}{\beta_s}\right) - \left(p_x^2 + p_y^2 + \frac{p_t^2}{\beta_s^2 \gamma_s^2}\right)}, & p_{t2} &= p_{t1}. \end{aligned} \quad (5.2)$$

This map is not used in MAD.

5.2.3 Lie-Algebraic Map for a Drift Space

The Lie-algebraic map is found by the techniques of reference [10]. The linear part is represented by the transfer matrix

$$R = \begin{pmatrix} 1 & L & 0 & 0 & 0 & 0 \\ 0 & 1 & 0 & 0 & 0 & 0 \\ 0 & 0 & 1 & L & 0 & 0 \\ 0 & 0 & 0 & 1 & 0 & 0 \\ 0 & 0 & 0 & 0 & 1 & \frac{L}{\beta_s^2 \gamma_s^2} \\ 0 & 0 & 0 & 0 & 0 & 1 \end{pmatrix}. \quad (5.3)$$

and the generators are

$$\begin{aligned} f_1 &= -\frac{\eta \delta_s}{\beta_s} p_t, \\ f_3 &= \frac{L}{2\beta_s} \left(p_x^2 + p_y^2 + \frac{p_t^2}{\beta_s^2 \gamma_s^2} \right) p_t, \\ f_4 &= -\frac{L}{2\beta_s^2} \left(p_x^2 + p_y^2 + \frac{p_t^2}{\beta_s^2 \gamma_s^2} \right) p_t^2 - \frac{L}{8} \left(p_x^2 + p_y^2 + \frac{p_t^2}{\beta_s^2 \gamma_s^2} \right)^2. \end{aligned} \quad (5.4)$$

5.2.4 TRANSPORT Map

The TRANSPORT map for a drift-like element can be derived by differentiation of the exact form, or from the Lie-algebraic map:

$$\begin{aligned} x_2 &= x_1 + L p_{x1} \left(1 - \frac{p_t}{\beta_s} \right), & p_{x2} &= p_{x1}, \\ y_2 &= y_1 + L p_{y1} \left(1 - \frac{p_t}{\beta_s} \right), & p_{y2} &= p_{y1}, \\ t_2 &= t_1 + \frac{L \eta \delta_s}{\beta_s} + \frac{p_{t1}}{\beta_s^2 \gamma_s^2} - \frac{L}{2\beta_s} \left(p_{x1}^2 + p_{y1}^2 + \frac{3p_{t1}^2}{\beta_s^2 \gamma_s^2} \right), & p_{t2} &= p_{t1}. \end{aligned} \quad (5.5)$$

5.3 Dipoles

Transfer maps for dipoles in MAD are composed of three maps, namely the fringing field at the magnet entrance $\mathcal{F}^{(1)}$, the body of the dipole \mathcal{B} , and the fringing field at the magnet exit $\mathcal{F}^{(2)}$:

$$\mathcal{F} = \mathcal{F}^{(1)} \mathcal{B} \mathcal{F}^{(2)}. \quad (5.6)$$

MAD presently (still) treats all dipoles as SBENDs, but for an RBEND it uses an additional pole face rotation angle equal to half the bend angle.

5.3.1 Dipole Fringing Fields

The TRANSPORT map for a fringing field has been derived in [2], and the required change of variables, together with an equivalent Lie transformation, is described in [16]. Let the pole-face rotation angles at entrance and exit be ψ_1 and ψ_2 respectively, and the curvature of the pole faces be described by the radii R_1 and R_2 . For a dipole of type RBEND half the bend angle is added to each of the ψ_i . If the fringing fields have a finite extent the vertical focussing angle is changed according to [2]:

$$\overline{\psi_i} = \psi_i - h g I_1 (1 + \sin^2 \psi_i). \quad (5.7)$$

h is the curvature of the reference orbit within the dipole, g is the *full* gap height, and I_1 is the first *fringing field integral*

$$I_1 = \int_{-\infty}^{\infty} \frac{B_y(s)(B_0 - B_y(s))}{g \cdot B_0^2} ds. \quad (5.8)$$

Lie-Algebraic Maps for Dipole Fringing Fields

For both entrance and exit the transfer matrix is

$$F^{(i)} = \begin{pmatrix} 1 & 0 & 0 & 0 & 0 & 0 \\ +h \tan \psi_i & 1 & 0 & 0 & 0 & 0 \\ 0 & 0 & 1 & 0 & 0 & 0 \\ 0 & 0 & -h \tan \overline{\psi_i} & 1 & 0 & 0 \\ 0 & 0 & 0 & 0 & 1 & 0 \\ 0 & 0 & 0 & 0 & 0 & 1 \end{pmatrix}. \quad (5.9)$$

The generator f_3 has been slightly improved with respect to reference [16]. At the magnet entrance, using the quadrupole coefficient K_1 for the magnet body, it takes the value

$$\begin{aligned} f_3^{(1)} &= \frac{1}{6} \left(\frac{h}{R_1} \sec^3 \psi_1 + 2K_1 \tan \psi_1 - 2h^2 \tan^3 \psi_1 \right) x^3 \\ &\quad - \frac{1}{2} \left(\frac{h}{R_1} \sec^3 \psi_1 + 2K_1 \tan \psi_1 - h^2 \tan \psi_1 (\sec^2 \psi_1 - \tan^2 \overline{\psi_1}) \right) xy^2 \\ &\quad + \frac{h}{2} \tan \psi_1 (x^2 p_x \tan \psi_1 - 2xyp_y \tan \overline{\psi_1}) - \frac{h}{2} p_x y^2 \sec^2 \psi_1. \end{aligned} \quad (5.10)$$

and for the exit it is

$$\begin{aligned} f_3^{(2)} &= \frac{1}{6} \left(\frac{h}{R_2} \sec^3 \psi_2 + 2K_1 \tan \psi_2 + h^2 \tan^3 \psi_2 \right) x^3 \\ &\quad - \frac{1}{2} \left(\frac{h}{R_2} \sec^3 \psi_2 + 2K_1 \tan \psi_2 - h^2 \tan \psi_2 \tan^2 \overline{\psi_2} \right) xy^2 \\ &\quad - \frac{h}{2} \tan \psi_2 (x^2 p_x \tan \psi_2 - 2xyp_y \tan \overline{\psi_2}) + \frac{h}{2} p_x y^2 \sec^2 \psi_2. \end{aligned} \quad (5.11)$$

The generator f_4 is not used by MAD.

TRANSPORT Map for Dipole Fringing Fields

For both entrance and exit the transfer matrix is

$$R = \begin{pmatrix} 1 & 0 & 0 & 0 & 0 & 0 \\ +h \tan \psi_i & 1 & 0 & 0 & 0 & 0 \\ 0 & 0 & 1 & 0 & 0 & 0 \\ 0 & 0 & -h \tan \overline{\psi_i} & 1 & 0 & 0 \\ 0 & 0 & 0 & 0 & 1 & 0 \\ 0 & 0 & 0 & 0 & 0 & 1 \end{pmatrix}. \quad (5.12)$$

The second-order terms for the entrance are

$$\begin{aligned}
T_{111} &= T_{234} = T_{414} = -\frac{h}{2} \tan^2 \psi_1, \\
T_{212} &= T_{313} = +\frac{h}{2} \tan^2 \psi_1, \\
T_{133} &= +\frac{h}{2} \sec^2 \psi_1, \\
T_{423} &= -\frac{h}{2} \sec^2 \psi_1, \\
T_{211} &= +\frac{h}{2R_1} \sec^3 \psi_1 + K_1 \tan \psi_1, \\
T_{233} &= -\frac{h}{2R_1} \sec^3 \psi_1 - K_1 \tan \psi_1 + \frac{h^2}{2} \tan \psi_1 (1 + \sec^2 \psi_1), \\
T_{413} &= -\frac{h}{2R_1} \sec^3 \psi_1 - K_1 \tan \psi_1.
\end{aligned} \tag{5.13}$$

and for the exit

$$\begin{aligned}
T_{111} &= T_{234} = T_{414} = +\frac{h}{2} \tan^2 \psi_2, \\
T_{212} &= T_{313} = -\frac{h}{2} \tan^2 \psi_2, \\
T_{133} &= -\frac{h}{2} \sec^2 \psi_2, \\
T_{423} &= +\frac{h}{2} \sec^2 \psi_2, \\
T_{211} &= +\frac{h}{2R_2} \sec^3 \psi_2 + K_1 \tan \psi_2 - \frac{h^2}{2} \tan^3 \psi_2, \\
T_{233} &= -\frac{h}{2R_2} \sec^3 \psi_2 - K_1 \tan \psi_2 - \frac{h^2}{2} \tan^3 \psi_2, \\
T_{413} &= -\frac{h}{2R_2} \sec^3 \psi_2 - K_1 \tan \psi_2 + \frac{h^2}{2} \tan \psi_2 \sec^2 \psi_2.
\end{aligned} \tag{5.14}$$

5.3.2 Body of a Sector Dipole

Hamiltonian for the Body of a Sector Dipole

Inserting the proper vector potential, the expanded Hamiltonian for a sector dipole has the terms

$$\begin{aligned}
H_1 &= (K_0 - h)x + \frac{\eta \delta_s}{\beta_s} p_t, \\
H_2 &= \frac{1}{2}(K_1 + hK_0)x^2 - \frac{1}{2}K_1 y^2 + \frac{1}{2} \left(p_x^2 + p_y^2 + \frac{p_t^2}{\beta_s^2 \gamma_s^2} \right), \\
H_3 &= \frac{1}{6}(K_2 + 2hK_1)x^3 - \frac{1}{2}(K_2 + hK_1)xy^2 + \frac{1}{2} \left(hx - \frac{p_t}{\beta_s} \right) \left(p_x^2 + p_y^2 + \frac{p_t^2}{\beta_s^2 \gamma_s^2} \right), \\
H_4 &= \frac{1}{24}(K_3 + 3hK_2)x^4 - \frac{1}{4}(K_3 + 2hK_2)x^2 y^2 + \frac{1}{24}(K_3 + hK_2 - h^2 K_1)y^4 - \\
&\quad \frac{p_t}{2\beta_s} \left(hx - \frac{p_t}{\beta_s} \right) \left(p_x^2 + p_y^2 + \frac{p_t^2}{\beta_s^2 \gamma_s^2} \right) + \frac{1}{8} \left(p_x^2 + p_y^2 + \frac{p_t^2}{\beta_s^2 \gamma_s^2} \right)^2.
\end{aligned} \tag{5.15}$$

We note the following differences with respect to reference [16]:

1. There is a term H_1 , generated by $h \neq K_0$, and by $p_s \neq p_0$.

2. The relativistic parameters $\beta_s = v/c$ and $\gamma_s = E/m$ are evaluated for the velocity and energy corresponding to p_s .
3. For the term in $x^2 y^2$ we have corrected a mis-print in the numeric factor.

Lie-Algebraic Map for a Sector Dipole

The Lie algebraic map of order three for a sector dipole has been derived in [16]. At present MAD knows only terms up to f_3 for dipoles. For notations refer to Section 1.3. The transfer matrix for the body of the dipole is

$$R = \begin{pmatrix} c_x & s_x & 0 & 0 & 0 & \frac{h}{\beta_s} d_x \\ -k_x^2 s_x & c_x & 0 & 0 & 0 & \frac{h}{\beta_s} s_x \\ 0 & 0 & c_y & s_y & 0 & 0 \\ 0 & 0 & -k_y^2 s_y & c_y & 0 & 0 \\ -\frac{h}{\beta_s} s_x - \frac{h}{\beta_s} d_x & -\frac{h}{\beta_s} d_x & 0 & 0 & 1 & \frac{L}{\beta_s^2 \gamma_s^2} - \frac{h^2}{\beta_s^2} J_1 \\ 0 & 0 & 0 & 0 & 0 & 1 \end{pmatrix} \quad (5.16)$$

The generator f_1 for the constant term and f_3 for the non-linear terms are

$$f_1 = -\frac{\eta \delta_s}{\beta_s} p_t, \quad f_3 = \frac{1}{6} \sum_{i=1}^6 \sum_{j=1}^6 \sum_{k=1}^6 F_{ijk} Z_i Z_j Z_k, \quad (5.17)$$

the latter has the coefficients

$$\begin{aligned} F_{111} &= -\frac{1}{3}(K_2 + 2hK_1)s_x(2 + c_x^2) - hk_x^4 s_x^3, \\ F_{112} &= +\frac{1}{3}(K_2 + 2hK_1)(d_x + s_x^2 c_x) - hk_x^2 s_x^2 c_x, \\ F_{116} &= -\frac{h}{6\beta_s}(K_2 + 2hK_1)(3J_1 - 3s_x d_x + 2s_x^3) + \frac{h^2}{\beta_s} k_x^2 s_x^3 + \frac{1}{2\beta_s} K_1(L - s_x c_x), \\ F_{122} &= -\frac{1}{3}(K_2 + 2hK_1)s_x^3 - hs_x c_x^2, \\ F_{126} &= +\frac{h}{6\beta_s}(K_2 + 2hK_1)d_x^2(1 + 2c_x) + \frac{h^2}{\beta_s} s_x^2 c_x + \frac{1}{2\beta_s} K_1 s_x^2, \\ F_{133} &= +2K_1 K_2(k_x^2 s_x J_d + c_x J_s) + (K_2 + hK_1)s_x, \\ F_{134} &= -K_2(k_x^2 s_x J_s + c_x J_c), \\ F_{144} &= +2K_2(k_x^2 s_x J_d + c_x J_s) - hs_x, \\ F_{166} &= -\frac{h^2}{3\beta_s^2}(K_2 + 2hK_1)(s_x d_x^2 - 2J_2) - \frac{h^3}{\beta_s^2} s_x^3 - \frac{h}{\beta_s^2} K_1(J_1 + s_x d_x) - \frac{h}{\beta_s^2 \gamma_s^2} s_x, \end{aligned} \quad (5.18)$$

$$\begin{aligned}
F_{222} &= +\frac{1}{3}(K_2 + 2hK_1)d_x^2(2 + c_x) + h(d_x + s_x^2c_x), \\
F_{226} &= -\frac{h}{3\beta_s}(K_2 + 2hK_1)(s_x d_x^2 + J_2) - \frac{h^2}{2\beta_s}(J_1 + s_x d_x(1 + 2c_x)) + \frac{1}{2\beta_s}(L + s_x c_x), \\
F_{233} &= +2K_1K_2(c_x J_d - s_x J_s) - (K_2 + hK_1)d_x, \\
F_{234} &= -K_2(c_x J_s - s_x J_c), \\
F_{244} &= 2K_2(c_x J_d - s_x J_s) + h d_x, \\
F_{266} &= +\frac{h^2}{3\beta_s^2}(K_2 + 2hK_1)d_x^3 - \frac{h^3}{\beta_s^2}s_x^2 d_x - \frac{h}{\beta_s^2}s_x^2 - \frac{h}{\beta_s^2\gamma_s^2}d_x, \\
F_{336} &= +\frac{2h}{\beta_s}K_1K_2(J_f + d_x J_s - s_x J_d) + \frac{h}{\beta_s}(K_2 + hK_1)J_1 - \frac{1}{2\beta_s}K_1(L - s_y c_y), \\
F_{346} &= -\frac{h}{\beta_s}K_2(J_d + d_x J_c - s_x J_s) - \frac{1}{2\beta_s}K_1s_y^2, \\
F_{446} &= +\frac{2h}{\beta_s}K_2(J_f + d_x J_s - s_x J_d) - \frac{h^2}{\beta_s}J_1 + \frac{1}{2\beta_s}(L + s_y c_y), \\
F_{666} &= -\frac{h^3}{\beta_s^3}(K_2 + 2hK_1)J_3 - \frac{h^4}{\beta_s^3}(s_x d_x^2 + J_2) + \frac{3h^2}{2\beta_s^3}(J_1 + s_x d_x) + \frac{3}{\beta_s^3\gamma_s^2}(L - h^2 J_1).
\end{aligned} \tag{5.19}$$

TRANSPORT Map for a Sector Dipole

The TRANSPORT map for bending magnets has been derived in [16], based on the work in [2]. For notations, refer to Chapter 1.3. The dipole changes the time reference by

$$\Delta t = \frac{L\eta\delta_x}{\beta_s}. \tag{5.20}$$

The transfer matrix for its body is

$$R = \begin{pmatrix} c_x & s_x & 0 & 0 & 0 & \frac{h}{\beta_s}d_x \\ -k_x^2 s_x & c_x & 0 & 0 & 0 & \frac{h}{\beta_s}s_x \\ 0 & 0 & c_y & s_y & 0 & 0 \\ 0 & 0 & -k_y^2 s_y & c_y & 0 & 0 \\ -\frac{h}{\beta_s}s_x & -\frac{h}{\beta_s}d_x & 0 & 0 & 1 & \frac{L}{\beta_s^2\gamma_s^2} - \frac{h^2}{\beta_s^2}J_1 \\ 0 & 0 & 0 & 0 & 0 & 1 \end{pmatrix}. \tag{5.21}$$

and the non-zero terms of second order:

$$\begin{aligned}
T_{111} &= -\frac{1}{6}(K_2 + 2hK_1)(s_x^2 + d_x) - \frac{h}{2}k_x^2 s_x^2, \\
T_{112} &= -\frac{1}{6}(K_2 + 2hK_1)s_x d_x + \frac{h}{2}s_x c_x, \\
T_{122} &= -\frac{1}{6}(K_2 + 2hK_1)d_x^2 + \frac{h}{2}c_x d_x, \\
T_{116} &= -\frac{h}{12\beta_s}(K_2 + 2hK_1)(3s_x J_1 - d_x^2) + \frac{h^2}{2\beta_s}s_x^2 + \frac{1}{4\beta_s}K_1 L s_x, \\
T_{126} &= -\frac{h}{12\beta_s}(K_2 + 2hK_1)(s_x d_x^2 - 2c_x J_2) + \frac{h^2}{4\beta_s}(s_x d_x + c_x J_1) - \frac{1}{4\beta_s}(s_x + L c_x), \\
T_{166} &= -\frac{h^2}{6\beta_s^2}(K_2 + 2hK_1)(d_x^3 - 2s_x J_2) + \frac{h^3}{2\beta_s^2}s_x J_1 - \frac{h}{2\beta_s^2}L s_x - \frac{h}{2\beta_s^2\gamma_s^2}d_x, \\
T_{133} &= K_1 K_2 J_d + \frac{1}{2}(K_2 + hK_1)d_x, \\
T_{134} &= \frac{1}{2}K_2 J_s, \\
T_{144} &= K_2 J_d - \frac{h}{2}d_x,
\end{aligned} \tag{5.22}$$

$$\begin{aligned}
T_{211} &= -\frac{1}{6}(K_2 + 2hK_1)s_x(1 + 2c_x), \\
T_{212} &= -\frac{1}{6}(K_2 + 2hK_1)d_x(1 + 2c_x), \\
T_{222} &= -\frac{1}{3}(K_2 + 2hK_1)s_x d_x - \frac{h}{2}s_x, \\
T_{216} &= -\frac{h}{12\beta_s}(K_2 + 2hK_1)(3c_x J_1 + s_x d_x) - \frac{1}{4\beta_s}K_1(s_x - L c_x), \\
T_{226} &= -\frac{h}{12\beta_s}(K_2 + 2hK_1)(3s_x J_1 + d_x^2) + \frac{1}{4\beta_s}K_1 L s_x, \\
T_{266} &= -\frac{h^2}{6\beta_s^2}(K_2 + 2hK_1)(s_x d_x^2 - 2c_x J_2) - \frac{h}{2\beta_s^2}K_1(c_x J_1 - s_x d_x) - \frac{h}{2\beta_s^2\gamma_s^2}s_x, \\
T_{233} &= K_1 K_2 J_s + \frac{1}{2}(K_2 + hK_1)s_x, \\
T_{234} &= \frac{1}{2}K_2 J_c, \\
T_{244} &= K_2 J_s - \frac{h}{2}s_x,
\end{aligned} \tag{5.23}$$

$$\begin{aligned}
T_{313} &= \frac{1}{2}K_2(c_y J_c - 2K_1 s_y J_s) + \frac{h}{2}K_1 s_x s_y, \\
T_{314} &= \frac{1}{2}K_2(s_y J_c - 2c_y J_s) + \frac{h}{2}s_x c_y, \\
T_{323} &= \frac{1}{2}K_2(c_y J_s - 2K_1 s_y J_d) + \frac{h}{2}K_1 d_x s_y, \\
T_{324} &= \frac{1}{2}K_2(s_y J_s - 2c_y J_d) + \frac{h}{2}d_x c_y, \\
T_{336} &= \frac{h}{2\beta_s}K_2(c_y J_d - 2K_1 s_y J_f) + \frac{h^2}{2\beta_s}K_1 J_1 s_y - \frac{1}{4\beta_s}K_1 L s_y, \\
T_{346} &= \frac{h}{2\beta_s}K_2(s_y J_d - 2c_y J_f) + \frac{h^2}{2\beta_s}J_1 c_y - \frac{1}{4\beta_s}(s_y + L c_y),
\end{aligned} \tag{5.24}$$

$$\begin{aligned}
T_{413} &= \frac{1}{2}K_1K_2(2c_yJ_s - s_yJ_c) + \frac{1}{2}(K_2 + hK_1)s_xc_y, \\
T_{414} &= \frac{1}{2}K_2(2K_1s_yJ_s - c_yJ_c) + \frac{1}{2}(K_2 + hK_1)s_xs_y, \\
T_{423} &= \frac{1}{2}K_1K_2(2c_yJ_d - s_yJ_s) + \frac{1}{2}(K_2 + hK_1)d_xc_y, \\
T_{424} &= \frac{1}{2}K_2(2K_1s_yJ_d - c_yJ_s) + \frac{1}{2}(K_2 + hK_1)d_xs_y, \\
T_{436} &= \frac{h}{2\beta_s}K_1K_2(2c_yJ_f - s_yJ_d) + \frac{h}{2\beta_s}(K_2 + hK_1)J_1c_y + \frac{1}{4\beta_s}K_1(s_y - Lc_y), \\
T_{446} &= \frac{h}{2\beta_s}K_2(2K_1s_yJ_f - c_yJ_d) + \frac{h}{2\beta_s}(K_2 + hK_1)J_1s_y - \frac{1}{4\beta_s}K_1Ls_y,
\end{aligned} \tag{5.25}$$

$$\begin{aligned}
T_{511} &= \frac{h}{12\beta_s}(K_2 + 2hK_1)(s_xd_x + 3J_1) - \frac{1}{4\beta_s}K_1(L - s_xc_x), \\
T_{512} &= \frac{h}{12\beta_s}(K_2 + 2hK_1)d_x^2 + \frac{1}{4\beta_s}K_1s_x^2, \\
T_{522} &= \frac{h}{6\beta_s}(K_2 + 2hK_1)J_2 - \frac{1}{2\beta_s}s_x - \frac{1}{4\beta_s}K_1(J_1 - s_xd_x), \\
T_{516} &= \frac{h^2}{12\beta_s^2}(K_2 + 2hK_1)(3d_xJ_1 - 4J_2) + \frac{h}{4\beta_s^2}K_1J_1(1 + c_x) + \frac{h}{2\beta_s^2\gamma_s^2}s_x, \\
T_{526} &= \frac{h^2}{12\beta_s^2}(K_2 + 2hK_1)(d_x^3 - 2s_xJ_2) + \frac{h}{4\beta_s^2}K_1s_xJ_1 + \frac{h}{2\beta_s^2\gamma_s^2}d_x, \\
T_{566} &= \frac{h^3}{6\beta_s^3}(K_2 + 2hK_1)(3J_3 - 2d_xJ_2) + \frac{h^2}{6\beta_s^3}K_1(s_xd_x^2 - J_2(1 + 2c_x)) + \frac{3}{2\beta_s^3\gamma_s^2}(h^2J_1 - L), \\
T_{533} &= -\frac{h}{\beta_s}K_1K_2J_f - \frac{h}{2\beta_s}(K_2 + hK_1)J_1 + \frac{1}{4\beta_s}K_1(L - c_y s_y), \\
T_{534} &= -\frac{h}{2\beta_s}K_2J_d - \frac{1}{4\beta_s}K_1s_y^2, \\
T_{544} &= -\frac{h}{\beta_s}K_2J_f + \frac{h^2}{2\beta_s}J_1 - \frac{1}{4\beta_s}(L + c_y s_y).
\end{aligned} \tag{5.26}$$

5.3.3 Body of a Rectangular Dipole

Hamiltonian for the Body of a Rectangular Dipole

For a rectangular Dipole with a straight reference one may set the curvature $h = 0$, and the expanded Hamiltonian for a sector dipole has the terms

$$\begin{aligned}
H_1 &= K_0x + \frac{\eta\delta_s}{\beta_s}p_t, \\
H_2 &= \frac{1}{2}K_1(x^2 - y^2) + \frac{1}{2}\left(p_x^2 + p_y^2 + \frac{p_t^2}{\beta_s^2\gamma_s^2}\right), \\
H_3 &= \frac{1}{6}(K_2x^3 - 3xy^2) - \frac{p_t}{2\beta_s}\left(p_x^2 + p_y^2 + \frac{p_t^2}{\beta_s^2\gamma_s^2}\right), \\
H_4 &= \frac{1}{24}(K_3x^4 - 6x^2y^2 + y^4) + \\
&\quad \frac{p_t^2}{2\beta_s^2}\left(p_x^2 + p_y^2 + \frac{p_t^2}{\beta_s^2\gamma_s^2}\right) + \frac{1}{8}\left(p_x^2 + p_y^2 + \frac{p_t^2}{\beta_s^2\gamma_s^2}\right)^2.
\end{aligned} \tag{5.27}$$

At this time the maps for this case have not been worked out yet.

5.4 Quadrupole

The transfer map for a quadrupole is the limit obtained by setting $h = K_2 = K_3 = 0$ in the map for a combined function dipole. We use the two quantities

$$k_x^2 = K_1 = (qB_1)/(p_s c), \quad k_y^2 = -K_1. \quad (5.28)$$

For other definitions refer to Section 1.3.

5.4.1 Hamiltonian for a Quadrupole

The expanded Hamiltonian for a quadrupole is

$$\begin{aligned} H_1 &= \frac{\eta\delta_s}{\beta_s} p_t, \\ H_2 &= \frac{1}{2} K_1 (x^2 - y^2) + \frac{1}{2} \left(p_x^2 + p_y^2 + \frac{p_t^2}{\beta_s^2 \gamma_s^2} \right), \\ H_3 &= -\frac{p_t}{2\beta_s} \left(p_x^2 + p_y^2 + \frac{p_t^2}{\beta_s^2 \gamma_s^2} \right), \\ H_4 &= \frac{p_t^2}{2\beta_s^2} \left(p_x^2 + p_y^2 + \frac{p_t^2}{\beta_s^2 \gamma_s^2} \right) + \frac{1}{8} \left(p_x^2 + p_y^2 + \frac{p_t^2}{\beta_s^2 \gamma_s^2} \right)^2. \end{aligned} \quad (5.29)$$

5.4.2 Lie-Algebraic map for a Quadrupole

The transfer matrix for a quadrupole is

$$F = \begin{pmatrix} c_x & s_x & 0 & 0 & 0 & 0 \\ -k_x^2 s_x & c_x & 0 & 0 & 0 & 0 \\ 0 & 0 & c_y & s_y & 0 & 0 \\ 0 & 0 & -k_y^2 s_y & c_y & 0 & 0 \\ 0 & 0 & 0 & 0 & 1 & \frac{L}{\beta_s^2 \gamma_s^2} \\ 0 & 0 & 0 & 0 & 0 & 1 \end{pmatrix}. \quad (5.30)$$

The generators for the quadrupole are [10]:

$$\begin{aligned} f_1 &= -\frac{L\eta\delta_s}{\beta_s} p_t, \\ f_3 &= \frac{p_t}{4\beta_s} (+K_1(L - s_x c_x)x^2 + 2K_1 s_x^2 x p_x + (L + s_x c_x)p_x^2 \\ &\quad - K_1(L - s_y c_y)y^2 - 2K_1 s_y^2 y p_y + (L + s_y c_y)p_y^2) + \frac{p_t^3}{2\beta_s^3 \gamma_s^2}, \\ f_4 &= \frac{1}{4!} \sum_{i=1}^6 \sum_{j=1}^6 \sum_{k=1}^6 \sum_{l=1}^6 F_{ijkl} Z_i Z_j Z_k Z_l \end{aligned} \quad (5.31)$$

and f_4 has the coefficients

$$\begin{aligned}
F_{1111} &= +\frac{K_1^2}{64} \left(-s(4k_x, L) + 4s(2k_x, L) - 3L \right), \\
F_{1112} &= -\frac{K_1^3}{8} s^4(k_x, L), \\
F_{1122} &= +\frac{3K_1}{32} \left(s(4k_x, L) - L \right), \\
F_{1222} &= +\frac{1}{8} \left(c^4(k_x, L) - 1 \right), \\
F_{2222} &= -\frac{1}{64} \left(s(4k_x, L) + 4s(2k_x, L) + 3L \right),
\end{aligned} \tag{5.32}$$

$$\begin{aligned}
F_{3333} &= +\frac{K_1^2}{64} \left(-s(4k_y, L) + 4s(2k_y, L) - 3L \right), \\
F_{3334} &= +\frac{K_1^3}{8} s^4(k_y, L), \\
F_{3344} &= -\frac{3K_1}{32} \left(s(4k_y, L) - L \right), \\
F_{3444} &= +\frac{1}{8} \left(c^4(k_y, L) - 1 \right), \\
F_{4444} &= -\frac{1}{64} \left(s(4k_y, L) + 4s(2k_y, L) + 3L \right),
\end{aligned} \tag{5.33}$$

$$\begin{aligned}
F_{1133} &= +\frac{K_1^2}{32} \left(-s(2k_y, L) \left(2 - c(2k_x, L) \right) - s(2k_x, L) \left(2 - c(2k_y, L) \right) + 2L \right), \\
F_{1134} &= +\frac{K_1}{32} \left(c(2k_y, L) \left(2 - c(2k_x, L) \right) - 4K_1 s(2k_x, L) s(2k_y, L) - 1 \right), \\
F_{1144} &= +\frac{K_1}{32} \left(s(2k_x, L) \left(2 + c(2k_y, L) \right) - s(2k_y, L) \left(2 - c(2k_x, L) \right) - 2L \right), \\
F_{1233} &= -\frac{K_1}{32} \left(c(2k_x, L) \left(2 - c(2k_y, L) \right) + 4K_1 s(2k_y, L) s(2k_x, L) - 1 \right), \\
F_{1234} &= +\frac{K_1}{8} \left(s(2k_x, L) c(2k_y, L) - c(2k_x, L) s(2k_y, L) \right), \\
F_{1244} &= +\frac{1}{32} \left(c(2k_x, L) \left(2 + c(2k_y, L) \right) - 4K_1 s(2k_x, L) s(2k_y, L) - 3 \right), \\
F_{2233} &= -\frac{K_1}{32} \left(s(2k_y, L) \left(2 + c(2k_x, L) \right) - s(2k_x, L) \left(2 - c(2k_y, L) \right) - 2L \right), \\
F_{2234} &= +\frac{1}{32} \left(c(2k_y, L) \left(2 + c(2k_x, L) \right) + 4K_1 s(2k_x, L) s(2k_y, L) - 3 \right), \\
F_{2244} &= -\frac{1}{32} \left(s(2k_x, L) \left(2 + c(2k_y, L) \right) + s(2k_y, L) \left(2 + c(2k_x, L) \right) + 2L \right),
\end{aligned} \tag{5.34}$$

$$\begin{aligned}
F_{1166} &= +\frac{K_1}{8} \left(L - s(2k_x, L) \right) + \frac{K_1}{16\beta_s^2} \left(3s(2k_x, L) + L(c(2k_x, L) - 4) \right), \\
F_{1266} &= -\frac{K_1}{4\beta_s^2} \left(Ls(2k_x, L) + (2 - \beta_s^2) s^2(k_x, L) \right), \\
F_{2266} &= +\frac{1}{8} \left(L + s(2k_x, L) \right) - \frac{1}{16\beta_s^2} \left(5s(2k_x, L) + L(6 + c(2k_x, L)) \right),
\end{aligned} \tag{5.35}$$

$$\begin{aligned}
F_{3366} &= -\frac{K_1}{8}(L - s(2k_y, L)) - \frac{K_1}{16\beta_s^2}(3s(2k_y, L) + L(c(2k_y, L) - 4)), \\
F_{3466} &= +\frac{K_1}{4\beta_s^2}(Ls(2k_y, L) + (2 - \beta_s^2)s^2(k_y, L)), \\
F_{4466} &= +\frac{1}{8}(L + s(2k_y, L)) - \frac{1}{16\beta_s^2}(5s(2k_y, L) + L(6 + c(2k_y, L))), \\
F_{6666} &= +\frac{1}{8\beta_s^2\gamma_s^2}\left(1 - \frac{5}{\beta_s^2}\right).
\end{aligned} \tag{5.36}$$

$$F_{6666} = +\frac{1}{8\beta_s^2\gamma_s^2}\left(1 - \frac{5}{\beta_s^2}\right). \tag{5.37}$$

5.4.3 TRANSPORT Map for a Quadrupole

The complete TRANSPORT map for a quadrupole is:

$$\begin{aligned}
x_2 &= c_x x_1 + s_x p_{x1} + \frac{1}{2\beta_s}(+K_1 L s_x x_1 p_{t1} - (s_x + L c_x) p_{x1} p_{t1}), \\
p_{x2} &= -K_1 s_x x_1 + c_x p_{x1} + \frac{K_1}{2\beta_s}(-(s_x - L c_x) x_1 p_{t1} + L s_x p_{x1} p_{t1}), \\
y_2 &= c_y y_1 + s_y p_{y1} + \frac{1}{2\beta_s}(-K_1 L s_y y_1 p_{t1} - (s_y + L c_y) p_{y1} p_{t1}), \\
p_{y2} &= +K_1 s_y y_1 + c_y p_{y1} + \frac{K_1}{2\beta_s}(+(s_y - L c_y) y_1 p_{y1} - L s_y p_{y1} p_{t1}), \\
t_2 &= t_1 + \frac{L\eta\delta_s}{\beta_s} - \frac{L}{\beta_s^2\gamma_s^2} p_{t1} \\
&\quad - \frac{1}{4\beta_s} K_1 (L - s_x c_x) x_1^2 + \frac{1}{2\beta_s} K_1 s_x^2 x_1 p_{x1} - \frac{1}{4\beta_s} (L + s_x c_x) p_{x1}^2 \\
&\quad + \frac{1}{4\beta_s} K_1 (L - s_y c_y) y_1^2 - \frac{1}{2\beta_s} K_1 s_y^2 y_1 p_{y1} - \frac{1}{4\beta_s} (L + s_y c_y) p_{y1}^2 \\
&\quad - \frac{3L}{2\beta_s^3\gamma_s^2} p_{t1}^2, \\
p_{t2} &= p_{t1}.
\end{aligned} \tag{5.38}$$

5.5 Sextupole

The transfer map for a sextupole is the limits obtained by setting $h = K_1 = K_3 = 0$ in the map for a combined function dipole.

5.5.1 Hamiltonian for a Sextupole

The expanded Hamiltonian for a sextupole is

$$\begin{aligned}
H_1 &= \frac{\eta\delta_s}{\beta_s} p_t, \\
H_2 &= \frac{1}{6} K_1 (x^3 - 3xy^2) + \frac{1}{2} \left(p_x^2 + p_y^2 + \frac{p_t^2}{\beta_s^2\gamma_s^2} \right), \\
H_3 &= -\frac{p_t}{2\beta_s} \left(p_x^2 + p_y^2 + \frac{p_t^2}{\beta_s^2\gamma_s^2} \right), \\
H_4 &= \frac{p_t^2}{2\beta_s^2} \left(p_x^2 + p_y^2 + \frac{p_t^2}{\beta_s^2\gamma_s^2} \right) + \frac{1}{8} \left(p_x^2 + p_y^2 + \frac{p_t^2}{\beta_s^2\gamma_s^2} \right)^2.
\end{aligned} \tag{5.39}$$

5.5.2 Lie-Algebraic Map for a Sextupole

A sextupole has the same transfer matrix as a drift space

$$F = \begin{pmatrix} 1 & L & 0 & 0 & 0 & 0 \\ 0 & 1 & 0 & 0 & 0 & 0 \\ 0 & 0 & 1 & L & 0 & 0 \\ 0 & 0 & 0 & 1 & 0 & 0 \\ 0 & 0 & 0 & 0 & 1 & \frac{L}{\beta_s^2 \gamma_s^2} \\ 0 & 0 & 0 & 0 & 0 & 1 \end{pmatrix}. \quad (5.40)$$

L is the sextupole length. The sextupole strength K_2 , defined as for a combined function dipole, produces the generators [10]:

$$\begin{aligned} f_1 &= -\frac{L\eta\delta_s}{\beta_s} p_t, \\ f_3 &= \frac{L}{2\beta_s} \left(p_x^2 + p_y^2 + \frac{p_t^2}{\beta_s^2 \gamma_s^2} \right) p_t - \frac{L}{6} K_2 (x^3 - 3xy^2) + \frac{L^2}{4} K_2 ((x^2 - y^2)p_x - 2xy p_y) - \\ &\quad \frac{L^3}{6} K_2 (x(p_x^2 - p_y^2) - 2yp_x p_y) + \frac{L^4}{24} K_2 (p_x^3 - 3p_x p_y^2), \\ f_4 &= \frac{L^3}{48} K_2^2 (x^2 + y^2)^2 - \frac{L^4}{24} K_2^2 (x^2 + y^2)(xp_x + yp_y) + \\ &\quad \frac{L^5}{480} K_2^2 ((x^2 + y^2)(p_x^2 + p_y^2) + 14(xp_x + yp_y)^2) - \\ &\quad \frac{L^6}{96} K_2^2 (xp_x + yp_y)(p_x^2 + p_y^2) + \frac{L^7}{672} K_2^2 (p_x^2 + p_y^2)^2 - \\ &\quad \frac{L^3}{12} K_2 (x(p_x^2 - p_y^2) - 2p_x p_y) p_t + \frac{L^4}{24} K_2 (p_x^3 - 3p_x p_y^2) p_t - \\ &\quad \frac{L}{2\beta_s^2} \left(p_x^2 + p_y^2 + \frac{p_t^2}{\beta_s^2 \gamma_s^2} \right) p_t^2 - \frac{L}{8} \left(p_x^2 + p_y^2 + \frac{p_t^2}{\beta_s^2 \gamma_s^2} \right)^2. \end{aligned} \quad (5.41)$$

5.5.3 TRANSPORT Map for a Sextupole

The complete TRANSPORT map for a thick sextupole is

$$\begin{aligned} x_2 &= x_1 + L \left(1 - \frac{p_{t1}}{\beta_s} \right) p_{x1} - K_2 \left(\frac{L^2}{4} (x_1^2 - y_1^2) + \frac{L^3}{12} (x_1 p_{x1} - y_1 p_{y1}) + \frac{L^4}{24} (p_{x1}^2 - p_{y1}^2) \right) - \frac{L}{2\beta_s} p_{x1} p_{t1}, \\ p_{x2} &= p_{x1} - K_2 \left(\frac{L}{2} (x_1^2 - y_1^2) + \frac{L^2}{4} (x_1 p_{x1} - y_1 p_{y1}) + \frac{L^3}{6} (p_{x1}^2 - p_{y1}^2) \right), \\ y_2 &= y_1 + L \left(1 - \frac{p_{t1}}{\beta_s} \right) p_{y1} + K_2 \left(\frac{L^2}{4} x_1 y_1 + \frac{L^3}{12} (x_1 p_{y1} + y_1 p_{x1}) + \frac{L^4}{24} p_{x1} p_{y1} \right) - \frac{L}{2\beta_s} p_{y1} p_{t1}, \\ p_{y2} &= p_{y1} + K_2 \left(\frac{L}{2} x_1 y_1 + \frac{L^2}{4} (x_1 p_{y1} + y_1 p_{x1}) + \frac{L^3}{6} p_{x1} p_{y1} \right), \\ t_2 &= \frac{L\eta\delta_s}{\beta_s} + t_1 + \frac{L}{\beta_s^2 \gamma_s^2} p_{t1} - \frac{L}{2\beta_s} \left(p_{x1}^2 + p_{y1}^2 + \frac{3p_{t1}^2}{\beta_s^2 \gamma_s^2} \right), \\ p_{t2} &= p_{t1}. \end{aligned} \quad (5.42)$$

5.6 Octupole

The transfer map for an octupole is limit obtained by setting $h = K_1 = K_2 = 0$ in the map for a combined function dipole.

5.6.1 Lie-Algebraic Map for an Octupole

In the Lie algebraic formalism an octupole can be handled as a lens of finite length. It has the same transfer matrix as a drift space

$$F = \begin{pmatrix} 1 & L & 0 & 0 & 0 & 0 \\ 0 & 1 & 0 & 0 & 0 & 0 \\ 0 & 0 & 1 & L & 0 & 0 \\ 0 & 0 & 0 & 1 & 0 & 0 \\ 0 & 0 & 0 & 0 & 1 & \frac{L}{\beta_s^2 \gamma_s^2} \\ 0 & 0 & 0 & 0 & 0 & 1 \end{pmatrix}. \quad (5.43)$$

L is the octupole length. The generators are [10]:

$$\begin{aligned} f_3 &= +\frac{L}{2\beta_s} \left(p_x^2 + p_y^2 + \frac{p_t^2}{\beta_s^2 \gamma_s^2} \right) p_t, \\ f_4 &= -\frac{L}{2\beta_s^2} \left(p_x^2 + p_y^2 + \frac{p_t^2}{\beta_s^2 \gamma_s^2} \right) p_t^2 - \frac{L}{8} \left(p_x^2 + p_y^2 + \frac{p_t^2}{\beta_s^2 \gamma_s^2} \right)^2 - \frac{K_3}{24} (x^4 - 6x^2 y^2 + y^4). \end{aligned} \quad (5.44)$$

5.6.2 TRANSPORT Map for a Thin Octupole

In TRANSPORT form an octupole is treated as a thin lens placed between two drifts of half the octupole length. The map for the thin lens with strength $K_3 L = (qB_3)/(p_s c)$, evaluated with respect to the actual orbit produces a kick

$$p_{x2} = p_{x1} - \frac{1}{6} K_3 L (x^3 - 3xy^2), \quad p_{y2} = p_{y1} + \frac{1}{6} K_3 L (3x^2 y - y^3). \quad (5.45)$$

Hence the transfer matrix for the thin lens with respect to a given orbit is the unit matrix augmented with the terms

$$-R_{21} = +R_{43} = \frac{1}{2} K_3 L (x^2 - y^2), \quad +R_{23} = +R_{41} = K_3 L xy, \quad (5.46)$$

and the second-order terms around that orbit are

$$-T_{211} = +T_{233} = +T_{413} = +T_{431} = \frac{1}{2} K_3 L x, \quad +T_{213} = +T_{231} = +T_{411} = -T_{433} = \frac{1}{2} K_3 L y. \quad (5.47)$$

5.7 Thin Multipole

A thin multipole affects the reference system like a dipole, i. e. the reference direction changes by the bend angle of its nominal dipole component. The total dipole strength thus generates dispersion only; but a dipole error, if present, also changes the orbit.

5.7.1 Lie-Algebraic Map for a Thin Multipole

A thin multipole affects the reference system like a dipole, i. e. the reference direction changes by the bend angle of its nominal dipole component. The total dipole strength thus generates dispersion only; but a dipole error, if present, also changes the orbit with respect to the reference.

With Lie algebraic maps truncated at order of f_4 , field components can be represented up to the octupole. The multipole deflects the orbit according to the complex kick

$$Z = \Delta K_0 L - K_0 L \frac{\delta}{\beta_s} + \sum_{n=1}^3 K_n L \frac{(x + iy)^n}{n!}. \quad (5.48)$$

The geometric terms of the transfer matrix are found by differentiation:

$$-F_{21} = +F_{43} = \Re Z', \quad +F_{23} = +F_{41} = \Im Z'. \quad (5.49)$$

The *total* dipole strength creates the dispersive terms

$$+F_{26} = -F_{51} = \frac{1}{\beta_s} \Re(K_0 L), \quad -F_{46} = +F_{53} = \frac{1}{\beta_s} \Im(K_0 L). \quad (5.50)$$

From the equation for Z one may derive the generators

$$f_1 = -\Re(\Delta K_0 L(x + iy)), \quad f_3 = -\frac{1}{3!} \Re(K_2 L(x - iy)^3), \quad f_4 = -\frac{1}{4!} \Re(K_3 L(x - iy)^4). \quad (5.51)$$

5.7.2 TRANSPORT Map for a Thin Multipole

The multipole deflects the orbit according to the complex kick

$$P = \Delta K_0 L - K_0 L \frac{p_t}{\beta_s} + \sum_{n=1}^N K_n L \frac{(x + iy)^n}{n!}, \quad (5.52)$$

i. e. it produces the orbit change

$$\begin{aligned} x_2 &= x_1, & p_{x2} &= p_{x1} - \Re P \\ y_2 &= y_1, & p_{y2} &= p_{y1} + \Im P \\ t_2 &= t_1 - \frac{1}{\beta_s} \Re(K_0 L(x + iy)), & p_{t2} &= p_{t1}. \end{aligned} \quad (5.53)$$

The transfer matrix can be obtained by differentiating the kick. Defining

$$P' = \sum_{n=1}^N K_n L \frac{(x + iy)^{n-1}}{(n-1)!}, \quad (5.54)$$

the geometric terms of the transfer matrix are

$$-R_{21} = +R_{43} = \Re P', \quad +R_{23} = +R_{41} = \Im P'. \quad (5.55)$$

The *total* dipole strength creates the dispersive terms

$$+R_{26} = -R_{51} = \frac{1}{\beta_s} \Re(K_0 L), \quad -R_{46} = +R_{53} = \frac{1}{\beta_s} \Im(K_0 L). \quad (5.56)$$

The second-order terms are due to components K_2 and higher. They are obtained by differentiating the kick twice. Defining

$$P'' = \sum_{n=2}^N K_n L \frac{(x + iy)^{n-2}}{(n-2)!}, \quad (5.57)$$

these terms become

$$-T_{211} = +T_{233} = +T_{413} = +T_{431} = \frac{1}{2} \Re P'', \quad +T_{213} = +T_{231} = +T_{411} = -T_{433} = \frac{1}{2} \Im P''. \quad (5.58)$$

5.8 Solenoid

5.8.1 Hamiltonian for a Solenoid

The expanded Hamiltonian is

$$\begin{aligned}
H_1 &= \frac{\eta\delta_s}{\beta_s}, \\
H_2 &= \frac{1}{2} \left((p_x + ky)^2 + (p_y - kx)^2 + \frac{p_t^2}{\beta_s^2 \gamma_s^2} \right), \\
H_3 &= -\frac{p_t}{2\beta_s} \left((p_x + ky)^2 + (p_y - kx)^2 + \frac{p_t^2}{\beta_s^2 \gamma_s^2} \right), \\
H_4 &= \frac{p_t^2}{\beta_s^2} \left((p_x + ky)^2 + (p_y - kx)^2 + \frac{p_t^2}{\beta_s^2 \gamma_s^2} \right) + \frac{1}{8} \left((p_x + ky)^2 + (p_y - kx)^2 + \frac{p_t^2}{\beta_s^2 \gamma_s^2} \right)^2.
\end{aligned} \tag{5.59}$$

5.8.2 Lie-Algebraic Map for a Solenoid

Solving the Hamiltonian by the techniques of [10] gives the transfer matrix

$$F = \begin{pmatrix} C^2 & \frac{1}{k}SC & SC & \frac{1}{k}S^2 & 0 & 0 \\ -kSC & C^2 & -kS^2 & SC & 0 & 0 \\ -SC & -\frac{1}{k}S^2 & C^2 & \frac{1}{k}SC & 0 & 0 \\ kS^2 & -SC & -kSC & C^2 & 0 & 0 \\ 0 & 0 & 0 & 0 & 1 & \frac{L}{\beta_s^2 \gamma_s^2} \\ 0 & 0 & 0 & 0 & 0 & 1 \end{pmatrix}, \tag{5.60}$$

where

$$k = \frac{qB_0}{2p_s}, \quad C = \cos(kL), \quad S = \sin(kL). \tag{5.61}$$

The third- and fourth-order parts of the Hamiltonian are invariant under the linear transformation. Hence the non-linear generators take a particularly simple form:

$$\begin{aligned}
f_1 &= -\frac{L\eta\delta_s}{\beta_s} p_t, \\
f_3 &= +\frac{L}{2\beta_s} \left((p_x + ky)^2 + (p_y - kx)^2 + \frac{p_t^2}{\beta_s^2 \gamma_s^2} \right) p_t, \\
f_4 &= -\frac{L}{2\beta_s^2} \left((p_x + ky)^2 + (p_y - kx)^2 + \frac{p_t^2}{\beta_s^2 \gamma_s^2} \right) p_t^2 - \frac{L}{8} \left((p_x + ky)^2 + (p_y - kx)^2 + \frac{p_t^2}{\beta_s^2 \gamma_s^2} \right)^2.
\end{aligned} \tag{5.62}$$

Two effects should be considered at the ends of the solenoid. First, the field lines cannot end abruptly at the ends; and second, the vector potential is zero outside the solenoid and finite inside. The first effect can be estimated by assuming that the magnetic flux lines bend sharply and concentrate in a radial plane at each end of the solenoid. The second effect causes the transverse canonical momentum to jump by the value of $e\vec{A}/B\rho$. Both transformations are non-symplectic, but fortunately they cancel in the approximation used.

5.8.3 TRANSPORT Map for a Solenoid

A solenoid changes the time reference by

$$\Delta t = \frac{L\eta\delta_s}{\beta_s}. \quad (5.63)$$

Its Lie transformation is easily transformed to the TRANSPORT map with the transfer matrix

$$R = \begin{pmatrix} C^2 & \frac{1}{k}SC & SC & \frac{1}{k}S^2 & 0 & 0 \\ -kSC & C^2 & -kS^2 & SC & 0 & 0 \\ -SC & -\frac{1}{k}S^2 & C^2 & \frac{1}{k}SC & 0 & 0 \\ kS^2 & -SC & -kSC & C^2 & 0 & 0 \\ 0 & 0 & 0 & 0 & 1 & \frac{L}{\beta_s^2\gamma_s^2} \\ 0 & 0 & 0 & 0 & 0 & 1 \end{pmatrix}. \quad (5.64)$$

The second-order terms become:

$$\begin{aligned} T_{116} &= \frac{kL}{2\beta_s} \sin(2kL), & T_{126} &= -\frac{L}{2\beta_s} \cos(2kL), & T_{136} &= -\frac{kL}{2\beta_s} \cos(2kL), & T_{146} &= -\frac{L}{2\beta_s} \sin(2kL), \\ T_{216} &= \frac{k^2L}{2\beta_s} \cos(2kL), & T_{226} &= \frac{kL}{2\beta_s} \sin(2kL), & T_{236} &= \frac{k^2L}{2\beta_s} \sin(2kL), & T_{246} &= -\frac{kL}{2\beta_s} \cos(2kL), \\ T_{316} &= \frac{kL}{2\beta_s} \cos(2kL), & T_{326} &= \frac{L}{2\beta_s} \sin(2kL), & T_{336} &= \frac{kL}{\beta_s} \sin(2kL), & T_{346} &= -\frac{L}{2\beta_s} \cos(2kL), \\ T_{416} &= -\frac{k^2L}{2\beta_s} \sin(2kL), & T_{426} &= \frac{kL}{2\beta_s} \cos(2kL), & T_{436} &= \frac{k^2L}{2\beta_s} \cos(2kL), & T_{446} &= \frac{kL}{2\beta_s} \sin(2kL), \\ T_{511} &= -\frac{k^2L}{2\beta_s}, & T_{514} &= \frac{kL}{2\beta_s}, & T_{544} &= -\frac{L}{2\beta_s}, \\ T_{533} &= -\frac{k^2L}{2\beta_s}, & T_{523} &= -\frac{kL}{2\beta_s}, & T_{522} &= -\frac{L}{2\beta_s}, \\ T_{566} &= -\frac{3L}{2\beta_s^2\gamma_s^2}. \end{aligned} \quad (5.65)$$

5.9 Orbit Correctors

An orbit corrector is modelled as a zero-length dipole between two drifts of half the corrector length. The reference system is *not changed* by the corrector. The effect of the thin dipole is simply

$$p_{x2} = p_{x1} + K_{0x}/(1 + \delta_s), \quad p_{y2} = p_{y1} + K_{0y}/(1 + \delta_s), \quad (5.66)$$

where K_{0x} and K_{0y} are the given kicks in the respective plane. There are no non-linear terms.

5.10 RF Cavity

An RF cavity is treated in the impulse approximation. The length of a cavity is simulated by placing the accelerating gap between two drifts of half the cavity length. The voltage of the thin cavity is

$$V = \hat{V} \sin(\phi_s - \omega t/c). \quad (5.67)$$

The phase lag of the cavity is defined as the RF phase seen by a particle arriving with a time difference of zero relative to the time frame. \hat{V} is the peak RF voltage, $f_{RF} = h_{RF}/T_s$ is the RF frequency, and h_{RF} is the harmonic number. The circular frequency of the RF cavity is

$$\omega = \frac{2\pi h_{RF}}{T_s} \quad (5.68)$$

5.10.1 Exact Solution for a Thin RF Cavity

The general particle sees an RF phase of

$$\phi = \phi_s - \omega t/c. \quad (5.69)$$

Hence the cavity causes an accelerating kick of

$$p_{t2} = p_{t1} + \frac{q\hat{V}}{p_s c} \sin \phi. \quad (5.70)$$

Higher-order terms are obtained easily by differentiation of this expression.

5.10.2 Lie-Algebraic Map for a Thin RF Cavity

The cavity produces an accelerating kick of

$$\delta_2 = \delta_1 + \frac{\hat{V}}{pc} \sin(\phi - \omega t). \quad (5.71)$$

With respect to the actual orbit it has the transfer matrix

$$F = \begin{pmatrix} 1 & 0 & 0 & 0 & 0 & 0 \\ 0 & 1 & 0 & 0 & 0 & 0 \\ 0 & 0 & 1 & 0 & 0 & 0 \\ 0 & 0 & 0 & 1 & 0 & 0 \\ 0 & 0 & 0 & 0 & 1 & 0 \\ 0 & 0 & 0 & 0 & -\omega \frac{e\hat{V}}{pc} \cos \phi & 1 \end{pmatrix}. \quad (5.72)$$

and the generators [10]:

$$f_1 = +\frac{e\hat{V}}{pc} t \sin \phi, \quad f_3 = -\frac{\omega^2}{3!} \frac{e\hat{V}}{pc} t^3 \sin \phi, \quad f_4 = +\frac{\omega^3}{4!} \frac{e\hat{V}}{pc} t^4 \cos \phi. \quad (5.73)$$

5.10.3 TRANSPORT Map for a Thin RF Cavity

Using the definitions in Section 5.10, we find the accelerating kick:

$$p_{t2} = p_{t1} + \frac{q\hat{V}}{p_s c} \sin \phi. \quad (5.74)$$

By differentiation one finds that the transfer matrix is

$$R = \begin{pmatrix} 1 & 0 & 0 & 0 & 0 & 0 \\ 0 & 1 & 0 & 0 & 0 & 0 \\ 0 & 0 & 1 & 0 & 0 & 0 \\ 0 & 0 & 0 & 1 & 0 & 0 \\ 0 & 0 & 0 & 0 & 1 & 0 \\ 0 & 0 & 0 & 0 & -\frac{\omega}{c} \frac{\hat{V}}{pc} \cos \phi & 1 \end{pmatrix}. \quad (5.75)$$

and one non-zero second-order term

$$T_{655} = -\frac{\omega^2}{c^2} \frac{\hat{V}}{2pc} \sin \phi. \quad (5.76)$$

5.10.4 Electrostatic Separator

By convention an electrostatic separator does *not* change the reference orbit. We use the definition

$$k = \frac{qE_y}{p_0 c} \quad (5.77)$$

5.10.5 Hamiltonian for an Electrostatic Separator

The exact Hamiltonian for a separator is

$$H = -\sqrt{\left(\frac{1}{\beta_s} + p_t + ky\right)^2 - \frac{1}{\beta_s^2 \gamma_s^2} - (p_x^2 + p_y^2)} + \frac{1 + \eta \delta_s}{\beta_s} \left(p_t + \frac{1}{\beta_s}\right). \quad (5.78)$$

5.10.6 Exact Solution for an Electrostatic Separator

The Hamiltonian is an integral of motion, and is constant on any orbit. It is easily verified that the exact solution for the equations of motion is

$$\begin{aligned} x_2 &= x_1 + \frac{s}{|H|} p_{x1}, \\ p_{x2} &= p_{x1}, \\ y_2 &= \cosh\left(\frac{ks}{|H|}\right) y_1 + \frac{1}{k} \sinh\left(\frac{ks}{|H|}\right) p_{y1} + \frac{1}{k} \left(\cosh\left(\frac{ks}{|H|}\right) - 1\right) E_1, \\ p_{y2} &= k \sinh\left(\frac{ks}{|H|}\right) y_1 + \cosh\left(\frac{ks}{|H|}\right) p_{y1} + \sinh\left(\frac{ks}{|H|}\right) E_1, \\ t_2 &= \frac{L\eta\delta_s}{\beta_s} - \sinh\left(\frac{ks}{|H|}\right) y_1 - \frac{1}{k} \left(\cosh\left(\frac{ks}{|H|}\right) - 1\right) p_{y1} + t_1 - \frac{1}{k} \sinh\left(\frac{ks}{|H|}\right) E_1, \\ p_{t2} &= p_{t1}. \end{aligned} \quad (5.79)$$

5.10.7 Lie-Algebraic Map for an Electrostatic Separator

The Lie algebraic map for a separator can be derived from the TRANSPORT map listed below. We use the abbreviations

$$C = \cosh(kL), \quad S = \sinh(kL). \quad (5.80)$$

The transfer matrix is

$$F = \begin{pmatrix} 1 & L & 0 & 0 & 0 & 0 \\ 0 & 1 & 0 & 0 & 0 & 0 \\ 0 & 0 & C - \frac{kL}{\beta_s^2} S & \frac{1}{k} S & 0 & \frac{1}{k} (C - 1) - \frac{L}{\beta_s^2} S \\ 0 & 0 & k \left(S - \frac{kL}{\beta_s^2} C\right) & C & 0 & S - \frac{kL}{\beta_s^2} C \\ 0 & 0 & -\left(S - \frac{kL}{\beta_s^2} C\right) & -\frac{1}{k} (C - 1) & 1 & -\frac{1}{k} S + \frac{L}{\beta_s^2} C \\ 0 & 0 & 0 & 0 & 0 & 1 \end{pmatrix}. \quad (5.81)$$

The generators are

$$\begin{aligned}
f_1 &= -\frac{L\eta\delta_s}{\beta_s}p_t + \frac{1}{\beta_s}\left(S - \frac{kL}{\beta_s^2}C\right)y + \frac{1}{k\beta_s}(C-1)p_y, \\
f_3 &= \frac{L}{2\beta_s}p_x^2\left(C(ky+p_t) - Sp_y\right) + \left(\frac{k^2L^3}{6\beta_s^5} + \frac{L}{2\beta_s^3\gamma_s^2}\right)\left(C(ky+p_t) - Sp_y\right)^3 \\
&\quad - \frac{kL^2}{2\beta_s^3}\left(C(ky+p_t) - Sp_y\right)^2\left(S(ky+p_t) - Cp_y\right) + \frac{L}{2\beta_s}\left(C(ky+p_t) - Sp_y\right)\left(S(ky+p_t) - Cp_y\right)^2.
\end{aligned} \tag{5.82}$$

The generator f_4 is ignored, because its coefficients are all small of order one.

5.10.8 TRANSPORT Map for an Electrostatic Separator

The TRANSPORT map is the expansion of the exact map to second order. We use the abbreviations

$$C = \cosh(kL), \quad S = \sinh(kL). \tag{5.83}$$

The TRANSPORT map becomes

$$\begin{aligned}
x_2 &= x_1 + Lp_{x1} - \frac{L}{\beta_s}p_{x1}(ky_1 + p_{t1}), \\
p_{x2} &= p_{x1}, \\
y_2 &= \frac{1}{k\beta_s}(C-1) + \left(C - \frac{kL}{\beta_s^2}S\right)y_1 + \frac{1}{k}Sp_{y1} + \frac{1}{k}\left(C-1 - \frac{kL}{\beta_s^2}S\right)p_{t1} \\
&\quad + \frac{L}{2\beta_s}S(p_{x1}^2 + p_{y1}^2) - \frac{L}{2\beta_s}C(ky_1 + p_{t1})p_{y1} + \frac{L}{2\beta_s^3}\left(kLC + \frac{3}{\gamma_s^2}S\right)(ky_1 + p_{t1})^2, \\
p_{y2} &= \frac{1}{\beta_s}S + k\left(S - \frac{kL}{\beta_s^2}C\right)y_1 + Cp_{y1} + \left(S - \frac{kL}{\beta_s^2}C\right)p_{t1} \\
&\quad + \frac{kL}{2\beta_s}C(p_{x1}^2 + p_{y1}^2) - \frac{kL}{2\beta_s}S(ky_1 + p_{t1})p_{y1} + \frac{kL}{2\beta_s^3}\left(kLS + \frac{3}{\gamma_s^2}C\right)(ky_1 + p_{t1})^2, \\
t_2 &= \frac{L\eta\delta_s}{\beta_s} - \left(S - \frac{kL}{\beta_s^2}C\right)y_1 - \frac{1}{k}(C-1)p_{y1} + t_1 - \frac{1}{k}\left(S - \frac{kL}{\beta_s^2}C\right)p_{t1} \\
&\quad - \frac{L}{2\beta_s}C(p_{x1}^2 + p_{y1}^2) + \frac{L}{2\beta_s}S(ky_1 + p_{t1})p_{y1} - \frac{L}{2\beta_s^3}\left(kLS + \frac{3}{\gamma_s^2}C\right)(ky_1 + p_{t1})^2, \\
p_{t2} &= p_{t1}.
\end{aligned} \tag{5.84}$$

5.11 Misalignments

Misalignments are defined by three displacements and three angles:

Δx	Horizontal displacement,
Δy	Vertical displacement,
Δs	Longitudinal displacement.
θ	Rotation about the s -axis,
ϕ	Rotation about the x -axis,
ψ	Rotation about the y -axis.

Lie algebraic maps for misalignments have been derived in [14] as separate maps for each of the six components of the misalignment. In practice misalignments are not known to high precision. For this and for speed reasons, MAD uses a linear approximation of its effects. The six transformations are also combined into one map.

5.11.1 Exact Map for Misalignments

The three translational components can be composed to form a vector

$$V = \begin{pmatrix} v_1 \\ v_2 \\ v_3 \end{pmatrix} = \begin{pmatrix} \Delta x \\ \Delta y \\ \Delta s \end{pmatrix}. \quad (5.85)$$

and the three rotational components are represented by an orthogonal matrix

$$W = \begin{pmatrix} w_{11} & w_{12} & w_{13} \\ w_{21} & w_{22} & w_{23} \\ w_{31} & w_{32} & w_{33} \end{pmatrix} \quad (5.86)$$

$$= \begin{pmatrix} +\cos\theta\cos\psi - \sin\theta\sin\phi\sin\psi & -\cos\theta\sin\psi - \sin\theta\sin\phi\cos\psi & \sin\theta\cos\phi \\ \cos\phi\sin\psi & \cos\phi\cos\psi & \sin\phi \\ -\sin\theta\cos\psi - \cos\theta\sin\phi\sin\psi & +\sin\theta\sin\psi - \cos\theta\sin\phi\sin\psi & \cos\theta\cos\phi \end{pmatrix}.$$

The *misalignment pivot*, i. e. the point around which the rotation takes place, is the origin of the reference system at element entrance. The misalignment generates a canonical transformation. With the abbreviations

$$s_2 = w_{13}(x_1 - v_1) + w_{23}(y_1 - v_2) - w_{33}v_3, \quad (5.87)$$

$$p_{si} = \sqrt{1 + \frac{2p_{ti}}{\beta_s} + p_{ti}^2 - p_{xi}^2 - p_{yi}^2}, \quad i = 1, 2.$$

the transformation for the entrance can be written as

$$\begin{aligned} p_{x2} &= w_{11}p_{x1} + w_{21}p_{y1} + w_{31}p_{s1}, \\ p_{y2} &= w_{12}p_{x1} + w_{22}p_{y1} + w_{32}p_{s1}, \\ p_{t2} &= p_{t1}. \end{aligned} \quad (5.88)$$

$$\begin{aligned} x_2 &= w_{11}(x_1 - v_1) + w_{21}(y_1 - v_2) - w_{31}v_3 - \frac{p_{x2}}{p_{s2}}s_2, \\ y_2 &= w_{12}(x_1 - v_1) + w_{22}(y_1 - v_2) - w_{32}v_3 - \frac{p_{y2}}{p_{s2}}s_2, \\ t_2 &= t_1 + \frac{\beta_s^{-1} + p_{t2}}{p_{s2}}s_2. \end{aligned} \quad (5.89)$$

5.11.2 Linear Approximation for Misalignments

The linear part for defines the transfer matrix

$$R = \begin{pmatrix} +\frac{w_{22}}{w_{33}} + \frac{w_{22}}{w_{33}}s & -\frac{w_{12}}{w_{33}} - \frac{w_{12}}{w_{33}}s & 0 & 0 \\ 0 & w_{11} & 0 & w_{21} & 0 & \frac{w_{31}}{\beta_s} \\ -\frac{w_{21}}{w_{33}} - \frac{w_{21}}{w_{33}}s & +\frac{w_{11}}{w_{33}} + \frac{w_{11}}{w_{33}}s & 0 & 0 \\ 0 & w_{12} & 0 & w_{22} & 0 & \frac{w_{32}}{\beta_s} \\ \frac{w_{13}}{\beta_s w_{33}} & \frac{w_{13}}{\beta_s w_{33}}s & \frac{w_{23}}{\beta_s w_{33}} & \frac{w_{23}}{\beta_s w_{33}}s & 1 & \frac{s}{\beta_s^2 \gamma_s^2} \\ 0 & 0 & 0 & 0 & 0 & 1 \end{pmatrix}, \quad (5.90)$$

where

$$s_2 = -w_{13}v_1 - w_{23}v_2 - w_{33}v_3, \quad (5.91)$$

The Lie-algebraic map contains a first-order generator

$$f_1 = -\left(w_{13}(x - sp_x) + w_{23}(y - sp_y)\right)/w_{33} + (v_1p_x + v_2p_y + \beta_s^{-1}v_3p_t), \quad (5.92)$$

which gives rise to the kick, to be used for the TRANSPORT map:

$$\begin{aligned} \Delta x &= -(w_{22}v_1 - w_{12}v_2)/w_{33}, & \Delta p_x &= w_{31}, \\ \Delta y &= -(w_{11}v_2 - w_{21}v_1)/w_{33}, & \Delta p_y &= w_{32}, \\ \Delta t &= 0 & \Delta p_t &= 0. \end{aligned} \quad (5.93)$$

5.11.3 Misalignment at Exit

For the misalignment at element exit the displacement and rotation must be transformed to the new reference system as follows:

$$\bar{V} = W_e^{-1}(V + WV_e - V_e), \quad \bar{W} = W_e^{-1}WW_e, \quad (5.94)$$

where V_e and W_e are the displacement vector and rotation matrix describing the change of reference when proceeding through the element. The inverse transformation has the transfer matrix

$$F = \begin{pmatrix} \bar{w}_{11} - \frac{\bar{w}_{22}s}{\bar{w}_{33}} & \bar{w}_{21} & \frac{\bar{w}_{21}s}{\bar{w}_{33}} & 0 & \frac{\bar{w}_{13}s}{\beta_s \bar{w}_{33}} \\ 0 & \frac{\bar{w}_{22}}{\bar{w}_{33}} & 0 & -\frac{\bar{w}_{21}}{\bar{w}_{33}} & 0 & \frac{\bar{w}_{13}}{\beta_s \bar{w}_{33}} \\ \bar{w}_{12} & \frac{\bar{w}_{12}s}{\bar{w}_{33}} & \bar{w}_{22} - \frac{\bar{w}_{11}s}{\bar{w}_{33}} & 0 & -\frac{\bar{w}_{23}s}{\beta_s \bar{w}_{33}} \\ 0 & -\frac{\bar{w}_{12}}{\bar{w}_{33}} & 0 & \frac{\bar{w}_{11}}{\bar{w}_{33}} & 0 & \frac{\bar{w}_{23}}{\beta_s \bar{w}_{33}} \\ \frac{\bar{w}_{31}}{\beta_s} & 0 & \frac{\bar{w}_{32}}{\beta_s} & 0 & 1 & \frac{s}{\beta_s^2 \gamma_s^2} \\ 0 & 0 & 0 & 0 & 0 & 1 \end{pmatrix}, \quad (5.95)$$

were

$$s = (w_{13}v_1 + w_{23}v_2 + w_{33}v_3)/w_{33}. \quad (5.96)$$

The Lie-algebraic map contains the generator

$$f_1 = -(\bar{w}_{31}x + \bar{w}_{32}y) - \left((+\bar{w}_{22}\bar{v}_1 - \bar{w}_{12}\bar{v}_2)p_x + (-\bar{w}_{21}\bar{v}_1 + \bar{w}_{11}\bar{v}_2)p_y\right)/\bar{w}_{33}, \quad (5.97)$$

For the TRANSPORT map the orbit kicks are

$$\begin{aligned} \Delta x &= (w_{22}v_1 - w_{12}v_2)/w_{33}, & \Delta p_x &= -w_{31}, \\ \Delta y &= (w_{21}v_2 - w_{11}v_1)/w_{33}, & \Delta p_y &= -w_{32}, \\ \Delta t &= -\beta_s^{-1}s, & \Delta p_t &= 0. \end{aligned} \quad (5.98)$$

5.12 Rotation of Reference about the s -Axis

A rotation about the s -axis by an angle ψ is a linear map \mathcal{R} . It is completely described by the transfer matrix

$$R = \begin{pmatrix} \cos \psi & 0 & \sin \psi & 0 & 0 & 0 \\ 0 & \cos \psi & 0 & \sin \psi & 0 & 0 \\ -\sin \psi & 0 & \cos \psi & 0 & 0 & 0 \\ 0 & -\sin \psi & 0 & \cos \psi & 0 & 0 \\ 0 & 0 & 0 & 0 & 1 & 0 \\ 0 & 0 & 0 & 0 & 0 & 1 \end{pmatrix}, \quad (5.99)$$

5.13 Rotation of Reference About y -Axis

A rotation about the y -axis is a special case of a misalignment, derived in [14]. With the rotation angle ϕ we have the transfer matrix

$$F = \begin{pmatrix} \cos \phi & 0 & 0 & 0 & 0 & 0 \\ 0 & 1/\cos \phi & 0 & 0 & 0 & -\frac{1}{\beta_s} \tan \phi \\ 0 & 0 & 1 & 0 & 0 & 0 \\ 0 & 0 & 0 & 1 & 0 & 0 \\ \frac{1}{\beta_s} \sin \phi & 0 & 0 & 0 & 1 & 0 \\ 0 & 0 & 0 & 0 & 0 & 1 \end{pmatrix}. \quad (5.100)$$

and only the first-order generator

$$r_1 = -x \sin \phi \quad (5.101)$$

is considered. For the TRANSPORT map this represents a kick

$$\Delta p_x = -\tan \phi. \quad (5.102)$$

5.14 Beam-Beam Interactions

5.14.1 Lie-Algebraic Map for Beam-Beam Interaction

The beam-beam interaction is not yet implemented in MAD for the Lie algebraic formalism.

5.14.2 TRANSPORT Map for Beam-Beam Interactions

For a two-dimensional Gaussian particle distribution a closed formula for the electric field has been given in [1]. It uses the following parameters:

σ_x	The horizontal standard deviation of the opposite beam,
σ_y	The vertical standard deviation of the opposite beam,
Δx	The horizontal displacement of the opposite beam with respect to the ideal orbit.
Δy	The vertical displacement of the opposite beam with respect to the ideal orbit.
q	The number of unit charges per particle in the beam under consideration.

q'	The number of unit charges per particle in the opposite beam.
N'	The number of particles per unit length in the opposite beam, or the number of particles per bunch in the opposite beam.
r_e	The classical particle radius.
E	The energy per particle.

Note that the electric field can be computed from a scalar potential ϕ . The kick acting on the particle can be computed as

$$K_y + iK_x = \frac{qq'N'}{E}(\phi_y + i\phi_x) = \frac{2\sqrt{\pi}r_eN'}{r\gamma_s} \left(w(z_1) - \exp(z_2^2 - z_1^2)w(z_2) \right). \quad (5.103)$$

w is the complex error function

$$w(z) = \exp(-z^2) \left(1 + \frac{2i}{\sqrt{\pi}} \int_0^z \exp(t^2) dt \right), \quad (5.104)$$

and

$$\xi = x + \Delta x, \quad \eta = y + \Delta y, \quad r = \sqrt{2(\sigma_x^2 - \sigma_y^2)}, \quad z_1 = \frac{\xi}{r} + i\frac{\eta}{r}, \quad z_2 = \frac{\sigma_y\xi}{\sigma_x r} + i\frac{\sigma_x\eta}{\sigma_y r}. \quad (5.105)$$

For a round beam the above formula produces 0/0, and must be replaced by the limit

$$K_y + iK_x = \frac{qq'N'}{E}(\phi_y + i\phi_x) = \frac{2ir_eN'}{\gamma_s} \frac{1 - \exp(-(\xi^2 + \eta^2)/2\sigma^2)}{\xi + i\eta}. \quad (5.106)$$

For optical calculations we need the transfer matrix with respect to the actual orbit. It is the identity matrix except for the elements

$$R_{21} = \frac{qq'N'}{E}\phi_{xx}, \quad R_{23} = R_{41} = \frac{qq'N'}{E}\phi_{xy}, \quad R_{43} = \frac{qq'N'}{E}\phi_{yy}. \quad (5.107)$$

and the second-order coefficients

$$\begin{aligned} T_{211} &= \frac{qq'N'}{2E}\phi_{xxx}, & T_{213} &= T_{231} = T_{411} = \frac{qq'N'}{2E}\phi_{xxy}, \\ T_{233} &= T_{413} = T_{431} = \frac{qq'N'}{2E}\phi_{xyy}, & T_{433} &= \frac{qq'N'}{2E}\phi_{yyy}. \end{aligned} \quad (5.108)$$

which are found by differentiation of the kick. For an elliptic beam we find

$$\begin{aligned} \phi_{xx} &= \frac{2}{r^2} \left(-(x\phi_x + y\phi_y) + \rho_0 \left(1 - \frac{\sigma_y}{\sigma_x} \exp \left(-\frac{x^2}{2\sigma_x^2} - \frac{y^2}{2\sigma_y^2} \right) \right) \right), \\ \phi_{xy} &= \frac{2}{r^2} (-(x\phi_y - y\phi_x)), \\ \phi_{yy} &= \frac{2}{r^2} \left(+(x\phi_x + y\phi_y) - \rho_0 \left(1 - \frac{\sigma_x}{\sigma_y} \exp \left(-\frac{x^2}{2\sigma_x^2} - \frac{y^2}{2\sigma_y^2} \right) \right) \right), \\ \phi_{xxx} &= \frac{1}{r^2} \left(-\phi_x - (x\phi_{xx} + y\phi_{xy}) + \rho_0 \frac{x\sigma_y}{\sigma_x^3} \exp \left(-\frac{x^2}{2\sigma_x^2} - \frac{y^2}{2\sigma_y^2} \right) \right), \\ \phi_{xxy} &= \frac{1}{r^2} (-\phi_y - (x\phi_{xy} - y\phi_{xx})), \\ \phi_{xyy} &= \frac{1}{r^2} (+\phi_x - (x\phi_{yy} - y\phi_{xy})), \\ \phi_{yyy} &= \frac{1}{r^2} \left(+\phi_y + (x\phi_{xy} + y\phi_{yy}) - \rho_0 \frac{y\sigma_x}{\sigma_y^3} \exp \left(-\frac{x^2}{2\sigma_x^2} - \frac{y^2}{2\sigma_y^2} \right) \right), \end{aligned} \quad (5.109)$$

and for a round beam

$$\begin{aligned}
\phi_{xx} &= \rho_0 \left(-\frac{x^2 - y^2}{(x^2 + y^2)^2} (1 - E) + \frac{x^2}{\sigma^2(x^2 + y^2)} E \right), \\
\phi_{xy} &= \rho_0 \left(-\frac{2xy}{(x^2 + y^2)^2} (1 - E) + \frac{xy}{\sigma^2(x^2 + y^2)} E \right), \\
\phi_{yy} &= \rho_0 \left(+\frac{x^2 - y^2}{(x^2 + y^2)^2} (1 - E) + \frac{y^2}{\sigma^2(x^2 + y^2)} E \right), \\
\phi_{xxx} &= \rho_0 \left(+\frac{x^3 - 3xy^2}{(x^2 + y^2)^3} (1 - E) - \frac{x^3 - 3xy^2}{2\sigma^2(x^2 + y^2)^2} E - \frac{x^3}{2\sigma^4(x^2 + y^2)} E \right), \\
\phi_{xxy} &= \rho_0 \left(+\frac{3x^2y - y^3}{(x^2 + y^2)^3} (1 - E) - \frac{3x^2y - y^3}{2\sigma^2(x^2 + y^2)^2} E - \frac{x^2y}{2\sigma^4(x^2 + y^2)} E \right), \\
\phi_{xyy} &= \rho_0 \left(-\frac{x^3 - 3xy^2}{(x^2 + y^2)^3} (1 - E) + \frac{x^3 - 3xy^2}{2\sigma^2(x^2 + y^2)^2} E - \frac{xy^2}{2\sigma^4(x^2 + y^2)} E \right), \\
\phi_{yyy} &= \rho_0 \left(-\frac{3x^2y - y^3}{(x^2 + y^2)^3} (1 - E) + \frac{3x^2y - y^3}{2\sigma^2(x^2 + y^2)^2} E - \frac{y^3}{2\sigma^4(x^2 + y^2)} E \right),
\end{aligned} \tag{5.110}$$

where

$$E = \exp \left(\frac{x^2 + y^2}{2\sigma^2} \right). \tag{5.111}$$

It is easy to check that

$$\phi_{xx} + \phi_{yy} = \rho, \quad \phi_{xxx} + \phi_{xyy} = \frac{\partial \rho}{\partial x}, \quad \phi_{xxy} + \phi_{yyy} = \frac{\partial \rho}{\partial y}. \tag{5.112}$$

where ρ is the relevant “space charge”.

Chapter 6. Uncoupled Linear Optics

In MAD lattice functions are always computed with respect to the computed closed orbit. Coupling is always ignored in OPTICS and ignored by default in TWISS. For a description of coupling effects refer to Chapters 7 and 8. The methods used for uncoupled calculations are described in [2, 6]. In the commands TWISS and OPTICS MAD uses TRANSPORT maps except for thin multipoles, where the exact thin multipole maps are used. When the closed orbit deviates from the design orbit, MAD uses the Jacobian of the TRANSPORT map for the linear transfer matrix. For thick elements this may perturb the symplecticity of the map. For this reason the Jacobian is by default made symplectic according to Section 4.7. Symplectification is controlled by the option SYMPLEC.

6.1 Courant-Snyder Lattice Functions

By default the TWISS and OPTICS commands track the lattice functions for *periodic* initial conditions. Any initial conditions specified (except β_x and β_y) override the periodic initial conditions.

However, if an initial condition is specified for at least one of β_x and β_y , the closed orbit is not computed, and MAD tracks the lattice functions for the initial conditions specified. Unspecified initial conditions are set to zero in this case. Unwary users may fool MAD into thinking that a value has been given for β_x . The most frequent case is entering the CENTRE flag on an OPTICS command in the American spelling:

```
OPTICS, CENTER ! should read OPTICS, CENTRE
```

The decoder assumes in this case that CENTRE is the name of an undefined global parameter, sets it to zero, and stores it in the slot for the initial value of β_x .

6.1.1 Initial Conditions for the Periodic Case

When the COUPLE option is not set, MAD computes the lattice functions as defined in [6]. Note that the integer parts of the betatron phases may be wrong when a beam line contains LUMP elements, or when it contains negative element lengths, as in these cases an incorrect branch of the arctangent function may be taken.

For the functions β, α, μ MAD uses the relevant diagonal blocks of the transfer matrix, denoted below as

$$R = \begin{pmatrix} R_{11} & R_{12} \\ R_{21} & R_{22} \end{pmatrix} \quad (6.1)$$

For optimal numeric precision MAD uses the following formulas for the tunes:

$$\begin{aligned} \cos \mu &= (R_{11} + R_{22})/2, \\ \sin \mu &= \text{sign } R_{12} \cdot \sqrt{R_{12}R_{21} - (R_{11} - R_{22})^2/4}, \\ Q &= \frac{1}{2\pi} \arctan \frac{\sin \mu}{\cos \mu} \end{aligned} \quad (6.2)$$

and the following for the initial lattice functions:

$$\begin{aligned} \beta_0 &= R_{12}/\sin \mu, \\ \alpha_0 &= (R_{11} - R_{22})/(2 \sin \mu). \end{aligned} \quad (6.3)$$

The way $\sin \mu$ is computed greatly improves the numerical accuracy for μ when its value is close to $1/2$.

6.1.2 Tracking the Lattice Functions

The formulas for advancing through an element are well known:

$$\begin{aligned}\beta_2 &= \frac{1}{\beta_1} ((R_{11}\beta_1 - R_{12}\alpha_1)^2 + R_{12}^2), \\ \alpha_2 &= -\frac{1}{\beta_1} ((R_{11}\beta_1 - R_{12}\alpha_1)(R_{21}\beta_1 - R_{22}\alpha_1) + R_{12}R_{22}), \\ \mu_2 &= \mu_1 + \arctan \frac{R_{12}}{R_{11}\beta_1 - R_{12}\alpha_1}.\end{aligned}\tag{6.4}$$

They are valid for both planes.

6.2 Dispersion

MAD computes the dispersion only for static machines, i. e. for machines whose momentum is constant.

6.2.1 Initial Values for Dispersion

Knowing the TRANSPORT map with respect to the closed orbit for one turn enables us to find two derivatives of the closed orbit with respect to p_t , named the first- and second-order dispersions. Defining

$$D = d/dp_t \tag{6.5}$$

the first derivative of the closed orbit

$$Z_0 = \begin{pmatrix} x_0 \\ p_{x0} \\ y_0 \\ p_{y0} \\ t_0 \\ p_{t0} \end{pmatrix}, \tag{6.6}$$

the first-order dispersion is its first derivative with respect to p_t :

$$DZ_0 = \begin{pmatrix} dx/dp_t \\ dp_x/dp_t \\ dy/dp_t \\ dp_y/dp_t \\ 0 \\ dp_{t0}/dp_t \end{pmatrix} = \begin{pmatrix} Dx \\ Dp_x \\ Dy \\ Dp_y \\ 0 \\ 1 \end{pmatrix} = \begin{pmatrix} Dz_1 \\ Dz_2 \\ Dz_3 \\ Dz_4 \\ Dz_5 \\ Dz_6 \end{pmatrix}. \tag{6.7}$$

The second derivative of the closed orbit with respect to p_t is the second-order dispersion:

$$D^2Z_0 = \begin{pmatrix} D^2z_1 \\ D^2z_2 \\ D^2z_3 \\ D^2z_4 \\ D^2z_5 \\ D^2z_6 \end{pmatrix} = \begin{pmatrix} d^2x/dp_t^2 \\ d^2p_x/dp_t^2 \\ d^2y/dp_t^2 \\ d^2p_y/dp_t^2 \\ 0 \\ 0 \end{pmatrix} = \begin{pmatrix} D^2x \\ D^2p_x \\ D^2y \\ D^2p_y \\ 0 \\ 1 \end{pmatrix} \tag{6.8}$$

The dispersions are computed following a method developed in [20]. With respect to the closed orbit the orbit behaves as

$$Z = Z_0 + p_t \cdot DZ_0 + \frac{p_t^2}{2} \cdot D^2 Z_0 + o(p_t^3) \quad (6.9)$$

The vectors DZ_0 and $D^2 Z_0$ are found by substitution of this expression in the TRANSPORT map and by separation of like powers of p_t . Substitution produces

$$\begin{aligned} z_k + p_t \cdot Dz_k + \frac{p_t^2}{2} \cdot D^2 z_k &= \sum_{l=1}^6 R_{kl}(z_l + p_t \cdot Dz_l + \frac{p_t^2}{2} \cdot D^2 z_l) + \\ &\sum_{l=1}^6 \sum_{m=1}^6 T_{klm}(z_l + p_t \cdot Dz_l + \frac{p_t^2}{2} \cdot D^2 z_l)(z_m + p_t \cdot Dz_m + \frac{p_t^2}{2} \cdot D^2 z_m) + o(p_t^3). \end{aligned} \quad (6.10)$$

The terms in p_t are:

$$Dz_k = \sum_{l=1}^6 R_{kl} Dz_l \quad (6.11)$$

Using $Dz_5 = 0, Dz_6 = 1$ and defining

$$A = \begin{pmatrix} R_{11} & R_{12} & R_{13} & R_{14} \\ R_{21} & R_{22} & R_{23} & R_{24} \\ R_{31} & R_{32} & R_{33} & R_{34} \\ R_{41} & R_{42} & R_{43} & R_{44} \end{pmatrix}, \quad (6.12)$$

we obtain

$$\begin{pmatrix} Dz_1 \\ Dz_2 \\ Dz_3 \\ Dz_4 \end{pmatrix} = (A - I)^{-1} \begin{pmatrix} R_{16} \\ R_{26} \\ R_{36} \\ R_{46} \end{pmatrix}. \quad (6.13)$$

The terms in p_t^2 give

$$D^2 z_k = \sum_{l=1}^6 R_{kl} D^2 z_l + 2 \sum_{l=1}^6 \sum_{m=1}^6 T_{klm} Dz_l Dz_m, \quad (6.14)$$

thus

$$\begin{pmatrix} D^2 z_1 \\ D^2 z_2 \\ D^2 z_3 \\ D^2 z_4 \end{pmatrix} = 2(A - I)^{-1} \begin{pmatrix} \sum_{l=1}^6 \sum_{m=1}^6 T_{1lm} Dz_l Dz_m \\ \sum_{l=1}^6 \sum_{m=1}^6 T_{2lm} Dz_l Dz_m \\ \sum_{l=1}^6 \sum_{m=1}^6 T_{3lm} Dz_l Dz_m \\ \sum_{l=1}^6 \sum_{m=1}^6 T_{4lm} Dz_l Dz_m \end{pmatrix}. \quad (6.15)$$

6.2.2 Tracking the Dispersion

The first-order dispersion is tracked through an element as follows:

$$Dz \leftarrow RDz. \quad (6.16)$$

By differentiation we find for the second-order dispersion:

$$D^2 z \leftarrow RD^2 z + DRDz. \quad (6.17)$$

The total derivative $DR = dR/dp_t$ of the transfer matrix must take into account the displacement of the orbit due to the dispersion. The particle orbit can be related to the dispersion orbit Dz by

$$Z = Z_0 + p_t \cdot Dz + \frac{p_t^2}{2} D^2 Z. \quad (6.18)$$

It transforms according to the equation

$$z_k + p_t \cdot Dz_k + \dots \leftarrow \sum_{l=1}^6 R_{kl}(z_l + p_t \cdot Dz_l + \dots) + \sum_{l=1}^6 \sum_{m=1}^6 T_{klm}(z_l + p_t \cdot Dz_l + \dots)(z_m + p_t \cdot Dz_m + \dots). \quad (6.19)$$

The total derivative of the transfer matrix is found by partial differentiation as

$$DR_{kl} = \frac{dR_{kl}}{dp_t} = 2 \sum_{m=1}^6 T_{klm} Dz_m. \quad (6.20)$$

6.3 Chromatic Effects

The chromatic effects are computed for the uncoupled case only.

6.3.1 Initial Values for Chromatic Functions

Using the total derivative of the transfer matrix for one turn we find the following equations:

$$\begin{aligned} \frac{1}{2}(DR_{11} + DR_{22}) &= D(\cos \mu) = -D\mu \sin \mu, \\ DR_{12} &= D(\beta \sin \mu) = D\beta \sin \mu - \beta D\mu \cos \mu, \\ \frac{1}{2}(DR_{11} - DR_{22}) &= D(\alpha \sin \mu) = D\alpha \sin \mu - \alpha D\mu \cos \mu. \end{aligned} \quad (6.21)$$

The derivative $DR = dR/dp_t$ of R has been given in Section 6.2.2. From these we derive the chromaticity

$$\begin{aligned} D\mu &= \frac{DR_{11} + DR_{22}}{2 \sin \mu}, \\ DQ &= \frac{D\mu}{2\pi}, \end{aligned} \quad (6.22)$$

and the initial values for the chromatic functions

$$\begin{aligned} D\beta_0 &= (DR_{12} + \beta_0 D\mu \cos \mu) / \sin \mu, \\ D\alpha_0 &= (DR_{11} - DR_{22} + 2\alpha_0 D\mu \cos \mu) / (2 \sin \mu), \\ B_0 &= D\beta_0 / \beta_0, \\ A_0 &= (D\alpha_0 \beta_0 - D\beta_0 \alpha_0) / \beta_0, \\ W_0 &= \sqrt{B_0^2 + A_0^2}, \\ \Phi_0 &= \arctan(A_0 / B_0). \end{aligned} \quad (6.23)$$

6.3.2 Tracking the Chromatic Functions

The derivative of the phase advance by p_t is found easily:

$$D\mu_2 = D\mu_2 = D\mu_1 + \frac{(R_{11}DR_{12} - R_{12}DR_{11})\beta_1 - R_{12}(R_{11}D\beta - R_{12}D\alpha)}{(R_{11}\beta - R_{12}\alpha)^2 + R_{P12}^2}. \quad (6.24)$$

Given the values W_1 and Φ_1 one may write

$$\begin{aligned}
A_1 &= W_1 \cos \Phi_1, \\
B_1 &= W_1 \sin \Phi_1, \\
D\beta_1 &= B_1 \beta_1, \\
D\alpha_1 &= A_1 + B_1 \alpha_1, \\
B_2 &= \frac{1}{\beta_1 \beta_2} \left(((R_{11}\beta_1 - R_{12}\alpha_1)^2 - R_{12}^2) B_1 - 2(R_{11}\beta_1 - R_{12}\alpha_1) R_{12} A_1 \right) \\
&\quad + \frac{2}{\beta_2} \left((R_{11}\beta_1 - R_{12}\alpha_1) D R_{11} - (R_{11}\alpha_1 - R_{12}\gamma_1) D R_{12} \right), \\
A_2 &= \frac{1}{\beta_1 \beta_2} \left(((R_{11}\beta_1 - R_{12}\alpha_1)^2 - R_{12}^2) A_1 + 2(R_{11}\beta_1 - R_{12}\alpha_1) R_{12} B_1 \right) \\
&\quad - \frac{1}{\beta_2} \left((R_{11}\beta_1 - R_{12}\alpha_1) (D R_{11} \alpha_2 + D R_{21} \beta_2) - (R_{11}\alpha_1 - R_{12}\gamma_1) (D R_{12} \alpha_2 + D R_{22} \beta_2) \right. \\
&\quad \left. + (R_{11} D R_{12} - R_{12} D R_{11}) \right), \\
W_2 &= \sqrt{B_2^2 + A_2^2}, \\
\Phi_2 &= \arctan \frac{A_2}{B_2}.
\end{aligned} \tag{6.25}$$

Note that the “partial” chromaticity $D\mu_2 - D\mu_1$ for a piece of the ring depends not only on the transfer map, but also on the initial values $D\beta_1$ and $D\alpha_1$.

Chapter 7. Transverse Coupling (Method by Edwards and Teng)

7.1 Initial Values

When the COUPLE option is set, the TWISS command uses a method similar to reference [22]. Consider the linear transfer map M in *two* degrees of freedom partitioned into four 2×2 blocks:

$$M = \begin{pmatrix} m_{11} & m_{12} & m_{13} & m_{14} \\ m_{21} & m_{22} & m_{23} & m_{24} \\ m_{31} & m_{32} & m_{33} & m_{34} \\ m_{41} & m_{42} & m_{43} & m_{44} \end{pmatrix} = \begin{pmatrix} A & B \\ C & D \end{pmatrix}. \quad (7.1)$$

The 4-dimensional phase space vector shall also be partitioned according to the horizontal and vertical planes. Edwards and Teng introduce a “symplectic rotation”

$$R = \begin{pmatrix} I \cos \phi & \bar{R} \sin \phi \\ -R \sin \phi & I \cos \phi \end{pmatrix} \quad (7.2)$$

R is a 2×2 matrix with unit determinant, and \bar{R} denotes its symplectic conjugate:

$$R = \begin{pmatrix} a & b \\ c & d \end{pmatrix}, \quad |R| = \begin{vmatrix} a & b \\ c & d \end{vmatrix} = 1, \quad \bar{R} = \begin{pmatrix} d & -b \\ -c & a \end{pmatrix}. \quad (7.3)$$

This leaves three free parameters for the elements of R , and a fourth parameter ϕ . Edwards and Teng then determine R such that M conjugated with R becomes block diagonal:

$$RMR^{-1} = \begin{pmatrix} E & 0 \\ 0 & F \end{pmatrix} \quad (7.4)$$

If $|B + \bar{C}| < 0$ both ϕ and all elements of R become imaginary. This may be avoided by redefining

$$R = \frac{1}{\sqrt{1 + |\bar{R}|}} \begin{pmatrix} I & \bar{R} \\ -R & I \end{pmatrix}. \quad (7.5)$$

where all four elements of R are free parameters. The solutions is:

$$\begin{aligned} R &= - \left(\frac{1}{2}(\text{Tr } A - \text{Tr } D) + \text{sign}(|B + \bar{C}|) \sqrt{|B + \bar{C}| + \frac{1}{4}(\text{Tr } A - \text{Tr } D)^2} \right)^{-1} (B + \bar{C}), \\ E &= A - BR, \quad F = D + \bar{R}C. \end{aligned} \quad (7.6)$$

The block diagonal matrix can be parametrised as usual. From the eigenvectors of the conjugated system

$$V_1 = \begin{pmatrix} \sqrt{\beta_1} & 0 \\ \frac{\alpha_1}{\sqrt{\beta_1}} & \frac{1}{\sqrt{\beta_1}} \end{pmatrix}, \quad V_2 = \begin{pmatrix} \sqrt{\beta_2} & 0 \\ \frac{\alpha_2}{\sqrt{\beta_2}} & \frac{2}{\sqrt{\beta_2}} \end{pmatrix} \quad (7.7)$$

one may find the eigenvectors of the coupled system:

$$V_1 = \frac{1}{\sqrt{1 + |\bar{R}|}} \begin{pmatrix} V_1 \\ \bar{R}V_1 \end{pmatrix}, \quad V_2 = \frac{1}{\sqrt{1 + |\bar{R}|}} \begin{pmatrix} -RV_2 \\ V_2 \end{pmatrix}. \quad (7.8)$$

7.2 Tracking the Edwards-Teng Functions

For tracking the coupled lattice functions we assume that the transfer matrix for one element is partitioned as above:

$$R_e = \begin{pmatrix} A_e & B_e \\ C_e & D_e \end{pmatrix}, \quad (7.9)$$

The symplectic rotation at element entrance changes the diagonal blocks to

$$E_e = (A_e - B_e R_1) / \sqrt{|A_e - B_e R_1|}, \quad F_e = (D_e + \overline{R_1} C_e) / \sqrt{|A_e - B_e R_1|}, \quad (7.10)$$

and the new coupling matrix at exit becomes

$$R_2 = -(C_e - D_e R_1) \overline{(A_e - B_e R_1)} / |A_e - B_e R_1|. \quad (7.11)$$

We may track the decoupled lattice functions using the matrices E_e for mode 1 and F_e for mode 2.

Chapter 8. Fully Coupled Motion

Throughout this chapter we make the assumption that all eigenvalues λ_k of a real symplectic matrix \mathbf{M} are distinct. This implies that the eigenvectors \mathbf{v}_k are all linearly independent and form a basis in $2N$ -dimensional space. Most facts derived remain valid when this condition is relaxed, but the proofs become much more difficult.

8.1 Eigenvectors of a $2N \times 2N$ Symplectic Matrix

An eigenvector of a general matrix \mathbf{M} obeys the relation

$$\mathbf{M}\mathbf{v}_k = \lambda_k \mathbf{v}_k. \quad (8.1)$$

where λ_k is the corresponding eigenvalue. If all eigenvalues λ_k are distinct the eigenvectors \mathbf{v}_k are all linearly independent and form a basis in $2N$ -dimensional space. Thus an arbitrary vector \mathbf{z} can be uniquely decomposed in terms of the eigenvectors:

$$\mathbf{z} = \sum_{k=1}^{2N} c_k \mathbf{v}_k = \mathbf{V}\mathbf{c}, \quad (8.2)$$

where the eigenvectors are arranged as the column vectors of a matrix \mathbf{V} . The vector

$$\mathbf{c} = \begin{pmatrix} c_1 \\ c_2 \\ \vdots \\ c_{2N} \end{pmatrix} = \mathbf{V}^{-1}\mathbf{z}, \quad (8.3)$$

is unique. Using the diagonal matrix formed from the eigenvalues

$$\Lambda = \begin{pmatrix} \lambda_1 & & \\ & \ddots & \\ & & \lambda_{2n} \end{pmatrix}, \quad (8.4)$$

the linear transformation for \mathbf{z} can be written as

$$\mathbf{M}\mathbf{z} = \mathbf{M}\mathbf{V}\mathbf{c} = (\mathbf{M}\mathbf{V})\mathbf{c} = (\mathbf{V}\Lambda)(\mathbf{V}^{-1}\mathbf{z}) = \mathbf{V}\Lambda\mathbf{V}^{-1}\mathbf{z}. \quad (8.5)$$

Since \mathbf{z} was arbitrary, there must hold an identity

$$\mathbf{M} = \mathbf{V}\Lambda\mathbf{V}^{-1}. \quad (8.6)$$

This representation is known as the Jordan normal form of the matrix. By definition two eigenvectors \mathbf{v}_k and \mathbf{v}_l obey the equations

$$\mathbf{M}\mathbf{v}_k = \lambda_k \mathbf{v}_k, \quad \mathbf{M}\mathbf{v}_l = \lambda_l \mathbf{v}_l. \quad (8.7)$$

The bilinear form

$$(\mathbf{M}\mathbf{v}_k)^T \mathbf{S} (\mathbf{M}\mathbf{v}_l) = (\lambda_k \mathbf{v}_k)^T \mathbf{S} (\lambda_l \mathbf{v}_l), \quad (8.8)$$

built using the matrix

$$\mathbf{S} = \begin{pmatrix} 0 & 1 & & \\ -1 & 0 & & \\ & & \ddots & \\ & & & 0 & 1 \\ & & & -1 & 0 \end{pmatrix} \quad (8.9)$$

is asymmetric, therefore it vanishes identically for $k = l$. Evaluation of both sides of the equation and use of the symplecticity of the transfer matrix \mathbf{M} leads to

$$\mathbf{v}_k^T (\mathbf{M}^T \mathbf{S} \mathbf{M}) \mathbf{v}_l = \mathbf{v}_k^T \mathbf{S} \mathbf{v}_l = \lambda_k \lambda_l \mathbf{v}_k^T \mathbf{S} \mathbf{v}_l. \quad (8.10)$$

This equation can only be true if either $\lambda_k \lambda_l = 1$ or if $\mathbf{v}_k^T \mathbf{S} \mathbf{v}_l = 0$.

It is well known that a symplectic matrix with all eigenvalues distinct has N pairs of eigenvalues for which $\lambda_k \lambda_l = 1$. If the motion is stable, these eigenvalue and the corresponding eigenvectors also form complex conjugate pairs. Due to the asymmetry of the bilinear form for all k

$$\mathbf{v}_k^T \mathbf{S} \mathbf{v}_k \equiv 0. \quad (8.11)$$

For all k the vector \mathbf{v}_k^* is an eigenvector with the eigenvalue λ_k^* . Inserting the eigenvectors \mathbf{v}_k and \mathbf{v}_k^* in equation 8.10 one gets an identity, and

$$\mathbf{v}_k^T \mathbf{S} \mathbf{v}_k^* = \text{arbitrary}. \quad (8.12)$$

where the arbitrary quantity on the right-hand side can be chosen freely. For all other pairs, $\lambda_k \lambda_l \neq 1$, and therefore equation 8.10 leads to the identities

$$\mathbf{v}_k^T \mathbf{S} \mathbf{v}_l \equiv 0, \quad \mathbf{v}_k^T \mathbf{S} \mathbf{v}_l^* \equiv 0. \quad (8.13)$$

8.2 Everything is Real ...

Since the transfer matrix is real, the eigenvalues and eigenvectors form complex conjugate pairs. Decomposing the eigenvalues and eigenvectors into their real and imaginary parts:

$$\mathbf{v}_k = \mathbf{a}_k + i\mathbf{b}_k, \quad \lambda_k = \cos \mu_k \pm i \sin \mu_k. \quad (8.14)$$

For stable motion the μ_k are real, but the following formulae are also valid if this is not the case. The definitions of the eigenvectors become

$$\mathbf{M} \mathbf{v}_k = \mathbf{M}(\mathbf{a}_k + i\mathbf{b}_k) = (\cos \mu_k \mathbf{a}_k - \sin \mu_k \mathbf{b}_k) + i(\cos \mu_k \mathbf{b}_k + \sin \mu_k \mathbf{a}_k). \quad (8.15)$$

The “real eigenvector matrix”

$$\mathbf{W} = \begin{pmatrix} a_{1,1} & b_{1,1} & a_{2,1} & b_{2,1} & \dots & a_{N,1} & b_{N,1} \\ a_{1,2} & b_{1,2} & a_{2,2} & b_{2,2} & \dots & a_{N,2} & b_{N,2} \\ \vdots & \vdots & \vdots & \vdots & \dots & \vdots & \vdots \\ a_{1,2N} & b_{1,2N} & a_{2,2N} & b_{2,2N} & \dots & a_{N,2N} & b_{N,2N} \end{pmatrix}, \quad (8.16)$$

is built by arranging the real and imaginary parts of the eigenvectors as alternating columns of the matrix. From Equation 8.15 and 8.16 it is obvious that the matrix \mathbf{W} transforms like

$$\mathbf{M} \mathbf{W} = \mathbf{W} \mathbf{R}, \quad (8.17)$$

where \mathbf{R} is the matrix

$$\mathbf{R} = \begin{pmatrix} \cos \mu_1 & \sin \mu_1 & & & & & \\ -\sin \mu_1 & \cos \mu_1 & & & & & \\ & & \ddots & & & & \\ & & & \cos \mu_N & \sin \mu_N & & \\ & & & -\sin \mu_N & \cos \mu_N & & \end{pmatrix}, \quad (8.18)$$

which rotates the phase space coordinates pairwise. Again an arbitrary vector \mathbf{z} can be written uniquely as

$$\mathbf{z} = \mathbf{W}\mathbf{d}, \quad \Rightarrow \quad \mathbf{d} = \mathbf{W}^{-1}\mathbf{z}. \quad (8.19)$$

In the same way as for the complex form one finds

$$\mathbf{M}\mathbf{z} = \mathbf{M}\mathbf{W}\mathbf{d} = (\mathbf{M}\mathbf{W})\mathbf{d} = (\mathbf{W}\mathbf{R})(\mathbf{W}^{-1}\mathbf{z}) = \mathbf{W}\mathbf{R}\mathbf{W}^{-1}\mathbf{z}. \quad (8.20)$$

and, since \mathbf{z} is arbitrary, the transfer matrix \mathbf{M} has the real representation

$$\mathbf{M} = \mathbf{W}\mathbf{R}\mathbf{W}^{-1}. \quad (8.21)$$

This is real equivalent to the Jordan normal form. The linear transformation for one turn around the machine can be written as

$$\mathbf{z}(C) = \mathbf{M}\mathbf{z}(0) = \mathbf{W}\mathbf{R}\mathbf{W}^{-1}\mathbf{z}(0), \quad (8.22)$$

Pre-multiplying with \mathbf{W}^{-1} gives

$$\mathbf{W}^{-1}\mathbf{z}(C) = \mathbf{R}\mathbf{W}^{-1}\mathbf{z}(0). \quad (8.23)$$

Now define the vector of *normalised coordinates*

$$\mathbf{u} = \mathbf{W}^{-1}\mathbf{z} = \begin{pmatrix} u_1 \\ u_2 \\ \vdots \\ u_{2N-1} \\ u_{2N} \end{pmatrix}, \quad (8.24)$$

and partition this vector into pairs of coordinates. Each pair is transformed under the action of \mathbf{R} like

$$\begin{pmatrix} u_{2k-1}(C) \\ u_{2k}(C) \end{pmatrix} = \begin{pmatrix} u_{2k-1}(0) \cos \mu_k & + & u_{2k}(0) \sin \mu_k \\ -u_{2k-1}(0) \sin \mu_k & + & u_{2k}(0) \cos \mu_k \end{pmatrix}. \quad (8.25)$$

Thus the quantities $I_k = \frac{1}{2}(u_{2k-1}^2 + u_{2k}^2)$ are invariant under the motion.

In Section 8.1 we introduced the bilinear form

$$\mathbf{v}_k^T \mathbf{S} \mathbf{v}_l = (\mathbf{a}_k + i\mathbf{b}_k)^T \mathbf{S} (\mathbf{a}_l + i\mathbf{b}_l) = (\mathbf{a}_k^T \mathbf{S} \mathbf{a}_l - \mathbf{b}_k^T \mathbf{S} \mathbf{b}_l) + i(\mathbf{a}_k^T \mathbf{S} \mathbf{b}_l + \mathbf{b}_k^T \mathbf{S} \mathbf{a}_l). \quad (8.26)$$

For various choices of k and l it has the values

$$\begin{aligned} \mathbf{v}_k^T \mathbf{S} \mathbf{v}_k &= (\mathbf{a}_k^T \mathbf{S} \mathbf{a}_k - \mathbf{b}_k^T \mathbf{S} \mathbf{b}_k) + i(\mathbf{a}_k^T \mathbf{S} \mathbf{b}_k + \mathbf{b}_k^T \mathbf{S} \mathbf{a}_k) = 0, \\ \mathbf{v}_k^T \mathbf{S} \mathbf{v}_k^* &= (\mathbf{a}_k^T \mathbf{S} \mathbf{a}_k + \mathbf{b}_k^T \mathbf{S} \mathbf{b}_k) + i(-\mathbf{a}_k^T \mathbf{S} \mathbf{b}_k + \mathbf{b}_k^T \mathbf{S} \mathbf{a}_k) = -2i, \\ \mathbf{v}_k^T \mathbf{S} \mathbf{v}_l &= (\mathbf{a}_k^T \mathbf{S} \mathbf{a}_l - \mathbf{b}_k^T \mathbf{S} \mathbf{b}_l) + i(\mathbf{a}_k^T \mathbf{S} \mathbf{b}_l + \mathbf{b}_k^T \mathbf{S} \mathbf{a}_l) = 0, \\ \mathbf{v}_k^T \mathbf{S} \mathbf{v}_l^* &= (\mathbf{a}_k^T \mathbf{S} \mathbf{a}_l + \mathbf{b}_k^T \mathbf{S} \mathbf{b}_l) + i(-\mathbf{a}_k^T \mathbf{S} \mathbf{b}_l + \mathbf{b}_k^T \mathbf{S} \mathbf{a}_l) = 0, \end{aligned} \quad (8.27)$$

where the right-hand side of the second equation has been chosen so as to achieve a simple normalisation of the eigenvectors. Note that this still leaves us free to multiply each eigenvector by a phase factor $\exp(i\mu)$ which will be determined later. Solving equations 8.27 for $k = l$ we obtain:

$$\mathbf{a}_k^T \mathbf{S} \mathbf{a}_k = \mathbf{b}_k^T \mathbf{S} \mathbf{b}_k = 0, \quad \mathbf{a}_k^T \mathbf{S} \mathbf{b}_k = -\mathbf{b}_k^T \mathbf{S} \mathbf{a}_k = 1. \quad (8.28)$$

and for $k \neq l$:

$$\mathbf{a}_k^T \mathbf{S} \mathbf{a}_l = \mathbf{a}_k^T \mathbf{S} \mathbf{b}_l = \mathbf{b}_k^T \mathbf{S} \mathbf{a}_l = \mathbf{b}_k^T \mathbf{S} \mathbf{b}_l = 0. \quad (8.29)$$

These results can be combined in matrix form and result in the condition for \mathbf{W}

$$\mathbf{W}^T \mathbf{S} \mathbf{W} = \mathbf{S}. \quad (8.30)$$

It turns out that with \mathbf{W} is symplectic under the normalisation chosen. Since \mathbf{W} is symplectic, its inverse is

$$\mathbf{W}^{-1} = \mathbf{S}^T \mathbf{W}^T \mathbf{S} = \mathbf{S}^T \begin{pmatrix} a_{1,1} & a_{1,2} & \cdots & a_{1,2N} \\ b_{1,1} & b_{1,2} & \cdots & b_{1,2N} \\ a_{2,1} & a_{2,2} & \cdots & a_{2,2N} \\ b_{2,1} & b_{2,2} & \cdots & b_{2,2N} \\ \vdots & \vdots & \ddots & \vdots \\ a_{N,1} & a_{N,2} & \cdots & a_{N,2N} \\ b_{N,1} & b_{N,2} & \cdots & b_{N,2N} \end{pmatrix} \mathbf{S}. \quad (8.31)$$

The components of $\mathbf{u} = \mathbf{W}^{-1} \mathbf{z}$ are

$$u_{2k-1} = \mathbf{b}_k^T \mathbf{S} \mathbf{z}, \quad u_{2k} = -\mathbf{a}_k^T \mathbf{S} \mathbf{z}, \quad (8.32)$$

and the invariants become

$$I_k = \frac{1}{2} \left((\mathbf{b}_k^T \mathbf{S} \mathbf{z})^2 + (\mathbf{a}_k^T \mathbf{S} \mathbf{z})^2 \right) = \frac{1}{2} \left(\left(\sum_{i=1}^N (a_{k,2i-1} \mathbf{z}_{2i} - a_{k,2i} \mathbf{z}_{2i-1}) \right)^2 + \left(\sum_{i=1}^N (b_{k,2i-1} \mathbf{z}_{2i} - b_{k,2i} \mathbf{z}_{2i-1}) \right)^2 \right). \quad (8.33)$$

8.3 Linear Invariants

Cutting the ring in two positions 1 and 2 produces two pieces with the matrices $\mathbf{M}_{1 \rightarrow 2}$ and $\mathbf{M}_{2 \rightarrow 1}$. The one-turn matrices for the two positions are

$$\mathbf{M}_1 = \mathbf{M}_{2 \rightarrow 1} \mathbf{M}_{1 \rightarrow 2} = \mathbf{W}_1 \mathbf{R}_1 \mathbf{W}_1^{-1}, \quad \mathbf{M}_2 = \mathbf{M}_{1 \rightarrow 2} \mathbf{M}_{2 \rightarrow 1} = \mathbf{W}_2 \mathbf{R}_2 \mathbf{W}_2^{-1}. \quad (8.34)$$

The two matrices are similar to each other:

$$\mathbf{M}_2 = \mathbf{M}_{1 \rightarrow 2} \mathbf{M}_1 \mathbf{M}_{1 \rightarrow 2}^{-1}, \quad (8.35)$$

Therefore they have the same eigenvalues, and $\mathbf{R}_1 = \mathbf{R}_2$. Also,

$$\mathbf{M}_2 = \mathbf{W}_2 \mathbf{R}_2 \mathbf{W}_2^{-1} = \mathbf{M}_{1 \rightarrow 2} \mathbf{W}_1 \mathbf{R}_1 \mathbf{W}_1^{-1} \mathbf{M}_{1 \rightarrow 2}^{-1}. \quad (8.36)$$

One sees easily that

$$\mathbf{W}_2 = \mathbf{M}_{1 \rightarrow 2} \mathbf{W}_1. \quad (8.37)$$

The transformation for \mathbf{u} from position 1 to 2 is

$$\mathbf{u}_2 = \mathbf{W}_2^{-1} \mathbf{z}_2 = \mathbf{W}_2^{-1} \mathbf{M}_{1 \rightarrow 2} \mathbf{z}_1 = \mathbf{W}_2^{-1} \mathbf{M}_{1 \rightarrow 2} \mathbf{W}_1 \mathbf{u}_1 = (\mathbf{M}_{1 \rightarrow 2} \mathbf{W}_1)^{-1} (\mathbf{M}_{1 \rightarrow 2} \mathbf{W}_1) \mathbf{u}_1 = \mathbf{u}_1. \quad (8.38)$$

Obviously the invariants are conserved. For each mode the motion can be written as

$$\mathbf{z}_k = \sqrt{2I_k} \Re \left(\mathbf{v}_k^*(s) e^{i\psi_k} \right), \quad (8.39)$$

or expressed in real quantities

$$\mathbf{z}_k = \sqrt{2I_k} (\mathbf{a}_k(s) \cos \psi_k + \mathbf{b}_k(s) \sin \psi_k), \quad (8.40)$$

where ψ_k is the *initial phase* of the motion. For a given value of the invariant the particle is found on an ellipse in $2N$ -dimensional phase space. The plane of the ellipse can have any orientation with respect to the $2N$ coordinate axes. Note that there is *no* plane of motion in physical space. However, the projections of this ellipse onto a plane spanned by two phase space coordinates can be easily determined, as we shall see below.

8.4 Phase Factors

We found $\mathbf{u}(s) = \mathbf{u}(0)$, which seems to imply that the phases μ_k are constant, but we also found $\mathbf{u}(C) = \mathbf{R}\mathbf{u}(0)$. This is only an apparent contradiction, since the eigenvectors contain the phase advances.

In general the projections of an eigenmode onto the $2N$ axes of phase space all have different phases relative to the initial phase ψ_k . However, all projections advance by the same phase difference, known as the tune, when moving once around the ring. For one degree of freedom [6] it is customary to force $b_{1,1} = 0$ along the ring by multiplying with a phase factor $\exp(\mu(s))$. To generalise to N degrees of freedom we associate each eigenvector \mathbf{v}_k with one coordinate direction q_k . We then multiply it in all positions s by a factor $\exp(\mu_k(s))$ such that its component along that direction is real:

$$b_{k,2k-1}(s) = 0, \quad k = 1, \dots, N. \quad (8.41)$$

Usually the k^{th} eigenvector has a largest component whose magnitude is its largest extent along the k^{th} axis of physical space. This a natural association of eigenvectors to directions, but it may also be made simply by arbitrary numbering. The re-normalisation does not affect the invariants. It merely causes the components of \mathbf{u} to proceed around the ring with a phase advance which reaches $2\pi Q_k$ after one turn. In the case of an uncoupled machine these phases become the usual Courant-Snyder phase functions.

The representation of one eigenmode along s takes the final form

$$\mathbf{z}_k = \sqrt{2I_k} \Re(\mathbf{v}_k^*(s) \exp(i\psi_k + \mu_k(s))), \quad (8.42)$$

or expressed in real quantities

$$\mathbf{z}_k = \sqrt{2I_k} (\mathbf{a}_k(s) \cos(\psi_k + \mu_k(s)) + \mathbf{b}_k(s) \sin(\psi_k + \mu_k(s))). \quad (8.43)$$

The ellipse generated by one mode varies with the position s , and the eigenvectors \mathbf{v}_k are re-normalised at each s such that

$$b_{k,2k-1}(s) = 0, \quad k = 1, \dots, N. \quad (8.44)$$

8.5 TRANSPORT Sigma Matrix

It is easily seen that the particle motion for mode k generates the second moments

$$\sigma_{m,n} = \langle z_m z_n \rangle = a_{k,m} a_{k,n} + b_{k,m} b_{k,n} = v_{k,m} b_{k,n}^*. \quad (8.45)$$

They can be assembled to form a matrix

$$\Sigma_k = \mathbf{v}_k \mathbf{v}_k^{*T}. \quad (8.46)$$

The Σ matrix has been introduced in TRANSPORT [2] for the first time. For a given value of I_k the largest extents of the eigenmode in each direction of phase space are

$$\begin{aligned} \sigma_{2m-1} &= \max q_{k,m} = \max z_{k,2m-1} = \sqrt{2I_k(a_{k,2m-1}^2 + b_{k,2m-1}^2)}, \\ \sigma_{2m} &= \max p_{k,m} = \max z_{k,2m} = \sqrt{2I_k(a_{k,2m}^2 + b_{k,2m}^2)}. \end{aligned} \quad (8.47)$$

The correlations between phase space coordinates are

$$r_{m,n} = \sqrt{\frac{4I_m I_n}{\max z_m \max z_n}} (a_{k,m} a_{k,n} + b_{k,m} b_{k,n}). \quad (8.48)$$

If one assumes a Gaussian distribution of $\sqrt{2I_k}$, each mode represents a Gaussian distribution in a plane with the density function

$$N(\mathbf{u}) \propto \exp(-I_k) = \exp\left(-\frac{1}{2}\mathbf{u}^T \mathbf{u}\right) = \exp\left(-\frac{1}{2}\mathbf{z}^T \Sigma_k^{-1} \mathbf{z}\right). \quad (8.49)$$

The three modes can be superposed and give a $2N$ -dimensional Gaussian distribution with the Σ matrix

$$\Sigma = \sum_{k=1}^3 E_k \Sigma_k. \quad (8.50)$$

where E_k is the emittance belonging to the mode k , and the distribution is

$$N(\mathbf{u}) \propto \exp\left(-\frac{1}{2}\mathbf{z}^T \Sigma^{-1} \mathbf{z}\right). \quad (8.51)$$

8.6 Coupling Angles

Since the canonical variables do not all have the same units, it is not possible to talk about an orientation of the ellipsoid in $2N$ -dimensional phase space. However, we can project the ellipsoid onto the planes (x, y) , (x, t) , and (y, t) . The momenta are conserved by this operation. They can be extracted as the relevant components from the phase space vector and the Σ matrix. The projection is then given by the equation

$$\frac{1}{2(\sigma_{x,x}\sigma_{y,y} - \sigma_{x,y}^2)} (\sigma_{y,y}x^2 - 2\sigma_{x,y}xy + \sigma_{x,x}y^2) = \text{constant}, \quad (8.52)$$

where we have denoted the selected phase planes by x and y . For each plane one has the situation of Fig. 8.1.

Analysing equation 8.52 gives the maximum extents

$$\sigma_x = \sqrt{\sigma_{x,x}}, \quad \sigma_y = \sqrt{\sigma_{y,y}}. \quad (8.53)$$

The correlation is as before

$$r_{x,y} = \sigma_{x,y} / (\sigma_x \sigma_y). \quad (8.54)$$

The points where the ellipse touches the circumscribed rectangle are indicated with their coordinates in figure 8.1. If and only if the units for both axes are the same, one may compute the principal axes a, b and the angle ϕ between the principal axes and the coordinate axes:

$$\begin{aligned} a^2 &= \frac{1}{2} \left(\sigma_{x,x} + \sigma_{y,y} + \sqrt{(\sigma_{x,x} - \sigma_{y,y})^2 + 4\sigma_{x,y}^2} \right), \\ b^2 &= \frac{1}{2} \left(\sigma_{x,x} + \sigma_{y,y} - \sqrt{(\sigma_{x,x} - \sigma_{y,y})^2 + 4\sigma_{x,y}^2} \right), \\ \tan 2\phi &= (2\sigma_{x,y}) / (\sigma_{x,x} - \sigma_{y,y}). \end{aligned} \quad (8.55)$$

Note that for $\sigma_{x,x} = \sigma_{y,y}$ the angle ϕ is not defined.

8.7 Implementation

8.7.1 EMIT Command

All commands described in the following sections *must* be preceded by the EMIT command. This fills in the RF frequencies using the revolution frequency and the harmonic number. Note that the RF lag must be set close to the stable phase, i. e. above the transition energy it should be close to 0.5.

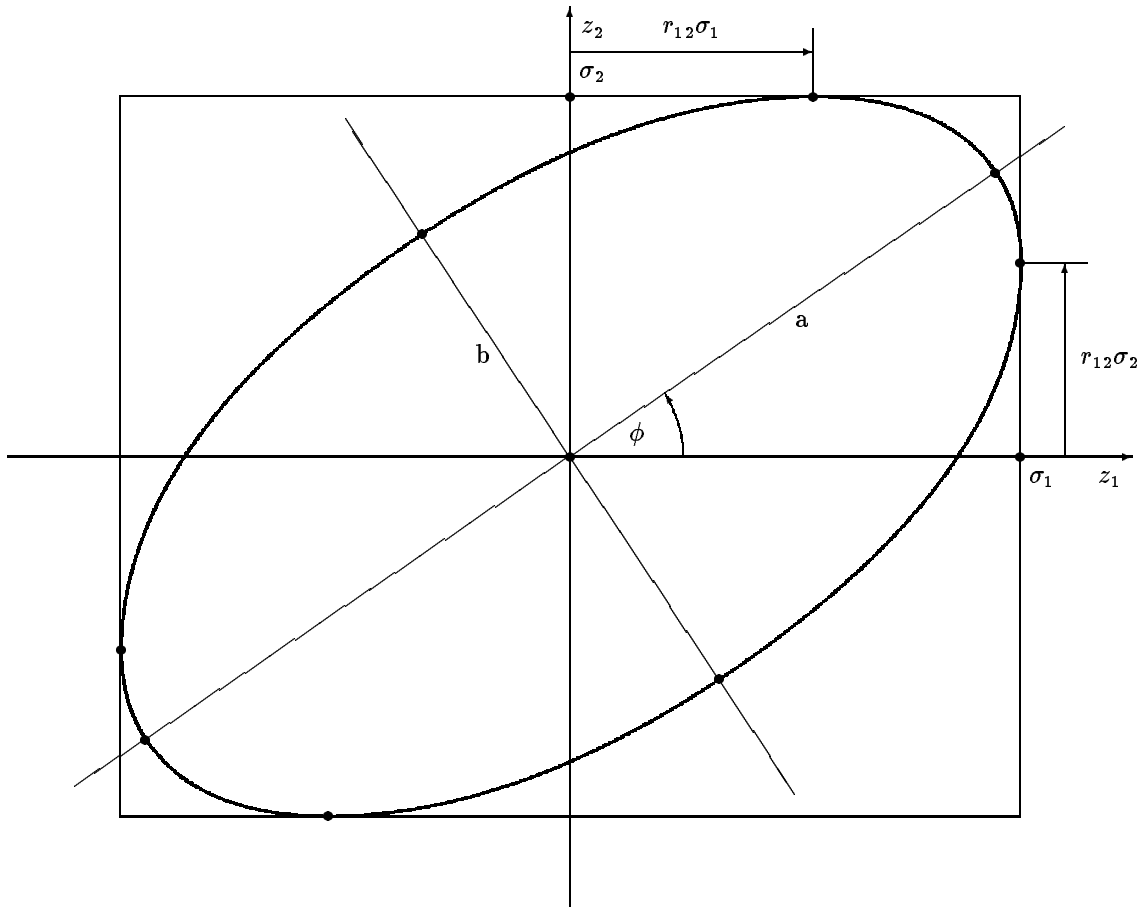


Figure 8.1: Projection of the phase space ellipsoid onto one plane

8.7.2 Eigenvectors

MAD lists them in selected position in the command EIGEN. They can be used to find the invariants.

8.7.3 Linear Invariants

The invariants can be built easily as shown above from the eigenvectors:

$$I_k = \frac{1}{2} \left((\mathbf{b}_k^T \mathbf{S} \mathbf{z})^2 + (\mathbf{a}_k^T \mathbf{S} \mathbf{z})^2 \right) = \frac{1}{2} \left(\left(\sum_{i=1}^N (a_{k,2i-1} \mathbf{z}_{2i} - a_{k,2i} \mathbf{z}_{2i-1}) \right)^2 + \left(\sum_{i=1}^N (b_{k,2i-1} \mathbf{z}_{2i} - b_{k,2i} \mathbf{z}_{2i-1}) \right)^2 \right). \quad (8.56)$$

8.7.4 Phase advances

MAD prints the phase advances in the commands TWISS3 and EIGEN. They are defined as described above; i. e. as the phase factors which re-normalise the principal components of the eigenvectors and makes them real.

8.7.5 Envelopes

The ENVELOPE command (must be preceded by EMIT !) computes the TRANSPORT Σ matrix from the eigenvectors. It is computed and listed in selected positions.

8.7.6 Mais-Ripken Lattice Functions

This method is due to H. Mais and G. Ripken [18, 21]. It is used in the TWISS3 command (which must be preceded by EMIT !), which computes the projections of the ellipses of motion onto the phase planes. The extents are expressed in the form similar to the Courant-Snyder parameters. The command lists these parameters along with the phases in selected positions. The projection of the Courant-Snyder lattice functions on the three planes (x, p_x) , (y, p_y) , and (t, p_t) are:

$$\begin{aligned}\beta_{k,j} &= a_{k,2j-1}a_{k,2j-1} + b_{k,2j-1}b_{k,2j-1}, \\ \gamma_{k,j} &= a_{k,2j}a_{k,2j} + b_{k,2j}b_{k,2j}, \\ \alpha_{k,j} &= a_{k,2j-1}a_{k,2j} + b_{k,2j}b_{k,2j-1}\end{aligned}\tag{8.57}$$

The index k refers to the eigenmode, and the index j to the plane. MAD prints the functions $\beta_{k,j}$, $\alpha_{k,j}$, and $\gamma_{k,j}$. It also prints the phase advances $\mu_{k,j}$ of the projections onto the three planes. Note that we have the equations

$$\beta_{k,j}\gamma_{k,j} - \alpha_{k,j}^2 = \left(\beta_{k,j}\frac{d\mu_{k,j}}{ds}\right)^2, \quad \text{but} \quad \beta_{k,j}\frac{d\mu_{k,j}}{ds} \neq 1.\tag{8.58}$$

Note that it is easy to convert the eigenvectors to the Mais-Ripken functions, but that this does not reduce the redundancy in information. A conversion in the opposite direction has not been found, it may well be impossible.

8.8 Transformations between Representations of Beam

8.8.1 Eigenvectors to Internal Sigma Matrix

Given the eigenvectors and the emittances for the three eigen-modes the beam ellipsoid Σ [2] can be computed as

$$\Sigma = \begin{pmatrix} \Sigma_{11} & \cdots & \Sigma_{14} \\ \vdots & & \vdots \\ \Sigma_{41} & \cdots & \Sigma_{44} \end{pmatrix} = \sum_{k=1}^3 E_k \Re(V_k^T V_k^*).\tag{8.59}$$

Assuming a Gaussian distribution, the particle distribution is then

$$N(Z) \propto \exp\left(\frac{1}{2}Z^T \Sigma^{-1}Z\right).\tag{8.60}$$

8.8.2 Internal Sigma Matrix to TRANSPORT Notation

Given the Σ matrix of the previous section the standard deviation of z_k is [2]:

$$\sigma_k = \sqrt{\Sigma_{kk}},\tag{8.61}$$

and the correlations between z_k and z_m as

$$r_{km} = \frac{\Sigma_{km}}{\sigma_k \sigma_m}.\tag{8.62}$$

MAD prints beam envelopes in this form.

8.8.3 TRANSPORT Notation to Internal Sigma Matrix

The formulas of the previous section can be inverted as:

$$\Sigma_{kk} = \sigma_k^2, \quad k = 1 \dots 4, \quad (8.63)$$

and the off-diagonal elements are

$$\Sigma_{km} = r_{km} \sigma_k \sigma_m, \quad k, m = 1 \dots 4, \quad k \neq m. \quad (8.64)$$

MAD uses this formula to find the internal Σ matrix from a SIGMA0 command.

Chapter 9. Survey

9.1 Global Reference System

The reference orbit of the accelerator is uniquely defined by the sequence of physical elements. The local reference system (x, y, s) may thus be referred to a global Cartesian coordinate system (X, Y, Z) (see Figure 9.1). The positions between beam elements are numbered $0, \dots, i, \dots, n$. The local reference system (x_i, y_i, z_i) at position i , i.e. the displacement and direction of the reference orbit with respect to the system (X, Y, Z) are characterised by three displacements (X_i, Y_i, Z_i) and three angles $(\theta_i, \phi_i, \psi_i)$. The above quantities are defined more precisely as follows:

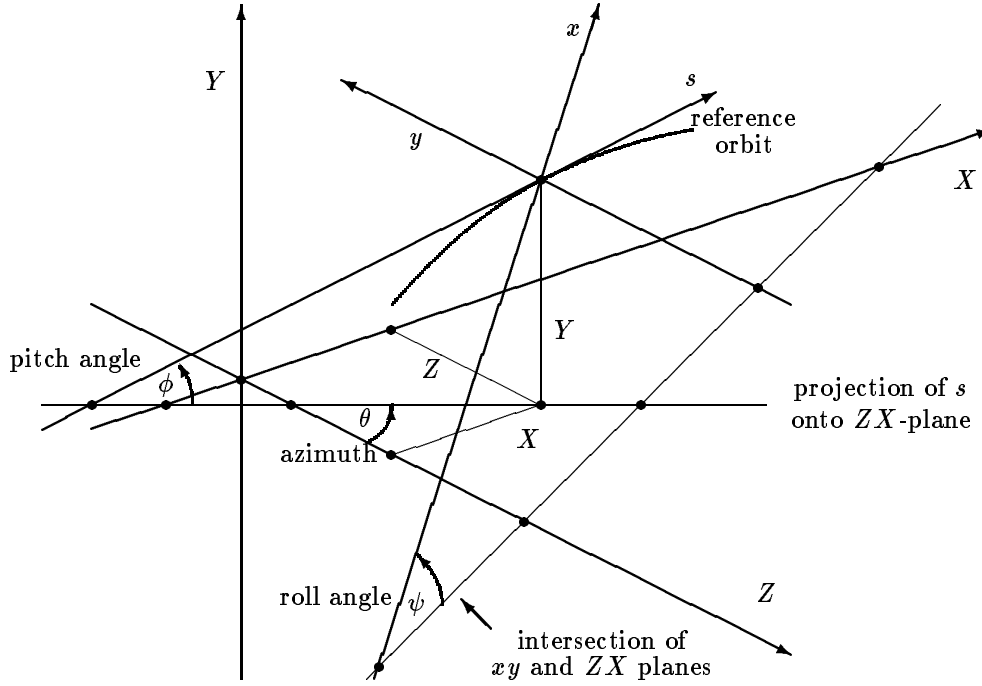


Figure 9.1: Global Reference System

X	Displacement of the local origin in X -direction.
Y	Displacement of the local origin in Y -direction.
Z	Displacement of the local origin in Z -direction.
θ	Angle of rotation (azimuth) about the global Y -axis, between the global Z -axis and the projection of the reference orbit onto the (Z, X) -plane. A positive angle θ forms a right-hand screw with the Y -axis.
ϕ	Elevation angle, i.e. the angle between the reference orbit and its projection onto the (Z, X) -plane. A positive angle ϕ correspond to increasing Y . If only horizontal bends are present, the reference orbit remains in the (Z, X) -plane. In this case ϕ is always zero.
ψ	Roll angle about the local s -axis, i.e. the angle between the intersection of the (x, y) and (Z, X) -planes and the local x -axis. A positive angle ψ forms a right-hand screw with the s -axis.

The angles (θ, ϕ, ψ) are *not* the Euler angles. The reference orbit starts at the origin and points by default in the direction of the positive Z -axis. The initial local axes (x, y, s) coincide with the global axes (X, Y, Z) in this order. The six quantities $(X_0, Y_0, Z_0, \theta_0, \phi_0, \psi_0)$, thus all have zero initial values by default. The program user may however specify different initial conditions.

Internally the displacement is described by a vector V , and the orientation by a unitary matrix W . The *column vectors* of W are the unit vectors spanning the local coordinate axes in the order (x, y, s) . V and W have the values

$$V = \begin{pmatrix} X \\ Y \\ Z \end{pmatrix}, \quad W = \Theta \Phi \Psi, \quad (9.1)$$

where

$$\Theta = \begin{pmatrix} \cos \theta & 0 & \sin \theta \\ 0 & 1 & 0 \\ -\sin \theta & 0 & \cos \theta \end{pmatrix}, \quad \Phi = \begin{pmatrix} 1 & 0 & 0 \\ 0 & \cos \phi & \sin \phi \\ 0 & -\sin \phi & \cos \phi \end{pmatrix}, \quad \Psi = \begin{pmatrix} \cos \psi & -\sin \psi & 0 \\ \sin \psi & \cos \psi & 0 \\ 0 & 0 & 1 \end{pmatrix}. \quad (9.2)$$

The reference orbit should be closed and it should not be twisted. This means that the displacement of the local reference system must be periodic with the revolution frequency of the accelerator, while the position angles must be periodic (modulo 2π) with the revolution frequency. If ψ is not periodic (modulo 2π), coupling effects are introduced. When advancing through a beam element, MAD computes V_i and W_i by the recurrence relations

$$V_i = W_{i-1} R_i + V_{i-1}, \quad W_i = W_{i-1} S_i. \quad (9.3)$$

The vector R_i is the displacement and the matrix S_i is the rotation of the local reference system at the exit of the element i with respect to the entrance of the same element. The values of R and S are listed below for each physical element type.

9.2 Single Elements

9.2.1 Markers

Marker elements do not affect the reference orbit. They are ignored for geometry calculations.

9.2.2 Straight Elements

The reference system for all straight elements is shown in Figure 9.2. It is valid for:

- | | | | |
|---------------|---------------|---------------|--------------|
| • DRIFT | • RCOLLIMATOR | • ECOLLIMATOR | • INSTRUMENT |
| • MONITOR | • HMONITOR | • VMONITOR | • QUADRUPOLE |
| • SEXTUPOLE | • OCTUPOLE | • SOLENOID | • RFCAVITY |
| • ELSEPARATOR | • KICKER | • HKICKER | • VKICKER |
| • MONITOR | • HMONITOR | • VMONITOR | |

The corresponding R and S are

$$R = \begin{pmatrix} 0 \\ 0 \\ L \end{pmatrix}, \quad S = \begin{pmatrix} 1 & 0 & 0 \\ 0 & 1 & 0 \\ 0 & 0 & 1 \end{pmatrix}. \quad (9.4)$$

A rotation of the *element* about the s -axis has an effect on R and S only for dipoles, since for all other elements the rotations of the reference system before and after the element cancel.

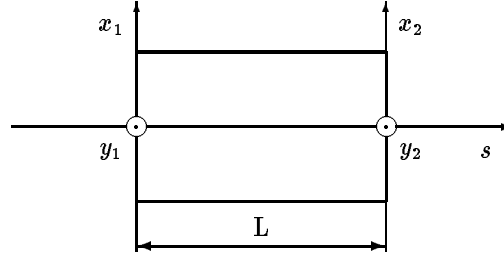


Figure 9.2: Reference System for Straight Beam Elements

9.2.3 Dipoles

Bending magnets affect the reference orbit due to their curvature. For both rectangular and sector bending magnets

$$R = \begin{pmatrix} \rho(\cos \alpha - 1) \\ 0 \\ \rho \sin \alpha \end{pmatrix}, \quad S = \begin{pmatrix} \cos \alpha & 0 & -\sin \alpha \\ 0 & 1 & 0 \\ \sin \alpha & 0 & \cos \alpha \end{pmatrix}, \quad (9.5)$$

where α is the bend angle. A positive bend angle represents a bend to the right, i.e. towards negative x values. For sector bending magnets, the bend radius is given by $\rho = L/\alpha$, and for rectangular bending magnets it has the value $\rho = L/(2 \sin(\alpha/2))$.

The reference system for type SBEND is shown in Figure 9.4, for type RBEND it is shown in Figure 9.3.

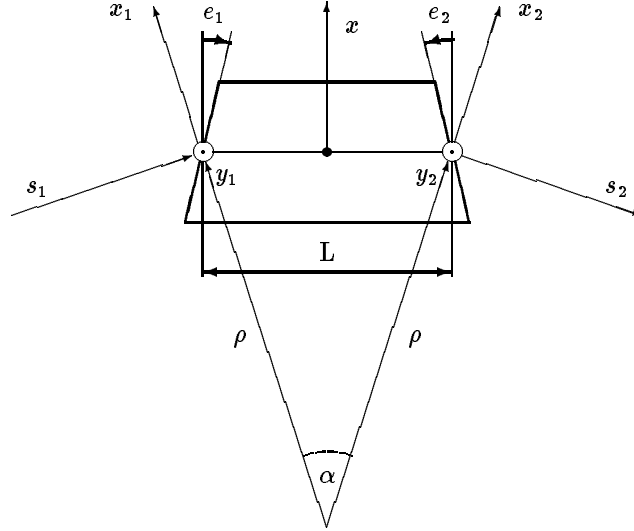


Figure 9.3: Reference System for a Rectangular Bending Magnet; the signs of pole-face rotations are positive as shown.

If the magnet is rotated about the s -axis by an angle ψ , R and S are transformed by

$$\bar{R} = TR, \quad \bar{S} = TST^{-1} \quad (9.6)$$

where T is the rotation matrix

$$T = \begin{pmatrix} \cos \psi & -\sin \psi & 0 \\ \sin \psi & \cos \psi & 0 \\ 0 & 0 & 1 \end{pmatrix}. \quad (9.7)$$

The special value $\psi = \pi/2$ represents a bend down.

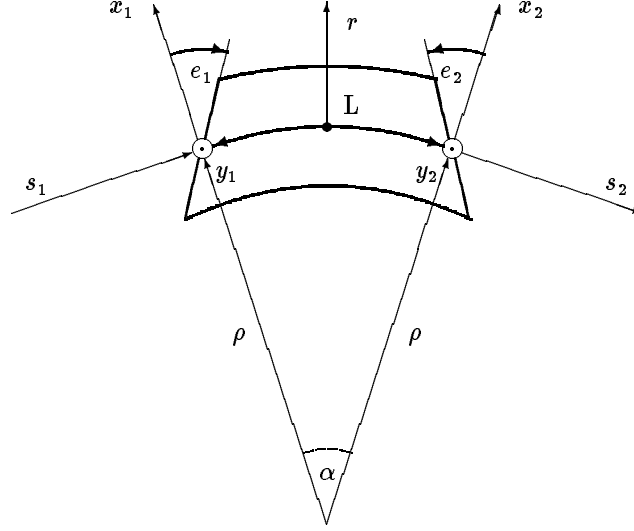


Figure 9.4: Reference System for a Sector Bending Magnet; the signs of pole-face rotations are positive as shown.

9.2.4 Rotation of Reference System about s -Axis

The reference system for the SROT element which rotates the local reference system about the longitudinal axis is shown in Figure 9.5. SROT has no effect on the beam, but it causes the beam to be referred to the new coordinate system

$$x_2 = x_1 \cos \psi + y_1 \sin \psi, \quad y_2 = x_1 \sin \psi + y_1 \cos \psi. \quad (9.8)$$

A positive angle means that the new reference system is rotated clockwise about the s -axis with respect to the old system. The *reference system* is changed using

$$R = \begin{pmatrix} 0 \\ 0 \\ 0 \end{pmatrix}, \quad S = \begin{pmatrix} \cos \psi & -\sin \psi & 0 \\ \sin \psi & \cos \psi & 0 \\ 0 & 0 & 1 \end{pmatrix}. \quad (9.9)$$

9.2.5 Rotation of Reference System about y -Axis

The reference system for a rotation by an angle θ about the vertical axis (YROT) the reference system is shown in Figure 9.6. YROT has no effect on the beam, but it causes the beam to be referred to the new coordinate system

$$x_2 = x_1 \cos \theta - s_1 \sin \theta, \quad s_2 = x_1 \sin \theta + s_1 \cos \theta. \quad (9.10)$$

A positive angle rotates the reference system clockwise about the local y -axis with respect to the old system:

$$R = \begin{pmatrix} 0 \\ 0 \\ 0 \end{pmatrix}, \quad S = \begin{pmatrix} \cos \theta & 0 & -\sin \theta \\ 0 & 1 & 0 \\ \sin \theta & 0 & \cos \theta \end{pmatrix}. \quad (9.11)$$

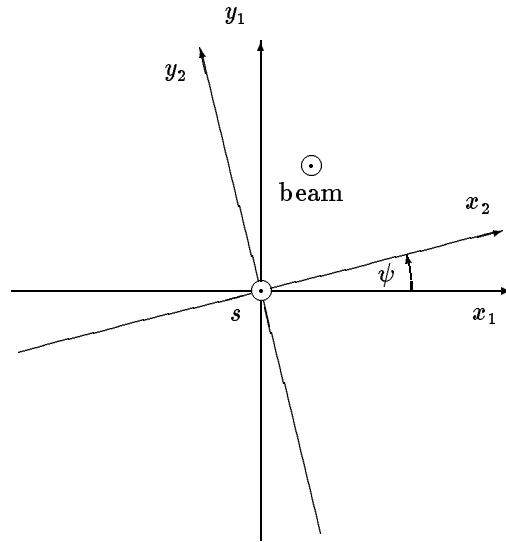


Figure 9.5: Reference System for a Rotation Around the s-Axis

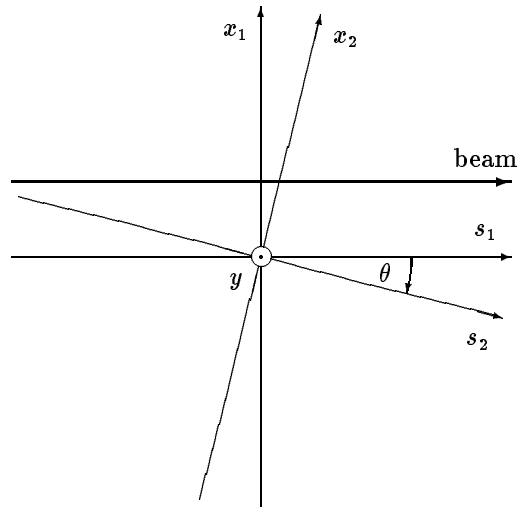


Figure 9.6: Reference System for a Rotation Around the y-Axis

9.3 Sequences of Elements

The displacement and rotation of the reference system due to an element sequence can be accumulated by the recurrence relations given above:

$$V_i = W_{i-1}R_i + V_{i-1}, \quad W_i = W_{i-1}S_i, \quad i = 1 \dots n. \quad (9.12)$$

Accumulating these quantities in *beam* order one finds for the sequence the values

$$R = V_n, \quad S = W_n. \quad (9.13)$$

Chapter 10. Closed Orbit and Dispersion Correction

This chapter describes the algorithms used for orbit and dispersion correction. The data structures used are documented in the MAD Programmer's Manual.

10.1 Influence of a Kick in a Plane on the Orbit

The betatron motion [6] with the initial conditions $q(s_0)$ and $p(s_0)$ is

$$\begin{aligned} q(s) &= \sqrt{\frac{\beta(s)}{\beta(s_0)}} (\cos \psi + \alpha(s_0) \sin \psi) q(s_0) + \sqrt{\beta(s)\beta(s_0)} \sin \psi p(s_0), \\ p(s) &= -\frac{(1 + \alpha(s)\alpha(s_0)) \sin \psi + (\alpha(s) - \alpha(s_0)) \cos \psi}{\sqrt{\beta(s)\beta(s_0)}} q(s_0) + \sqrt{\frac{\beta(s_0)}{\beta(s)}} (\cos \psi - \alpha(s) \sin \psi) p(s_0). \end{aligned} \quad (10.1)$$

where $\psi = \mu(s) - \mu(s_0)$ is the phase difference. The position q must be replaced by x or y , the transverse momentum p by p_x or p_y , and the optical functions must be taken for the plane in question.

The influence of a kick with the strength Δp at an azimuth s_0 in the ring by setting

$$q(s_0) = q(s_0 + C), \quad p(s_0) = p(s_0 + C) + \Delta p \quad (10.2)$$

in equation 10.1. It produces a closed orbit with the transverse position

$$q(s) = \frac{\sqrt{\beta(s)\beta(s_0)}}{2 \sin(\pi Q)} \times \begin{cases} \cos(\mu(s_0) - \mu(s) - \pi Q), & s < s_0, \\ \cos(\mu(s) - \mu(s_0) - \pi Q), & s > s_0. \end{cases} \quad (10.3)$$

This can be rewritten as

$$q(s) = \frac{\sqrt{\beta(s)\beta(s_0)}}{2 \sin(\pi Q)} \cos(|\mu(s_0) - \mu(s)| - \pi Q). \quad (10.4)$$

Note that taking the absolute value of the phase difference produces the proper jump in transverse momentum at position $s = s_0$ while leaving the transverse position unaffected.

If the machine is symmetric, MAD assumes that there is a second kick at the symmetric point $s = -s_0$ with the phase $\mu = -\mu(s_0)$, and the position of the orbit becomes

$$q(s) = \frac{\sqrt{\beta(s)\beta(s_0)}}{2 \sin(\pi Q)} (\cos(|\mu(s) - \mu(s_0)| - \pi Q) + \cos(\mu(s) + \mu(s_0) - \pi Q)). \quad (10.5)$$

Note that the second cosine term has no absolute value, since the symmetric kick falls outside the computation region.

The influence matrix for the orbit displacements at monitor positions as a function of corrector strengths is found by using the set of corrector azimuths for s_0 and the set of monitor azimuths for s .

10.2 Orbit Correction by MICADO Algorithm

The algorithm for solving the normal equations for the correctors is described in [4] as an Algol procedure.

***** section to be filled in *****

10.3 Influence Matrix for Orbit and Dispersion for a Plane

***** section to be filled in *****

10.4 Orbit and Dispersion Correction by MICADO Algorithm

**** section to be filled in ****

Chapter 11. Synchrotron Radiation and Equilibrium Emittances

Synchrotron radiation effects are optional in MAD:

- If RADIATE on the BEAM command is false, synchrotron radiation is ignored in *all commands*.
- If RADIATE is true, all commands apply synchrotron radiation as a *systematic effects*. The energy loss due to radiation changes the closed orbit, and the instantaneous momentum on the *closed orbit* affects the optics. In all magnetic elements MAD tracks the closed orbit in a three-step process:
 1. Compute the local magnetic field on the closed orbit where it enters the magnetic element. Assume that this field acts for half the length of the element on the particle, and use it to compute the energy radiated at the entrance of the element.
 2. Track the particle through the element, leaving its momentum unchanged.
 3. Compute the local magnetic field on the closed orbit where it leaves the magnetic element. Assume that this field acts for half the length of the element on the particle, and use it to compute the energy radiated at the exit of the element.

The TRACK command has two additional flags, DAMP and QUANTUM:

- If DAMP is false, the value of QUANTUM is ignored, and all particles loose energy as described above, the radiation being determined by the curvature of the *closed orbit*. Hence tracking uses the optics defined by the instantaneous momentum on the closed orbit and the particles see *no damping*. However, the *saw-tooth* like energy variation due to synchrotron radiation exists.
- If DAMP is true and QUANTUM is false, the local curvature of the actual particle orbit determines the systematic component of the radiation loss. The orbits are damped but there is no quantum excitation. This causes all trajectories to be attracted to the closed orbit, and allows to verify the damping times computed in EMIT.
- If both DAMP and QUANTUM are true, the local curvature of the actual particle orbit determines the radiation damping and quantum excitation. This is the most realistic model for the particle behaviour.

11.1 Local Curvature for Different Elements

11.1.1 Dipole

For radiation effects MAD ignores the dipole fringing fields. The reason is that the fringing field acts like a thin lens, it changes only the orbit angles but not its position. To determine the local curvature, the orbit must first be related to the mid-plane of the possibly rotated dipole:

$$x_r = x \cos \psi + y \sin \psi, \quad y_r = -x \sin \psi + y \cos \psi, \quad (11.1)$$

where ψ is the roll angle of the dipole. The total curvature h is then computed from the curvature in both planes:

$$\begin{aligned} h_x &= K_0 + K_1 x_r + K_2 (x_r^2 - y_r^2)/2 - K_0 K_1 y_r^2/2, \\ h_y &= -K_1 y_r - K_2 x_r y_r, \\ h &= \sqrt{h_x^2 + h_y^2}. \end{aligned} \quad (11.2)$$

11.1.2 Quadrupole, Sextupole, Octupole

The total local curvature is

$$h = K_n (x^2 + y^2)^{(n/2)}. \quad (11.3)$$

where $n = 1$ for a quadrupole, $n = 2$ for a sextupole, and $n = 3$ for an octupole.

11.1.3 Thin Multipole

For thin multipole the change in orbit direction is instantaneous, hence the energy loss would be infinite. To avoid this problem, MAD defines a fictitious length L_{rad} as a parameter for the multipole, which is used for the radiation loss calculation. The local curvature is then $h = |P|/L_{\text{rad}}$, where P is the *total kick* of the multipole. The value of P can be found in Section 5.7.

11.2 Systematic Energy Loss by Synchrotron Radiation

The total relative energy lost over half the element length by a particle is

$$\Delta E/(2p_s) = \frac{2r_e}{3} \gamma_s^3 h^2 \frac{1}{2} L, \quad (11.4)$$

where the local curvature is evaluated separately for the entrance and the exit. r_e is the classical radius for the particle in metres. The particle momentum vector is then changed at the entrance and at the exit by

$$p_{x2} = p_{x1} - \Delta E/p_s (1 + p_{t1}) p_{x1}, \quad p_{y2} = p_{y1} - \Delta E/p_s (1 + p_{t1}) p_{y1}, \quad p_{t2} = p_{t1} - \Delta E/p_s (1 + p_{t1})^2. \quad (11.5)$$

11.3 Quantum Excitation by Synchrotron Radiation in Tracking

The algorithm for quantum excitation is based on [17]. The first step is to determine the mean number of photons emitted over half the length of the element as

$$\frac{1}{2} \langle N \rangle = \frac{5\sqrt{3}r_e}{6\hbar c} p_s h \frac{1}{2} L, \quad (11.6)$$

and the actual number N of photons generated over half the length is selected from the Poisson distribution with average $\langle N \rangle$. The critical energy, divided by p_s , is computed as

$$U_c/p_s = \frac{3\hbar c}{2m_e} \gamma_s^2 h. \quad (11.7)$$

The local curvature is evaluated separately for the entrance and the exit. r_e is the classical radius for the particle in metres, and m_e is its mass in GeV. The second step is to sample N photons from the distribution

$$\xi, \quad (11.8)$$

and to sum up the energies of the photons, divided by p_s :

$$\Delta E/p_s = \sum_{k=1}^N U_c/p_s \xi_k. \quad (11.9)$$

Finally the particle momentum vector is changed by

$$p_{x2} = p_{x1} - \Delta E/p_s (1 + p_{t1}) p_{x1}, \quad p_{y2} = p_{y1} - \Delta E/p_s (1 + p_{t1}) p_{y1}, \quad p_{t2} = p_{t1} - \Delta E/p_s (1 + p_{t1})^2. \quad (11.10)$$

11.4 Equilibrium Emittances

The algorithm for damping is based on [5]. ***** section to be filled in *****

Chapter 12. HARMON Module

The HARMON calculations are based on a program originally written by M. Donald and linked to MAD by D. Schofield [8]. Various changes and improvements have been made later in this module.

12.1 General Organisation of HARMON

HARMON ignores all coupling effects. It uses thin lens approximations for all computations. Integrations around the ring are replaced by summations over the elements; all functions appearing in the integrands are approximated by their average over the element. Thus, for example, the integral $\int \sqrt{\beta_x} ds$ over the length of an element is replaced by $L\sqrt{\langle \beta_x \rangle}$.

When the HARMON module is started by the command HARMON, it sets up a table containing the averaged lattice functions for all dipoles, quadrupoles, sextupoles, and thin multipoles. It stores the averaged lattice functions

$$\begin{aligned} \langle \beta_x \rangle &= \int \beta_x ds / L, & \langle \alpha_x \rangle &= \int \alpha_x ds / L, & \langle \mu_x \rangle &= \int \mu_x ds / L, \\ \langle Dx \rangle &= \int Dx ds / L, & \langle Dp_x \rangle &= \int Dp_x ds / L, \\ \langle \beta_y \rangle &= \int \beta_y ds / L, & \langle \alpha_y \rangle &= \int \alpha_y ds / L, & \langle \mu_y \rangle &= \int \mu_y ds / L, \\ \langle Dy \rangle &= \int Dy ds / L, & \langle Dp_y \rangle &= \int Dp_y ds / L \end{aligned} \tag{12.1}$$

in this table. In subsequent print-outs HARMON lists these *averaged functions* for all active elements.

HARMON evaluates multiple integrals in a very efficient way. Applying addition theorems for trigonometric functions it separates functions of different positions. This makes it possible to evaluate a double integral as a double sum whose outer sum runs over partial sums of the inner sum, which may be evaluated in a single loop. A similar method applies to triple integrals.

12.2 First-Order Chromaticity

The linear chromaticity is found according to a formula given by Jäger and Möhl [15]. Defining

$$D = \frac{d}{dp_t}, \quad D^n = \frac{d^n}{dp_t^n}, \quad ' = \frac{d}{ds} \tag{12.2}$$

the chromaticities can be written as:

$$\begin{aligned} \frac{dQ_x}{dp_t} &= \frac{1}{4\pi} \left(- \int_0^C (K_1 + h^2) \beta_x ds + \int_0^C h Dx (2K_1 \beta_x + \gamma_x) ds - 2 \int_0^C h Dx' \alpha_x ds + \int_0^C K_2 Dx \beta_x ds \right), \\ \frac{dQ_y}{dp_t} &= \frac{1}{4\pi} \left(+ \int_0^C K_1 \beta_x ds + \int_0^C h Dx (-K_1 \beta_y + \gamma_y) ds + \int_0^C h' Dx' \beta_y ds - \int_0^C K_2 Dx \beta_y ds \right), \end{aligned} \tag{12.3}$$

These authors have shown the importance that the term containing h' is not omitted. The first-order chromaticities are evaluated by exact integration, and the results agree very well with the results found from TWISS (see 6.3.1).

12.3 Higher-order Chromaticities

The second- and third-order chromaticities consider only the effects of quadrupoles and higher-order multipoles. We introduce the functions

$$\begin{aligned}
f_{x1}(s) &= \beta_x(s) \left(K_1(s) - K_2(s) D x(s) \right), \\
f_{y1}(s) &= \beta_y(s) \left(K_1(s) - K_2(s) D x(s) \right), \\
f_{x2}(s) &= -f_{x1} - \beta_x(s) \left(K_2(s) D^2 x(s) + \frac{1}{2} K_3(s) (D x(s))^2 \right), \\
f_{y2}(s) &= -f_{y1} - \beta_y(s) \left(K_2(s) D^2 x(s) + \frac{1}{2} K_3(s) (D x(s))^2 \right), \\
f_{x3}(s) &= -f_{x2} - \beta_x(s) \left(K_2(s) D^3 x(s) + K_3(s) D x(s) D^2 x(s) + \frac{1}{6} K_4(s) (D x(s))^3 \right), \\
f_{y3}(s) &= -f_{y2} - \beta_y(s) \left(K_2(s) D^3 x(s) + K_3(s) D x(s) D^2 x(s) + \frac{1}{6} K_4(s) (D x(s))^3 \right).
\end{aligned} \tag{12.4}$$

The second-order and third-order chromaticities can be found by the methods given in reference [6] as the following integrals:

$$\begin{aligned}
\frac{d^2 Q_x}{dp_i^2} &= -\frac{1}{4\pi} \int_0^C f_{x2}(s) ds \\
&\quad - \frac{1}{4\pi \sin(2\pi Q_x)} \int_0^C \int_0^{s_1} f_{x1}(s_1) f_{x1}(s_2) \times \\
&\quad \times \sin(\mu_x(s_2) - \mu_x(s_1)) \sin(2\pi Q_x + \mu_x(s_1) - \mu_x(s_2)) ds_2 ds_1 \\
\frac{d^2 Q_y}{dp_i^2} &= +\frac{1}{4\pi} \int_0^C f_{y2}(s) ds \\
&\quad - \frac{1}{4\pi \sin(2\pi Q_y)} \int_0^C \int_0^{s_1} f_{y1}(s_1) f_{y1}(s_2) \times \\
&\quad \times \sin(\mu_y(s_2) - \mu_y(s_1)) \sin(2\pi Q_y + \mu_y(s_1) - \mu_y(s_2)) ds_2 ds_1 \\
\frac{d^3 Q_x}{dp_i^3} &= -\frac{1}{4\pi} \int_0^C f_{x3}(s) ds \\
&\quad - \frac{1}{4\pi \sin(2\pi Q_x)} \int_0^C \int_0^{s_1} (f_{x1}(s_1) f_{x2}(s_2) + f_{x2}(s_1) f_{x1}(s_2)) \times \\
&\quad \times \sin(\mu_x(s_2) - \mu_x(s_1)) \sin(2\pi Q_x + \mu_x(s_1) - \mu_x(s_2)) ds_2 ds_1 \\
&\quad + \frac{1}{4\pi \sin(2\pi Q_x)} \int_0^C \int_0^{s_1} \int_0^{s_2} f_{x1}(s_1) f_{x1}(s_2) f_{x1}(s_3) \times \\
&\quad \times \sin(\mu_x(s_3) - \mu_x(s_2)) \sin(\mu_x(s_2) - \mu_x(s_1)) \sin(2\pi Q_x + \mu_x(s_1) - \mu_x(s_3)) ds_3 ds_2 ds_1 \\
\frac{d^3 Q_y}{dp_i^3} &= +\frac{1}{4\pi} \int_0^C f_{y3}(s) ds \\
&\quad - \frac{1}{4\pi \sin(2\pi Q_y)} \int_0^C \int_0^{s_1} (f_{y1}(s_1) f_{y2}(s_2) + f_{y2}(s_1) f_{y1}(s_2)) \times \\
&\quad \times \sin(\mu_y(s_2) - \mu_y(s_1)) \sin(2\pi Q_y + \mu_y(s_1) - \mu_y(s_2)) ds_2 ds_1 \\
&\quad - \frac{1}{4\pi \sin(2\pi Q_y)} \int_0^C \int_0^{s_1} \int_0^{s_2} f_{y1}(s_1) f_{y1}(s_2) f_{y1}(s_3) \times \\
&\quad \times \sin(\mu_y(s_3) - \mu_y(s_2)) \sin(\mu_y(s_2) - \mu_y(s_1)) \sin(2\pi Q_y + \mu_y(s_1) - \mu_y(s_3)) ds_3 ds_2 ds_1
\end{aligned} \tag{12.5}$$

12.4 Variation of the Dispersion with Energy

The variation of the dispersion with energy can be found by the method given in Section 10.1. The closed orbit due to a distributed kick is

$$x(0) = \frac{1}{2 \sin(\pi Q_x)} \int_0^C \sqrt{\beta_x(0)\beta_x(s)} \cos(\pi Q_x - \mu_x(s)) k(s) ds \quad (12.6)$$

Expanding the orbit as

$$x(p_t) = x + Dx p_t + D^2 x p_t^2 + D^3 x p_t^3 + \dots \quad (12.7)$$

and separating like powers of p_t one gets the differential equations

$$\begin{aligned} \frac{d^2 Dx}{ds^2} + K_1 Dx &= -h^2, \\ \frac{d^2 D^2 x}{ds^2} + K_1 D^2 x &= +h^2 - K_1 Dx + \frac{1}{2} K_2 (Dx)^2, \\ \frac{d^2 D^3 x}{ds^2} + K_1 D^3 x &= -h^2 - K_1 Dx + \frac{1}{2} K_2 (Dx)^2 - K_1 D^2 x + K_2 Dx D^2 x + \frac{1}{6} K_3 (Dx)^3. \end{aligned} \quad (12.8)$$

The first-order dispersion $Dx = dx/dp_t$ is already known in the table of averaged values. At the origin of the ring the second-order dispersion $D^2 x$ is:

$$D^2 x(0) = -Dx(0) + \frac{1}{2 \sin(\pi Q_x)} \int_0^C \sqrt{\beta_x(0)\beta_x(s)} \cos(\pi Q_x - \mu_x(s)) \left(K_1(s) Dx(s) - \frac{1}{2} K_2(s) (Dx(s))^2 \right) ds. \quad (12.9)$$

The integral is evaluated as two sums to facilitate computation of $D^2 x$ around the ring:

$$\begin{aligned} S_c &= \sum_{\text{elements}} \sqrt{\langle \beta_x \rangle} \cos(\langle \mu_x \rangle) \left(K_1 \langle Dx \rangle - \frac{1}{2} K_2 \langle Dx(s) \rangle^2 \right) ds, \\ S_s &= \sum_{\text{elements}} \sqrt{\langle \beta_x \rangle} \sin(\langle \mu_x \rangle) \left(K_1 \langle Dx \rangle - \frac{1}{2} K_2 \langle Dx(s) \rangle^2 \right) ds, \\ D^2 x(0) &\approx -Dx(0) + \frac{\sqrt{\beta_x(0)}}{2 \sin(\pi Q_x)} \left(S_c \cos(\pi Q_x) + S_s \sin(\pi Q_y) \right) \end{aligned} \quad (12.10)$$

One may now proceed from one element to the next as follows:

$$\langle D^2 x_i \rangle \approx -\langle Dx_i \rangle + \frac{\sqrt{\langle \beta_x \rangle}}{2 \sin(\pi Q_x)} \left(S_c \cos(\pi Q_x + \langle \mu_x \rangle) + S_s \sin(\pi Q_x + \langle \mu_x \rangle) \right). \quad (12.11)$$

After each element one has to step the sums by

$$\begin{aligned} S_c &\leftarrow S_c + \sqrt{\langle \beta_x \rangle} \left(K_1 \langle Dx \rangle - \frac{1}{2} K_s (\langle Dx \rangle)^2 \right) \cos(2\pi Q_x + \langle \mu_x \rangle), \\ S_s &\leftarrow S_s + \sqrt{\langle \beta_x \rangle} \left(K_1 \langle Dx \rangle - \frac{1}{2} K_s (\langle Dx \rangle)^2 \right) \sin(2\pi Q_x + \langle \mu_x \rangle), \end{aligned} \quad (12.12)$$

Once the value of $D^2 x(s)$ is known, $D^3 x(0)$ is found from the integral:

$$\begin{aligned} D^3 x(0) &= -D^2 x(0) + \frac{1}{2 \sin(\pi Q_x)} \int_0^C \sqrt{\beta_x(0)\beta_x(s)} \cos(\pi Q_x - \mu_x(s)) \times \\ &\quad \times \left((K_1(s) - K_2(s) Dx(s)) D^2 x(s) - \frac{1}{6} K_3(s) (Dx(s))^3 \right) ds. \end{aligned} \quad (12.13)$$

Evaluation of the integral and stepping around the ring is done as for $D^2 x$.

12.5 Variation of β with Energy

Using the techniques of reference [6], the total derivatives of the β functions at the origin are:

$$\begin{aligned}\frac{1}{\beta_x(0)} \frac{d\beta_x(0)}{dp_t} &= + \frac{1}{2 \sin(2\pi Q_x)} \int_0^C \beta_x(s) (K_1(s) - K_2(s) D_x(s)) \cos(2\pi Q_x - 2\mu_x(s)(s)) ds \\ \frac{1}{\beta_y(0)} \frac{d\beta_y(0)}{dp_t} &= - \frac{1}{2 \sin(2\pi Q_x)} \int_0^C \beta_x(s) (K_1(s) - K_2(s) D_x(s)) \cos(2\pi Q_x - 2\mu_x(s)(s)) ds\end{aligned}\quad (12.14)$$

These integrals are evaluated and stepped in HARMON like the ones in the preceding section.

12.6 Variation of Tunes with Amplitude

The variation of tunes with amplitude has been described in reference [7, 9]. The tune shifts due to the betatron amplitudes are

$$\Delta Q_x = G_{xx} \hat{x}^2 + G_{xy} \hat{y}^2, \quad \Delta Q_y = G_{xy} \hat{x}^2 + G_{yy} \hat{y}^2. \quad (12.15)$$

With the abbreviations

$$\phi_x = Q_x - \mu_x(s_2) + \mu_x(s_1), \quad \phi_y = Q_y - \mu_y(s_2) + \mu_y(s_1), \quad (12.16)$$

the coefficients are given as sums of double integrals:

$$\begin{aligned}G_{xx} &= - \frac{1}{64\pi \sin(3\pi Q_x)} \int_0^C \int_0^{s_2} \beta_x^{3/2}(s_1) K_2(s_1) \beta_x^{3/2}(s_2) K_2(s_2) \cos(3\phi_x) ds_1 ds_2 \\ &\quad - \frac{3}{64\pi \sin(\pi Q_x)} \int_0^C \int_0^{s_2} \beta_x^{3/2}(s_1) K_2(s_1) \beta_x^{3/2}(s_2) K_2(s_2) \cos(\phi_x) ds_1 ds_2 \\ G_{xy} &= + \frac{1}{16\pi \sin(\pi Q_x)} \int_0^C \int_0^{s_2} \beta_x^{3/2}(s_1) K_2(s_1) \beta_x^{1/2}(s_2) \beta_y(s_2) K_2(s_2) \cos(\phi_x) ds_1 ds_2 \\ &\quad - \frac{1}{32\pi \sin(\pi(Q_x + 2Q_y))} \int_0^C \int_0^{s_2} \beta_x^{1/2}(s_1) \beta_y(s_1) K_2(s_1) \beta_x^{1/2}(s_2) \beta_y(s_2) K_2(s_2) \cos(\phi_x + 2\phi_y) ds_1 ds_2 \\ &\quad + \frac{1}{32\pi \sin(\pi(Q_x - 2Q_y))} \int_0^C \int_0^{s_2} \beta_x^{1/2}(s_1) \beta_y(s_1) K_2(s_1) \beta_x^{1/2}(s_2) \beta_y(s_2) K_2(s_2) \cos(\phi_x - 2\phi_y) ds_1 ds_2, \\ G_{yy} &= - \frac{1}{16\pi \sin(\pi Q_x)} \int_0^C \int_0^{s_2} \beta_x^{1/2}(s_1) \beta_y(s_1) K_2(s_1) \beta_x^{1/2}(s_2) \beta_y(s_2) K_2(s_2) \cos(\phi_x) ds_1 ds_2 \\ &\quad - \frac{1}{64\pi \sin(\pi(Q_x + 2Q_y))} \int_0^C \int_0^{s_2} \beta_x^{1/2}(s_1) \beta_y(s_1) K_2(s_1) \beta_x^{1/2}(s_2) \beta_y(s_2) K_2(s_2) \cos(\phi_x + 2\phi_y) ds_1 ds_2 \\ &\quad - \frac{1}{64\pi \sin(\pi(Q_x - 2Q_y))} \int_0^C \int_0^{s_2} \beta_x^{1/2}(s_1) \beta_y(s_1) K_2(s_1) \beta_x^{1/2}(s_2) \beta_y(s_2) K_2(s_2) \cos(\phi_x - 2\phi_y) ds_1 ds_2.\end{aligned}\quad (12.17)$$

12.7 Resonances

***** section is incomplete *****

12.7.1 HRESONANCE Command

The HRESONANCE command computes the effect of an n -order resonance.

12.7.2 Sum Resonances

For all combinations $n_1 + n_2 = n$ HRESONANCE computes the two multiples of the number of super-periods N_s just above and below the expression $(n_1 Q_x + n_2 Q_y)$. Defining

$$f_s = 2\pi(n_1 Q_x + n_2 Q_y - p)/C \quad (12.18)$$

For the k -th sextupole the resonance contribution is

$$c_k = \frac{1}{2^n \pi n_1! n_2!} \int_0^{L_k} K_2 \beta_x(s)^{|n_1|/2} \beta_y(s)^{|n_2|/2} \exp(i(n_1 \mu_x(s) + n_2 \mu_y(s) - f_s s)) ds, \quad (12.19)$$

where the integration is over the sextupole length. The integral is evaluated by fitting a cubic polynomial through the values of the integrand and its derivatives at both ends of the sextupole, and integrating this polynomial. The results are given in the form of real part (cosine terms), imaginary part (sine terms) and modulus (amplitude). The random effects are

$$\text{random} = \sqrt{\sum_{\text{sextupoles}} (2|c_k|^2)}. \quad (12.20)$$

12.8 Third-Integer Resonances in HFUNCTION Command

***** section to be filled in *****

12.9 Fourth-Order Resonances

***** section to be filled in ***** Find fourth-order resonance coefficients

Bibliography

- [1] M. Bassetti and G. A. Erskine. *Closed expression for the electrical field of a two-dimensional Gaussian charge*. CERN-ISR-TH/80-06.
- [2] Karl L. Brown. *A First-and Second-Order Matrix Theory for the Design of Beam Transport Systems and Charged Particle Spectrometers*. SLAC 75, Revision 3, SLAC, 1972, and SLAC-PUB-3381, July 1984.
- [3] K. L. Brown, D. C. Carey, Ch. Iselin, and F. Rothacker, *TRANSPORT — A Computer Program for Designing Charged Particle Beam Transport Systems*. CERN 73-16, revised as CERN 80-4, CERN, 1980.
- [4] P. Businger and G. H. Golub, *Linear LeastSquares Solutions by Householder Transformations*, in *Handbook for Automatic Computation, Vol. II, Linear Algebra*, pg. 111. Springer, Berlin, 1971.
- [5] A. Chao. Evaluation of beam distribution parameters in an electron storage ring. *Journal of Applied Physics*, 50:595–598, 1979.
- [6] E. D. Courant and H. S. Snyder. *Theory of the alternating gradient synchrotron*. *Annals of Physics*, 3:1–48, 1958.
- [7] M. Donald, P. L. Morton, and H. Wiedemann. *Chromaticity Correction in Large Storage Rings*. *IEEE Transaction on Nuclear Science*, Vol. NS-24, No. 3, June 1977.
- [8] M. Donald and D. Schofield. *A User's Guide to the HARMON Program*. LEP Note 420, CERN, 1982.
- [9] M. Donald, Private Communication.
- [10] D. R. Douglas, *Lie Algebraic Methods for Particle Accelerator Theory*. Doctoral thesis, University of Maryland, unpublished, 1982.
- [11] A. Dragt, *Lectures on Nonlinear Orbit Dynamics, 1981 Summer School on High Energy Particle Accelerators, Fermi National Accelerator Laboratory, July 1981*. American Institute of Physics, 1982.
- [12] H. Grote, F. C. Iselin, *The MAD Program (Methodical Accelerator Design) Version 8.1, User's Reference Manual*, CERN/SL/90-13 (AP).
- [13] L. M. Healy, *Concatenation of Lie Algebraic Maps*. CERN, LEP Note No. ???.
- [14] L. M. Healy, *Lie Algebraic Methods for Treating Lattice Parameter Errors in Particle Accelerators*. Doctoral thesis, University of Maryland, unpublished, 1986.
- [15] J. Jäger and D. Möhl, *Comparison of Methods to Evaluate the Chromaticity in LEAR*. CERN PS/DL/LEAR/Note 81-7.
- [16] F. Ch. Iselin, *Lie Transformations and Transport Equations for Combined-Function Dipoles*, *Particle Accelerators*, 1985, **17**, 143-155.
- [17] J. Jowett, .
- [18] H. Mais and G. Ripken, *Theory of Coupled Synchro-Betatron Oscillations*, DESY internal Report, DESY M-82-05, 1982.

- [19] J. Milutinovic and S. Ruggiero. *Comparison of Accelerator Codes for a RHIC Lattice.* AD/AP/TN-9, BNL, 1988.
- [20] S. Peggs, *Some Aspects of Machine Physics in the Cornell Electron Storage Ring*, Doctoral thesis, Cornell University, unpublished, 1981.
- [21] G. Ripken, *Untersuchungen zur Strahlführung und Stabilität der Teilchenbewegung in Beschleunigern und Storage-Ringen unter strenger Berücksichtigung einer Kopplung der Betatronschwingungen.*, DESY internal Report R1-70/4, 1970.
- [22] L. C. Teng, *Concerning n-Dimensional Coupled Motion.* FN 229, FNAL, 1971.

Index

- ϕ , 54
- ψ , 54
- θ , 54
- angle of rotation, 54
- auxiliary functions, 2
- azimuth, 54
- beam
 - covariance matrix, 49, 51
 - transformation, 52
- beam-beam
 - Lie transformation, 35
 - TRANSPORT map, 35
- bending magnet, 56
- canonical variables, 1
- cavity, 55
- CENTRE, 38
- chromatic functions, 41, 66, 67
- chromaticity
 - first order, 64
 - second order, 65
 - third order, 65
- collimator, 14, 55
- composition
 - Lie transformation, 6
 - survey, 58
 - TRANSPORT map, 11
- conventions, 1
- coordinates, 54
- corrector, 29, 55
- COUPLE, 38, 43
- coupled motion, 45, 50
- coupled phases, 51
- coupling, 1
- coupling angles, 50
- Courant, 38
- covariance matrix, 52, 53
- covariance matrix of beam, 49, 51
- curvature, 3
- dipole, 3, 56
- dipole body
 - Hamiltonian, 17
 - Lie transformation, 18
 - synchrotron radiation, 61
 - TRANSPORT map, 19
- dispersion, 39
- displacement, 55
- drift, 14, 55
 - exact motion, 14
 - Hamiltonian, 14
 - Lie transformation, 15
 - TRANSPORT map, 15
- Edwards, 43
- EIGEN, 51
- eigenvectors, 51, 52
 - complex, 45
 - components, 46
- electric field, 4
- electrostatic separator, 55
- element
 - map, 14
- elevation angle, 54
- EMIT, 50
- emittances
 - equilibrium, 63
- energy error, 1
- ENVELOPE, 51
- exact map
 - misalignment, 33
- exact motion
 - drift, 14
 - RF cavity, 30
 - separator, 31
- field
 - electric, 4
 - magnetic, 3, 4
- fixed point
 - Lie transformation, 9
 - TRANSPORT map, 12
- fringing field
 - Lie transformation, 16
 - TRANSPORT map, 16
- functions
 - auxiliary, 2
- geometry, 54
- global axes, 55
- global coordinates, 54
- global reference, 54
- Hamiltonian, 3, 4
 - dipole body, 17
 - drift, 14

- quadrupole, 22
- rectangular dipole, 21
- referred to ideal orbit, 5
- scaled, 4
- separator, 31
- sextupole, 24
- solenoid, 28
- HARMON, 64
 - anharmonicity, 67
 - chromatic functions, 66, 67
 - chromaticity, 64, 65
 - multiple integrals, 64
 - organisation, 64
 - tune shift with amplitude, 67
- instrument, 14, 55
- integrals, 2
- invariants
 - linear, 48, 51
- inversion
 - Lie transformation, 9
 - TRANSPORT map, 11
- lattice functions
 - chromatic, 41
 - coupled, 45
 - Courant-Snyder, 38
 - Edwards-Teng, 43
 - Mais-Ripken, 52
- Lie transformation, 6
 - beam-beam, 35
 - composition, 6
 - dipole body, 18
 - drift, 15
 - fixed point, 9
 - fringing field, 16
 - inversion, 9
 - octupole, 26
 - quadrupole, 22
 - reflection, 9
 - reverse factorisation, 8
 - RF cavity, 30
 - separator, 31
 - sextupole, 25
 - solenoid, 28
 - thin multipole, 27
 - tilted element, 6
 - tracking, 9
- linear invariants, 48, 51
- linear map
 - misalignment, 33, 34
- linear optics
 - uncoupled, 38
- local axes, 55
- local origin, 54
- LUMP, 38
- magnetic field, 3, 4
- Mais, 52
- map
 - beam-beam, 35
 - composition, 6, 11
 - corrector, 29
 - dipole body, 18, 19
 - drift, 15
 - element, 14
 - fixed point, 9, 12
 - fringing field, 16
 - inversion, 9, 11
 - Lie algebraic, 6
 - octupole, 26
 - quadrupole, 22, 24
 - reflection, 9, 12
 - reverse factorisation, 8
 - RF cavity, 30
 - rotation, 35
 - separator, 31, 32
 - sextupole, 25
 - solenoid, 28, 29
 - thin multipole, 27
 - tilted element, 6, 11
 - TRANSPORT form, 11
- MARKER, 14, 55
- marker, 14
- mid-plane symmetry, 3
- misalignment
 - exact map, 33
 - linear map, 33, 34
- misalignment pivot, 33
- momentum error, 1
- monitor, 14, 55
- multiple integrals in HARMON, 64
- multipole, 3
- notations, 1
- octupole, 3, 55
 - Lie transformation, 26
 - synchrotron radiation, 62
 - TRANSPORT map, 26
- OPTICS, 13, 38
- orbit

- reference, 3
- slope, 1
- orbit corrector, 29
- orientation, 55
- phase factors, 49
- phase space, 1
- phase space vector, 1
- phases
 - coupled, 51
- potential
 - scalar, 4
 - vector, 3, 4
- quadrupole, 3, 55
 - Hamiltonian, 22
 - Lie transformation, 22
 - synchrotron radiation, 62
 - TRANSPORT map, 24
- radiation, 61
- RBEND, 15, 56
- rectangular dipole
 - Hamiltonian, 21
- reference orbit, 3
- reference system, 57
- reflection
 - Lie transformation, 9
 - TRANSPORT map, 12
- reverse factorisation
 - Lie transformation, 8
- RF cavity, 4, 55
 - exact motion, 30
 - Lie transformation, 30
 - model, 29
 - TRANSPORT map, 30
- Ripken, 52
- roll angle, 54
- rotation, 57
 - map, 35
- rotation angle, 54
- SBEND, 56
- scalar potential, 4
- separator, 4, 55
 - exact motion, 31
 - Hamiltonian, 31
 - Lie transformation, 31
 - TRANSPORT map, 32
- sextupole, 3, 55
 - Hamiltonian, 24
 - Lie transformation, 25
- synchrotron radiation, 62
 - TRANSPORT map, 25
- Sigma matrix, 49, 52, 53
- SIGMA0, 53
- slope of orbit, 1
- Snyder, 38
- solenoid, 4, 55
 - Hamiltonian, 28
 - Lie transformation, 28
 - TRANSPORT map, 29
- SROT, 57
- survey, 54
 - composition, 58
- SYMPLEC, 38
- symplectification, 13, 38
- synchrotron radiation, 61
 - damping, 61
 - equilibrium emittances, 63
 - quantum effects, 61, 62
 - systematic effects, 61, 62
- Taylor expansion, 3
- Teng, 43
- thin multipole
 - Lie transformation, 27
 - synchrotron radiation, 62
 - TRANSPORT map, 27
- TILT, 6, 11
- tilt angle, 54
- tilted element, 6, 11
- tracking
 - Lie method, 9
 - TRANSPORT map, 13
- Transfer matrix
 - symplectification, 13
- transformation of beam, 52
- TRANSPORT map, 11
 - beam-beam, 35
 - closed orbit, 12
 - composition, 11
 - dipole body, 19
 - drift, 15
 - fixed point, 12
 - fringing field, 16
 - inversion, 11
 - octupole, 26
 - quadrupole, 24
 - reflection, 12
 - RF cavity, 30
 - separator, 32
 - sextupole, 25

- solenoid, 29
 - thin multipole, 27
 - tilted element, 11
 - tracking, 13
- tune
 - shift with amplitude, 67
 - shift with energy, 64, 65
- TWISS, 38, 43, 64
- uncoupled motion, 38
- variables
 - canonical, 1
- vector potential, 3, 4
- X, 54
- Y, 54
- YROT, 57
- Z, 54